F I N A L

NAPA PLANT SITE RESTORATION PROJECT

MODELING TECH MEMO #1B

Prepared for

California Department of Fish and Game
7329 Silverado Trail
Napa, California 94558

December 2005

URS Corporation
1333 Broadway, Suite 800
Oakland, California 94612

26815044.00003

TABLE OF CONTENTS

Tables

Figures

CIMIS	California Irrigation and Management Information System
DTM	Digital Terrain Model
NOS	National Oceanic Survey
NSMR	Napa Sonoma Marsh Restoration

This technical memorandum corresponds to Task 3 deliverable #1b entitled "Modeling Technical Memorandum #1b." The purpose of the document is to present the modeling approach, setup and calibration for existing conditions, as well as the modeling for the three selected alternatives. It incorporates the comments received from the CDFG science review team upon the peer review of "Modeling Tech Memo #1a," and as such forms the basis for the final submittal of Technical Memorandum 1.

This memorandum is divided into the following sections:

- Model Selection
- Modeling Approach
- Model Description
- Model Extent
- Dimensionality of the System
- Model Setup
- Model Calibration and Validation
- Alternatives Summary and Base Case for Alternative Evaluation
- Alternative 1 Modeling and Results
- Alternative 2 Modeling and Results
- Alternative 3 Modeling and Results
- Conclusions and Future Studies

Numerical modeling will be used to support the site restoration design, study impacts of the design on the site and Napa River, and evaluate potential flooding of adjacent land and properties. The model results will also aid in the permitting process. It is recognized that the model should be defensible vis-à-vis the scientific community and public.

To optimize resources, this project leveraged the existing models already developed for the Napa Sonoma Marsh Restoration (NSMR) project, which focused on the salt ponds west of the Napa River. In particular, two models developed for the NSMR project were adapted for this study. Both models have a coupled one-dimensional MIKE11 and two-dimensional MIKE21 setup (the combined model is referred to as MIKEFLOOD). The first one consists of a one-dimensional model for the Napa River, Sonoma Creek, and the slough network including South Slough, Dutchman Slough, etc. and a two-dimensional model for the former salt ponds. The model setup is shown in Figure 1.

The second model is an expanded version of the first model that covers the entire San Francisco Bay from the Pacific Ocean to the Delta, with the two-dimensional model extending into the lower Napa River up to the NSMR site, as depicted in Figure 2. This model was used to determine the impacts of the NSMR project on the Bay. In view of the large model domain, nested two-dimensional models with cell sizes varying from 25m to 225m were employed in the NSMR study to cut down the computational resources required. To select and subsequently modify the existing model for this current study, the following questions were considered.

- What are the design questions that the models are being used to help answer?
- How much certainty is required in the answer (or in other words, what is the acceptable level of uncertainty in the results?)
- How much time is available to conduct the modeling?
- Will the public and scientific community accept the approach?

Hydrodynamic modeling is being used to analyze the tides and currents in the Napa River and in the former Napa Plant Site salt ponds for the different proposed restoration alternatives (described in Section 9). The model(s) are being used to answer questions relating to tidal prism, water depths and hydroperiod in the restored ponds, optimal breach size and location, local scour velocity and breach protection, and altered flood levels in the site and the surrounding properties. It may also be used to evaluate potential changes resulting from the proposed project, in tidal range and currents in the Napa River, Fagan Slough, and other sloughs, as well as for the sensitive users (e.g., float docks for residences on the western side of the Napa River).

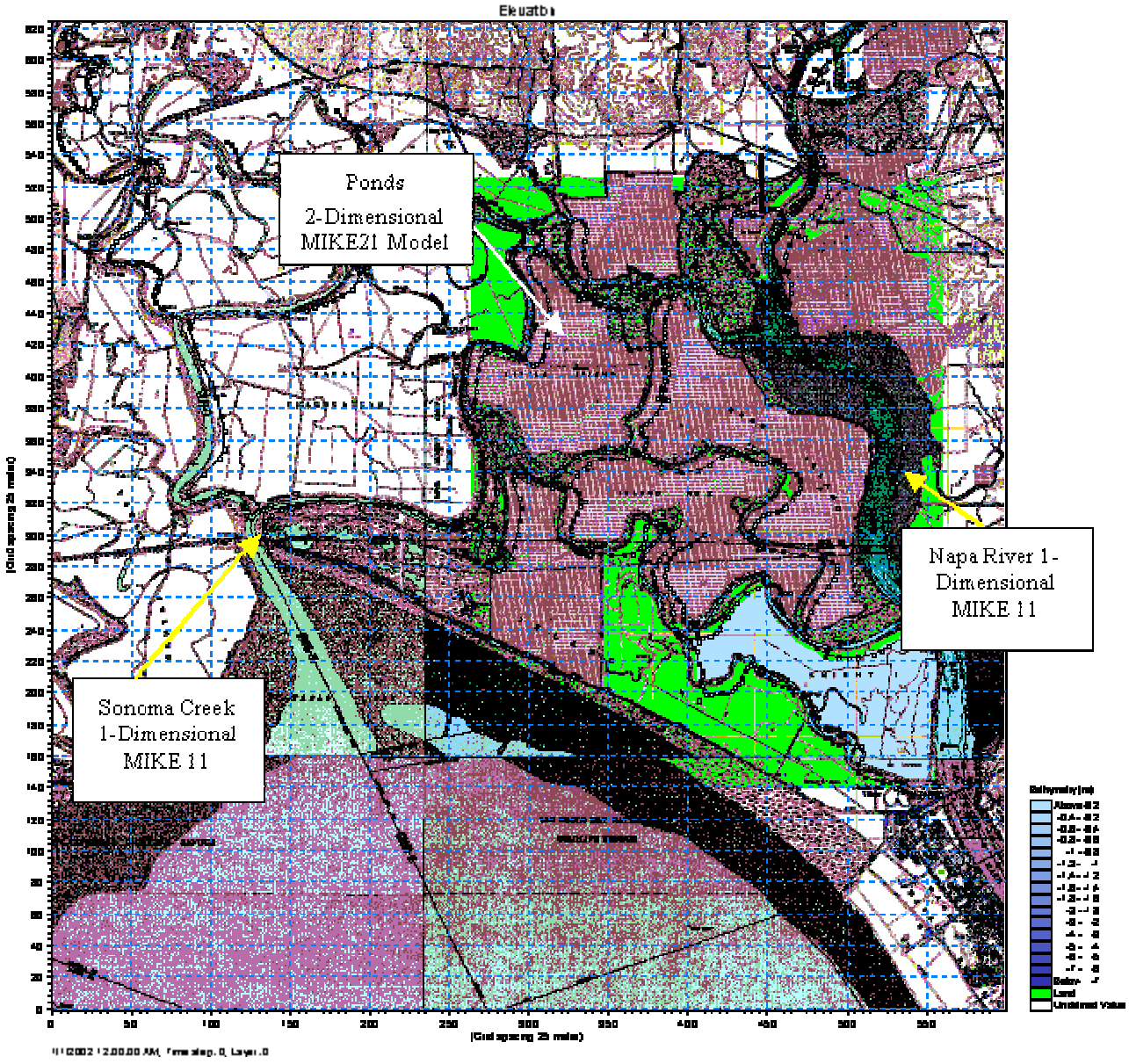

Figure 1 Napa River and Ponds MIKEFLOOD Setup from NMSR Project

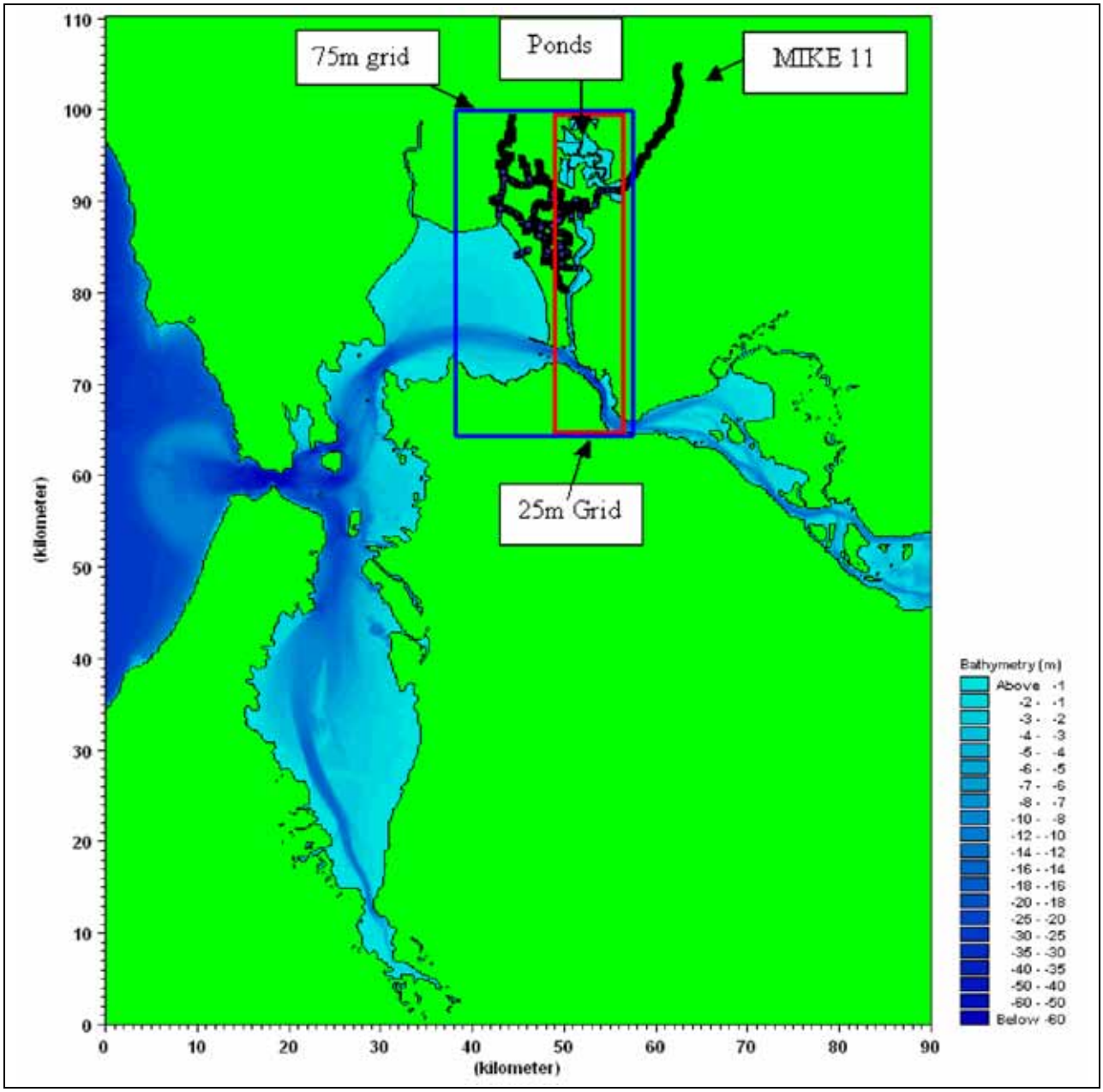

Figure 2 Bay-Wide MIKEFLOOD Model Setup from NMSR Project

A water quality model of the salt ponds will not be developed for this project. To evaluate the impacts of the project on water quality (such as methyl-mercury), procedures similar to those used in the NSMR project will be adopted. A simple dilution model for the ponds will be developed. The dilution model will provide information on the far-field mixing between the River and ponds and the dilution in the ponds. The estimated dilution combined with data on the average concentrations of constituents of concern in the River and ponds can be used to estimate the expected concentrations in the River with the ponds open. The simple dilution model will be based on tracking a tracer input into the hydrodynamic model developed for this project. Although this simplistic model will not be able to resolve local variation in concentration arising

from vertical stratification in the River, it is expected to provide a reasonable estimate of the concentration in the River at a large scale as long as the hydrodynamics are adequately reproduced in the river-pond system. However, this method is only applicable if the transport of constituent is predominated by advection and dispersion. Different methods should be considered if other physico-chemical processes such as dissolution and adsorption/desorption have a substantial influence on the concentration of the particular constituent.

As part of the property purchase agreement, Cargill has the responsibility to reduce surface salt concentrations to facilitate restoration. Salinity in Ponds 9 and 10 has been reduced and Cargill plans to sample these ponds in the summer or fall of 2005 to determine the residual salinity concentrations. Salt reduction activities in the remaining pickle ponds and crystallizer beds are expected to continue over the next 5 to 7 years.

In addition, the ponds are smaller than the ponds that will be restored as part of the NSMR project; therefore, salinity is not anticipated to be as significant an issue for this project as it was for the NSMR project. If salinity issues arise during the design of the restoration alternatives, the model used for the hydrodynamic study can address the impact on salinity. Alternatively, depending on the level of detail required, a simple box model could be adopted to evaluate the water quality changes brought about by the restoration project. Also, water quality and salinity data will be available for the NSMRP pond 4 breach in early 2006 and this data could be used to evaluate the salinity issues for the Napa Plant Site prior to finalizing the EIS/EIR.

According to the NSMR study, the creation of sediment sinks in the ponds may affect the sediment dynamics in San Pablo Bay in several ways, including: (1) erosion of shallows in San Pablo Bay to balance the ponds' sedimentation; and, (2) reduced accretion in sub-tidal channels in San Pablo Bay as the resuspended sediment is advected up-estuary to the restored ponds. Another possibility is that restoration of the ponds will cause a minor perturbation to the sediment dynamics in San Pablo Bay with the source of sediment to fill the ponds originating from the sediment in suspension that passes through the North and Central Bay and leaves the Golden Gate.

Considering the relative magnitude of the NSMR project compared with the Napa Plant project, the sediment supply should be sufficient for pond accretion. The NSMR project made a worst case estimate of sedimentation in the restored western ponds assuming that no additional sediment supply will be available from outside of San Pablo Bay. The total sediment demand from the west ponds was estimated to be about 5% of the sediment reservoir in San Pablo Bay. Therefore, using the same reasoning, the depletion in the sediment reservoir in San Pablo Bay will be less than 7-8% for the cumulative impact of the two projects under the worst-case scenario. No detailed sediment transport modeling will be conducted. Based on estimates of sediment supply from the NSMR project, together with the results from the hydrodynamic model, inferences will be made on the sedimentation rate within the site, as well as the associated impacts on the surrounding environment.

MIKE 11 is a one-dimensional numerical model that uses an implicit, finite-difference scheme for the computation of unsteady flows in rivers and estuaries. It is a modular model with the hydrodynamic module forming the backbone, upon which advection-dispersion processes, sediment transport and other water quality related phenomena can be added to the simulation system. The hydrodynamic module describes subcritical as well as supercritical flow conditions through a numerical scheme that adapts according to the local flow conditions, both temporally and spatially. A variety of structures can be incorporated into the model including bridges, culverts, gates, weirs and dams.

MIKE 21 is a two-dimensional, free-surface flow modeling system used to simulate hydraulics and hydraulics-related phenomena in estuaries, coastal waters and seas where stratification can be neglected. It consists of an assembly of computational modules that address different problems including advection-dispersion, short waves, sediment transport, water quality, eutrophication and transport of heavy metals. The hydrodynamic module, MIKE 21 HD, simulates the water level variations and flows in response to bathymetry, a variety of forcing functions (such as tide, wind, radiation stress) and various parameter values (bed resistance, eddy coefficients). It solves the time-dependent, vertically integrated equations of continuity and conservation of momentum in two horizontal dimensions. The water levels and flows are thus resolved on a rectangular grid covering the area of interest when provided with the bathymetry, topography, bed resistance, wind field, hydrographic boundary conditions (surface elevations or flux densities), etc.

The MIKE FLOOD model integrates the MIKE 11 and MIKE 21 models by linking MIKE 21 grid cells to a MIKE 11 reach and solving the flow exchange between the two models. It is a robust dynamic model, and it has the flexibility to address other constituent transport processes (e.g. salinity). The following effects are included in the equations:

- Convective and cross momentum;
- Wind shear stress at the surface;
- Bottom shear stress (by Chezy's equation);
- Barometric pressure gradients;
- Coriolis forces;
- Momentum dispersion (eddy effects);
- Sources and sinks (both mass and impulse);
- Evaporation;
- Flooding and drying.

The computational resources and run-time required for the NSMR bay-wide model are significantly greater than that for the river system and the site model alone. The bay-wide model is needed to evaluate potential impacts of the restoration project on the bay and areas beyond the mouth of the Napa River (e.g., local shoreline erosion at Mare Island Strait). Since the Napa Plant Site restoration is expected to have a similar but smaller influence on the Bay compared to the NSMR project (because of the substantially smaller restored area), a model encompassing the river network and ponds and excluding the bay is proposed for this study. Results from the NSMR project will be used to estimate project impacts outside the modeled area. The reduced run-time will allow for greater flexibility in deciding the scenarios to be included in the analysis.

Excluding the bay from the model domain requires that a tidal boundary condition be applied in San Pablo Bay near the mouths of the Napa River and Sonoma Creek (instead of in the Pacific Ocean as is done in the bay-wide model). Sonoma Creek is included in the model setup because the flows in the slough network are controlled by the tidal propagation along both the Napa River and Sonoma Creek, as well as the tidal phase difference between the two rivers. To apply the same boundary condition for the scenarios with and without the project, it should be demonstrated that the project would not have an impact on the water level in San Pablo Bay near the river mouths. Two simulations were conducted as part of the preliminary investigation using the NSMR bay-wide model to examine the changes in tidal elevation in the Napa River and Sonoma Creek, before and after the restoration of NSMR ponds 3, 4 and 5, which include a total area of about 3,000 acres. Results of this test indicate that the tidal elevations near the mouths of the two rivers are unaltered when opening up NSMR ponds 3,4, and 5 (see Figure 3), providing support to the assumption of applying consistent tidal boundary conditions at the downstream end of the rivers for both existing and proposed conditions.

The upstream boundary of the model in the Napa River is extended to about 6.5 miles north of the City of Napa, such that it is beyond the zone of tidal influence and a proper flow boundary condition can be specified. On Sonoma Creek, the upstream boundary is near the limit of tidal influence, at State Highway 12/121 near Schellville.

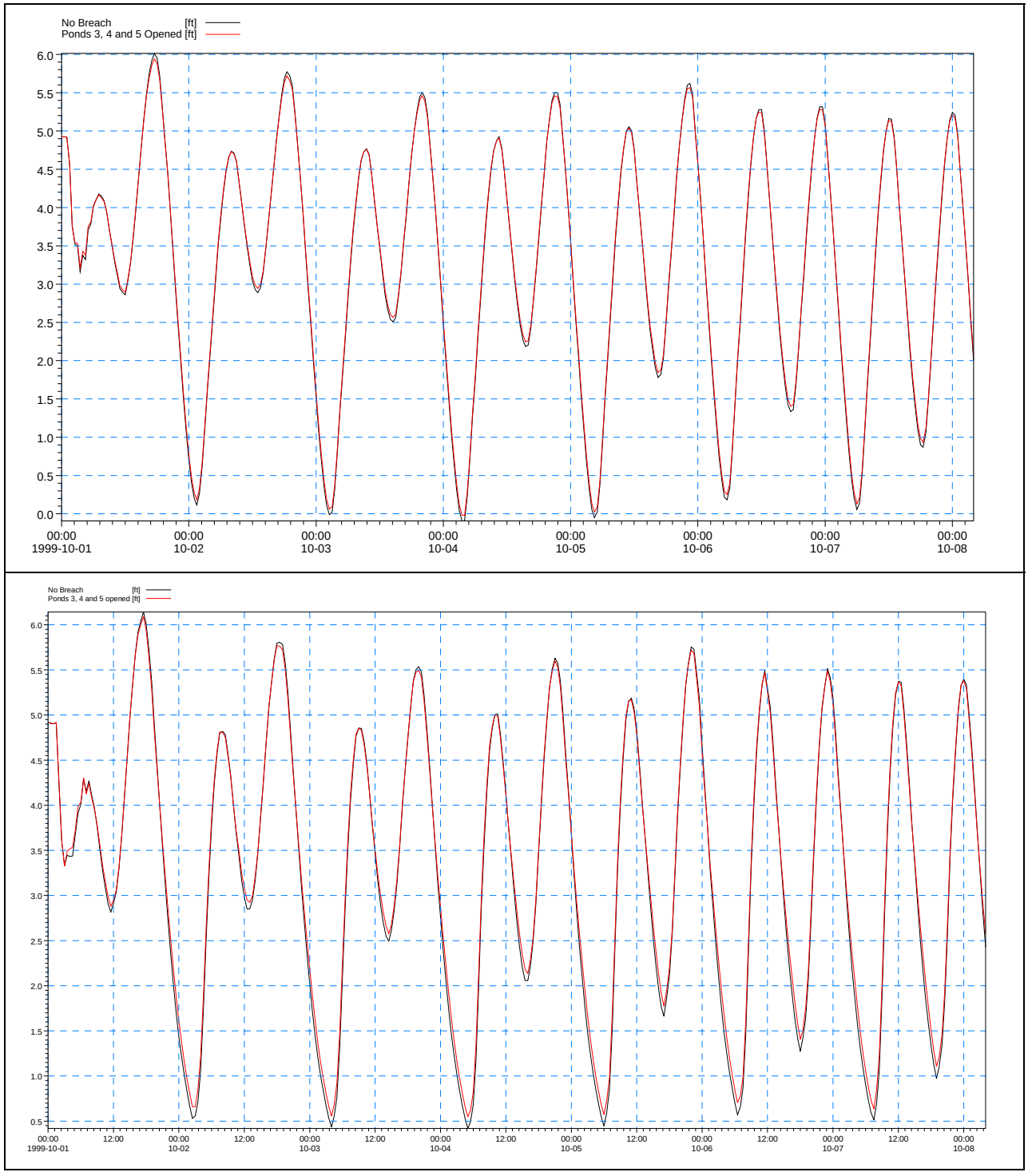

Figure 3 Tides at the Mouth of Napa River (top) and Sonoma Creek (bottom) with and without Breached NSMR Ponds 3, 4 and 5

The one-dimensional MIKE11 model will be used for the Napa River and the interconnected slough network since, in general, river flow is one-dimensional. Although it has been widely recognized that density gradients play an important role in the circulation at Mare Island Strait at the mouth of the Napa River, the focus of this study is on the tidal regime of the Napa River and how it influences the inundation of the former salt ponds. Therefore, it is considered that the use of a one-dimensional model for the river is commensurate with the resolution power required for the analyses.

The ponds in the Napa Plant Site can be represented as storage elements in the one-dimensional MIKE11 model or a collection of grid cells in the two-dimensional MIKE21 model. Model selection is dependent on the answers the model is supposed to provide. With a one-dimensional model, the water level and tidal prism can be predicted and flooding can be approximated from a stage-storage curve. Using the two-dimensional model, detailed information inside each pond such as local velocity and circulation patterns can be generated from the model results. In addition, the two-dimensional model may provide a lower level of uncertainty in the results and more elaborate graphical output that can be used for public meetings or presented to regulatory agencies.

For this analysis, a two-dimensional model of the salt ponds will be connected to the one-dimensional model of the River and Fagan Slough. This model will be used to assist in designing the breach sizes and locations, and to predict the wetting and drying cycle for the wetland restoration areas. Using a two-dimensional approach will provide flexibility in the event that internal channels are required based on biological assessment and needs.

The two-dimensional model will also provide information the biologists can use to predict habitats that are likely to develop. Separate models could be developed incorporating different assumptions on the future channel network to predict habitat types that are likely to occur over time.

In an effort to shorten the run-times, the western ponds (NSMR project) are simplified into one-dimensional elements that are linked with the slough network. This will ensure the inclusion of the effects of the western ponds on the hydrodynamics and tidal prism of the Napa River and the sloughs, while no detailed simulation will be done inside those ponds. In addition, representing the lower portion of the Napa River with the one-dimensional model can further shorten the run-time. Figure 4 presents the comparison of water level and velocity at several locations along the Napa River predicted from the one-dimensional pond model versus the two-dimensional pond model used for the NSMR study. The three locations selected were: (1) downstream of all the breaches; (2) between breaches to the ponds; and (3) upstream of all the breaches, in order to evaluate the potential difference in model predictions associated with the breached flows. The close resemblance between the model outputs indicates that the effects of NSMR Ponds 3, 4 and 5 can be adequately represented with one-dimensional river branches.

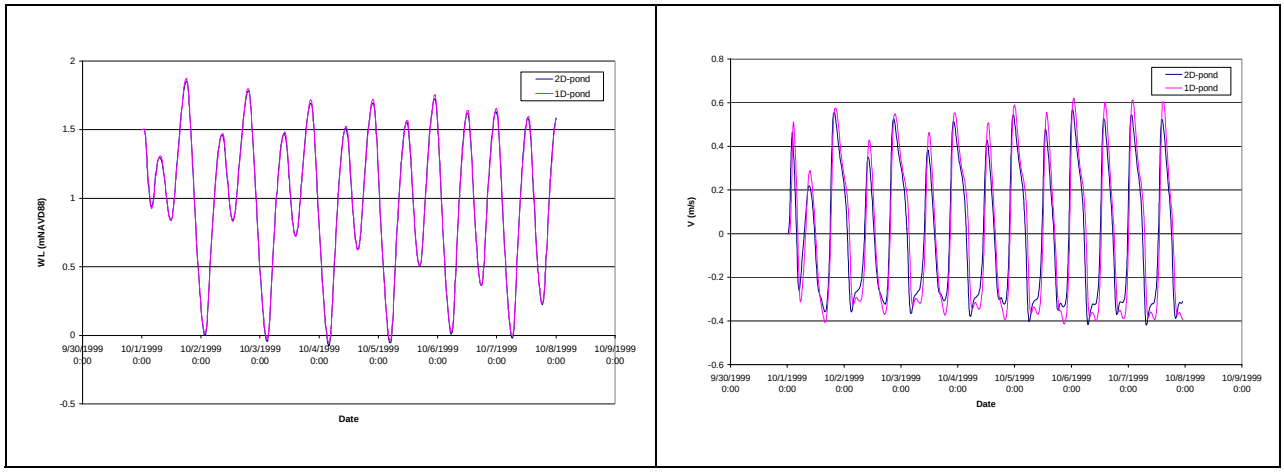

Figure 4a Comparison of Model Outputs Between 1-d and 2-d Setup of NSMR Ponds
Water Level and Velocity in Napa River Downstream of Dutchman Slough

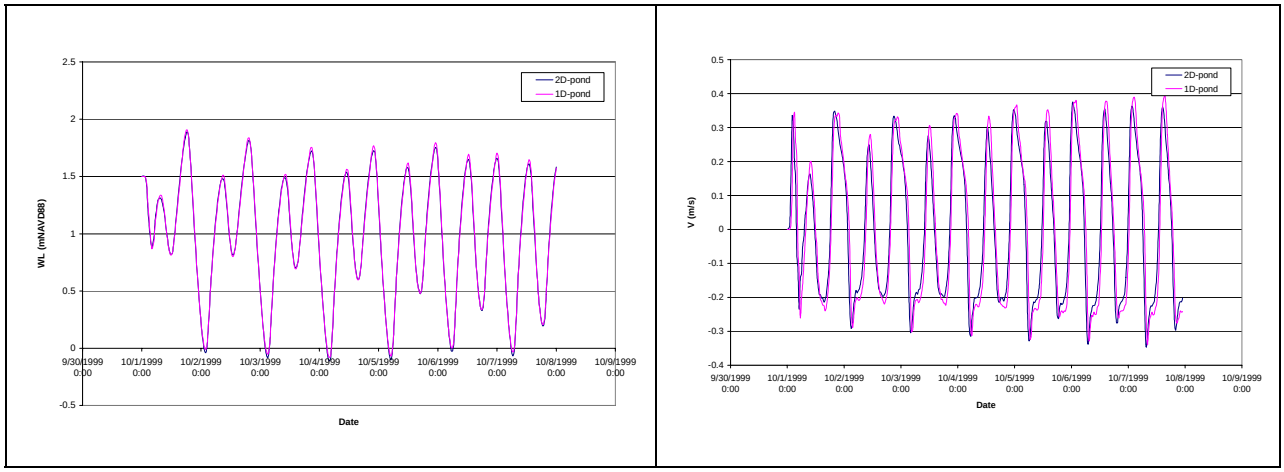

Figure 4b Comparison of Model Outputs Between 1-d and 2-d Setup of NSMR Ponds
Water Level and Velocity in Napa River Upstream of First Breach to Pond 4

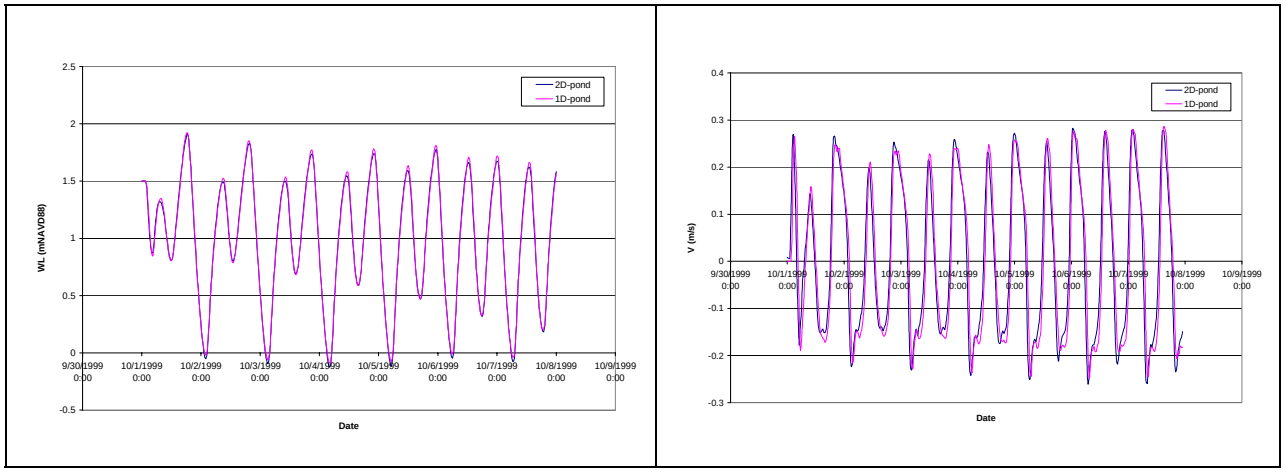

Figure 4c Comparison of Model Outputs Between 1-d and 2-d Setup of NSMR Ponds
Water Level and Velocity in Napa River Downstream of Napa Slough

Two types of data are required for model setup: geometry and boundary conditions. In addition, if there are any inflows or hydraulic structures, they need to be included with the input data. For MIKE11 the geometry data consist of channel cross-sections. For MIKE21 the geometry data consist of a two-dimensional evenly spaced bathymetry grid.

7.1 GEOMETRIC DATA OF RIVERS AND TIDAL SLOUGHS

MIKE11 was used to model the Napa River, Sonoma Creek and the tidal sloughs including Fagan Slough. Cross-sectional data of the upper Napa River, Sonoma Creek, and the tidal sloughs bounded by these two streams were obtained from the NSMR project (PWA 2004). The upper Napa River extends from the Southern Pacific Railroad Bridge near the northern end of the Napa Plant Site, to the USGS Oak Knoll gauging station, located about 6.5 miles north of the City of Napa. The Napa River cross-sections were created for the Napa River Flood Protection Project (USACE, 1998) using surveys conducted by the USACE. These cross-sections do not reflect conditions in the River following the construction of the Napa River Flood Protection Project, which involves reconnecting the River to its historic floodplains at selected reaches and widening of the River, with the work to be implemented in phases. These changes are not expected to significantly influence the hydrodynamics of the lower Napa River or the Napa Plant Site, as the flow in the system is driven primarily by the tides in San Pablo Bay. However, there will be an exception during large flood events since the peak flow arriving at the lower Napa River will be attenuated as a result of the reconfiguration in the upper reach of the River. Horizontal and vertical projections of the data are in NAD83 and NAVD88, respectively.

The cross-sections for the lower Napa River were extracted from the 25m MIKE21 grid created for the NSMR project (PWA, 2004). This grid incorporated information from the National Oceanic Survey (NOS), a survey conducted by Warner (2000) and USGS aerial photos. To ensure that the tidal boundary condition would be appropriately imposed, the most downstream section of the River was extended a short distance past the river mouth into Carquinez Strait. Locations of the cross-sections along the lower Napa River are shown on Figure 5.

Cross-sections of the lower Sonoma Creek, from the mouth at San Pablo Bay to its confluence with the Second Napa Slough, were derived from the Digital Terrain Model (DTM) created by Towill, Inc. using a variety of techniques including aerial photogrammetry and land based surveying (Towill, Inc., 2001). A combination of a survey conducted for the NSMR study and cross-sections developed by the Southern Sonoma County Resource Conservation District provided the sources for cross-sections in the upper Sonoma Creek.

The geometry data for the major tidal sloughs including Napa Slough, Second Napa Slough, Third Napa Slough, Dutchman Slough, South Slough, China Slough, Devils Slough, Hudeman Slough and Mud Slough were obtained from the DTM developed by Towill, Inc. Since Fagan Slough was not included in the NSMR model setup, cross-sections of Fagan Slough were surveyed as part of this project. A total of 9 transects between the mouth and the confluence with Fagan Creek were surveyed (see Figure 5) and used in the MIKE11 model setup.

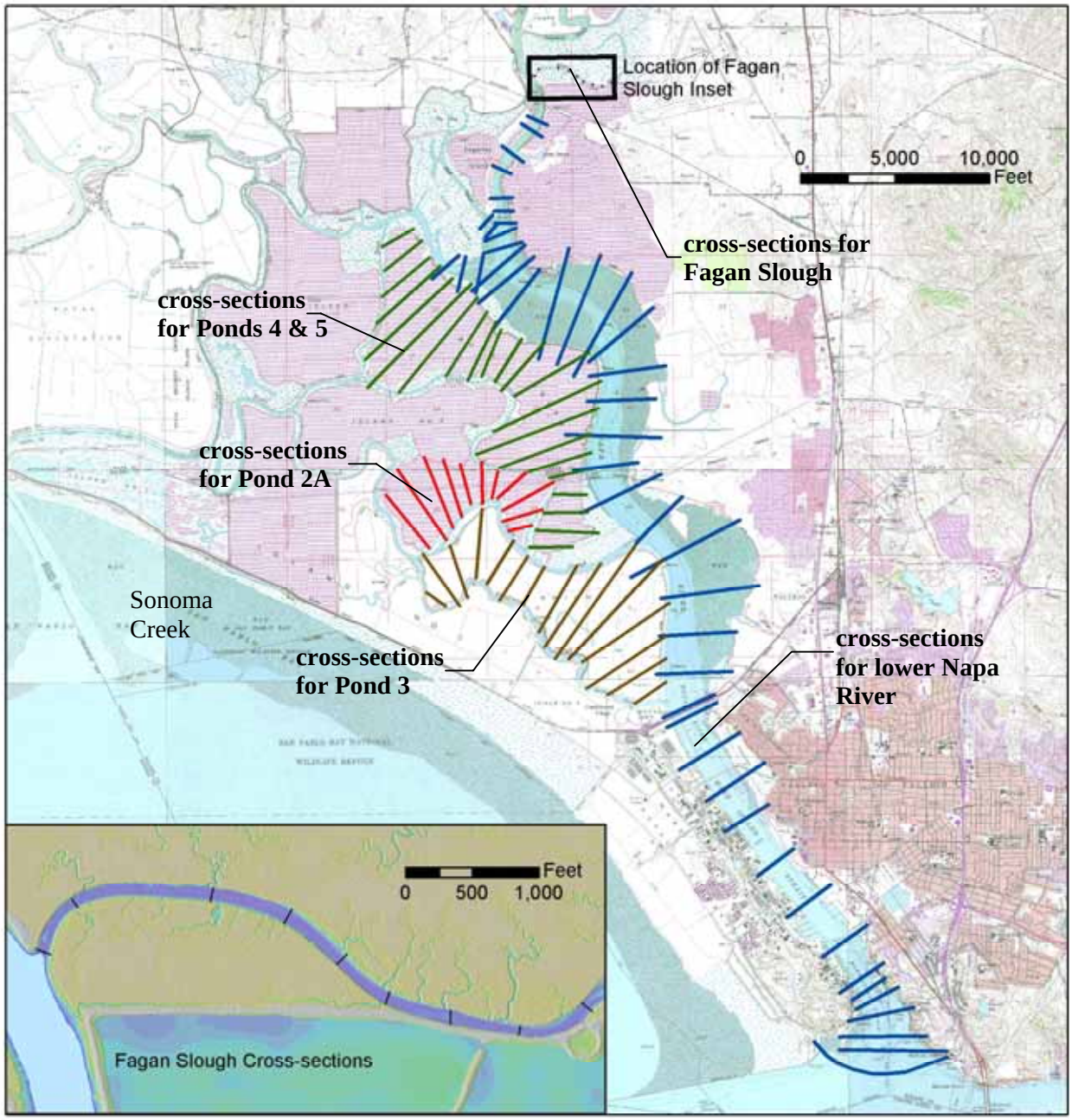

Figure 5 Cross Sections Extracted from MIKE 21 Grid Developed for the NSMR Project and Fagan Slough Sections

7.2 GEOMETRIC DATA OF SALT PONDS

Cross sections for Ponds 2A, 3, 4 and 5, located west of the Napa River, were extracted from the 25m MIKE21 grid developed for the NSMR study (PWA, 2004). The NSMR grid was generated from a DTM created from three to six transects across each pond to form the surface representing the bottom of the ponds.

A DTM with a one-meter cell size covering the Napa Plant Site was created in ArcGIS using a combination of LIDAR and ground survey data collected as part of this study. The ground survey provided point data at about 200 meter spacing to supplement the LIDAR survey, which did not include information for submerged areas of the ponds. To achieve a balance between model resolution and computer run-time, a 20-meter grid was created for the model input grid from the one-meter DTM. Figure 6 presents the grid created for the ponds for use in the MIKE21 model.

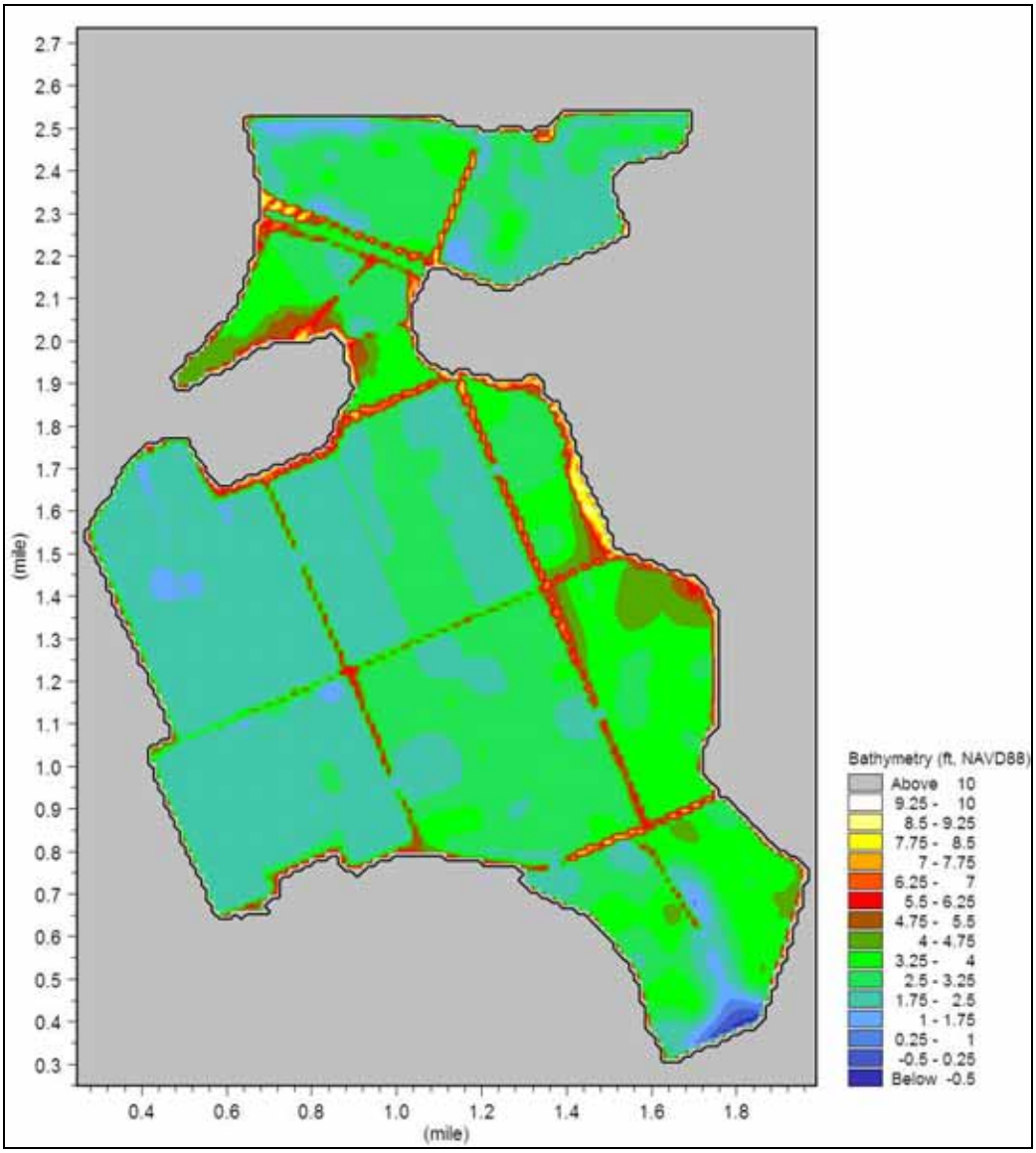

Figure 6 Bathymetric Grid Used in the MIKE21 Model

7.3 BOUNDARY CONDITIONS

Two boundary conditions are needed by the model. Tides are the primary driving force for flows in the river-slough system. Therefore, tidal boundary conditions are required at the downstream end of the model, at the mouths of both the Napa River and Sonoma Creek. Since the tides are transformed as they propagate from the Pacific Ocean up-estuary into San Pablo Bay, they are slightly different in amplitude and phase between the mouths of the two rivers. At the upstream boundaries of the model, above the tidal zone, stream flows are required as boundary conditions.

The NOAA tide stations at the mouths of Sonoma Creek (Station 9415338) and the Napa River at Mare Island (Station 9415218) were only in commission for a short period and were not concurrent. These data can therefore not be used directly as boundary conditions. Warner et al. (1999) collected concurrent tidal data at the mouths of both streams from September 1997 to March 1998. The water level data were subsequently converted to the NAVD88 datum under the NSMR study (PWA, 2002a). However, some of the measured data appear to have datum errors, which could in part be associated with land subsidence in the locality leading to inaccurate benchmark elevations.

In view of the limitation in data availability, predicted tides at the mouths of the two streams were adopted for this study. Predicted water levels were obtained from the output of the bay-wide model developed for the NSMR project.

Freshwater inflows from the contributing watersheds are prescribed at the upstream end of the rivers. The USGS gauging station at Oak Knoll Avenue (north of the City of Napa) (Station #11458000) on the Napa River has daily flow data from 1929 to 1932, and from 1960 to the present. It has a drainage area of approximately 218 square miles, or about half the size of the total watershed. For Sonoma Creek, the USGS gauging station at Agua Caliente (Station #11458500) has daily flow data from 1955 to 1981, and in water years 2002 to 2004. The drainage area for this station is approximately 58 square miles. To apply the data to the upstream boundary at Highway 12/121, which has a drainage area of 91 square miles, the hydrograph obtained from the USGS station is weighted by the drainage areas. During the ungaged period, the synthetic hydrograph developed for the NSMR project was adopted, which is based on statistical correlation between the flows in Sonoma Creek at Agua Caliente and in Napa River at the Oak Knoll Avenue Station using the concurrent records.

7.4 OTHER HYDROLOGIC INPUTS

To include the flows from the major tributaries of the Napa River downstream of the Oak Knoll station, the synthetic hydrographs created for the NSMR project were adopted (PWA, 2004). The synthetic hydrographs were scaled from the daily discharge measured at the Oak Knoll station, with the scaling factor determined by the ratio of tributary's peak discharge to that at Oak Knoll. The method and assumption for generating these synthetic hydrographs were provided by the Napa County Resource Conservation District (Zlomke, 1996). In addition, the synthetic hydrographs were shifted forward in time to account for the fact that smaller catchments typically respond faster to precipitation than large ones. The amount of time shift was estimated in accordance with the catchment size. Table 1 summarizes the properties of the synthetic hydrographs for the tributaries.

Table 1
Properties of Synthetic Hydrographs for Tributaries to Napa River

Name of Tributary	% Flow of Oak Knoll Ave Station	Time shift from Oak Knoll Ave Station
Milliken Creek	19.4	+3.0 hours
Napa Creek	10	+3.6 hours
Tulucay Creek	9	+3.7 hours
Carneros Creek	6	+4.0 hours

Wind stresses on the water surface can cause wind driven circulation and enhance the mixing process, especially in shallow waters. Wind waves also play an important role in the resuspension of benthic sediments. Although water quality or sediment transport modeling is not included in the project at present, the wind data are included for completeness of the model setup. Hourly wind data including wind speed and direction were obtained from the CIMIS (California Irrigation and Management Information System) station #109 in Carneros for input into the MIKE21 model, and assumed to be spatially constant throughout the ponds. The CIMIS wind data was available from 1993 to 2001. Although Cargill has an on-site meteorological station with wind measurement, the data were not available at the time of this analysis.

In riverine and estuarine systems, direct precipitation on the water surface normally has an insignificant contribution to the total inflows. In the case of salt ponds or managed ponds, however, precipitation can be a major source of water, and can have a large influence on the salinity. Similarly, evaporation can effect changes in salinity. Therefore, hourly precipitation and evaporation data obtained from the CIMIS station in Carneros were included in the MIKE21 model. The hourly evaporation rate was computed using measurements from CIMIS on net radiation, air temperature, relative humidity and wind speed, and corrected for salinity effect with a coefficient. The computation on evaporation rate was undertaken by PWA for the NSMR project and adopted for this study.

7.5 HYDRAULIC STRUCTURES

There are a several existing water control structures in both the NSMR ponds and the Napa Plant ponds that were constructed for the operation of the former salt production plants. Most are siphons built in the 1950s to convey flow between the ponds, but a few gate structures also exist. Although they had been the primary means for moving water through the system, their conveyance has been largely impaired as a result of subsidence and sediment deposition. Moreover, their influence on the hydrodynamics of the ponds will be minimal once the ponds are opened to tidal action. Therefore, these existing structures are omitted from the model.

A numerical model requires calibration to define the values of model parameters. Calibration is used to demonstrate that the model correctly simulates the physical processes included in the model, and ensures that model predictions are defensible.

A similar model to that developed for this study was calibrated for the NSMR project (PWA, 2004). In that project report, some uncertainties were discussed regarding the datum of the water level measurements in the river-slough network. In particular, the accuracy of the boundary condition at the mouth of the Napa River was questioned. Therefore, a calibration check has been performed for the current study as an independent evaluation of the validity of the model. The period selected for the calibration check is September 6-20, 1997. This period was selected since the discharges in the rivers were low, and the transformation of tides in response to bathymetry and friction losses could be diagnosed separately from the influence due to freshwater inflows.

8.1 CALIBRATION DATA

Between September 1997 and March 1998, Warner, UC Davis and USGS, in support of the NSMR study, undertook the most extensive data collection effort in the river-slough network (Warner et al., 1999). Water depths were logged and subsequently converted to the NAVD88 datum using the permanent and temporary benchmarks. Current velocities were measured at several points along the vertical profile depending on the station. In addition, conductivity, temperature and suspended sediment concentrations were measured at about 17 sites (locations shown in Figure 7). Not all parameters were available at each monitoring station. The calibration data were compiled in a format compatible with the MIKE model under the NSMR study (PWA, 2004) and were also adopted for this study.

Figure 7 Locations of Calibration Stations

8.2 CALIBRATION PROCEDURE

The primary calibration parameter in the MIKE11 and MIKE21 models is Manning's n, which is used to calculate frictional losses due to bed resistance. Typical values of Manning's n are published (Chow, 1959) for different fluvial and estuarine environments based on the degree of irregularities and the types of vegetation cover. Separate Manning's n values can be prescribed for the main channel and the overbank areas in MIKE11. In general, the Napa River and Sonoma Creek have little vegetation within the main channel and therefore the Manning's n values are typically in the range of 0.020 to 0.035. The tidal sloughs have moderate to dense vegetation cover and more meanderings and irregularities, so typical Manning's n would range from 0.030 to 0.045. The Manning's n values are adjusted within the reasonable range to minimize the difference between model predictions and the field measurements.

Horizontal mixing coefficients (eddy diffusivities) are specified in the MIKE21 model to account for turbulence and mixing not included in the model. Although these parameters can be used as calibration parameters, they will be assigned as a constant in this study due to the absence of calibration data in the ponds.

8.3 CALIBRATION RESULTS

The predicted water levels at the mouths of the Napa River and Sonoma Creek from the NSMR bay-wide model were compared to the UCD/USGS field measurements at stations M5 and PABLO before applying them as the boundary conditions for the current river-pond model. As shown on Figure 8, the predicted water levels (presented as black lines) are slightly higher (<0.1m) than the measured data, but reasonable agreement is achieved at both stations. Also, the predicted low tides appear to be dampened at both stations, but more so at the Sonoma Creek mouth. This could be caused by inadequate resolution of the inlet channel in the 75m grid used in the Bay wide model for this location. To help mitigate this effect, the location of water levels to use as a model boundary condition was moved farther into the Bay. There is a shift in the predicted tidal signals starting from the second week of simulation. The reason is unclear, but it is possible that a phase shift was introduced into the ocean boundary conditions used for the bay-wide model during that period.

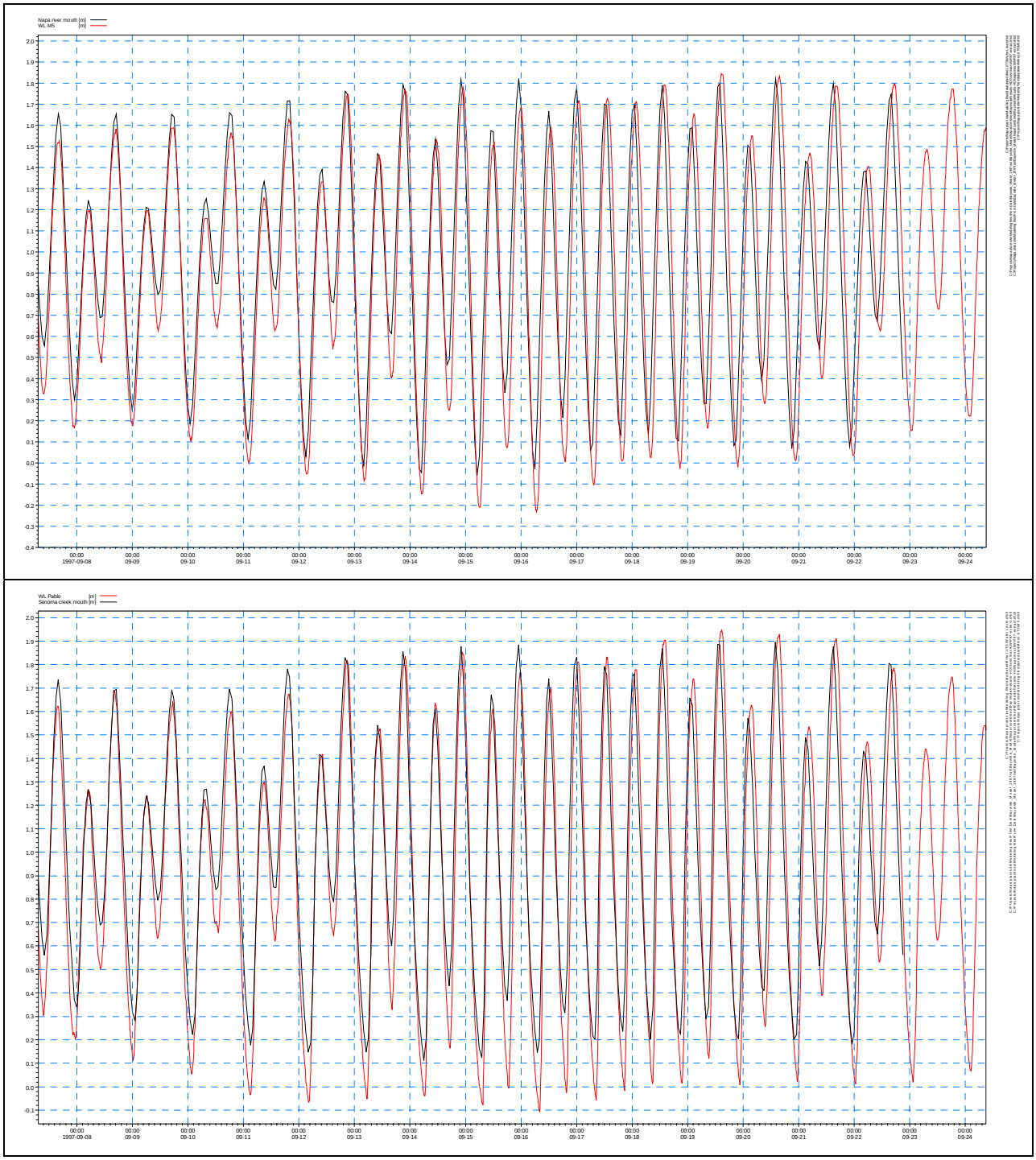

Figure 8 Comparison of Predicted and Measured Water Levels at the Mouth of Napa River (top) and Sonoma Creek (bottom) in September 1997 (taken from DHI Baywide Model)

The results obtained from the MIKE11 model are compared to the measured water levels and velocities at the stations where data are available for the simulation period, and presented in Figures 9a through 9c, and 10a through 10f, respectively.

With the exception of China Slough, of the 6 stations with available water level data, the predicted water levels are higher than the measured data in Napa River and the tidal sloughs but very close to the measured tides in Sonoma Creek. The water level at Station CHINA is remarkably higher than the remaining stations and it is suspected that there is an error in the station datum. This issue was discussed in the NSMR study (PWA, 2002a), which suggested that the water level measurement at M5 might be too high. However, it appears that there is also an error with the data collected at the other stations based on the following reasons:

- The water level predicted by the bay-wide model at the mouth of Napa River matches reasonably well with M5;
- The measured tidal signals, both at high and low tides, at the stations in the tidal sloughs (e.g. DUTCH, PIPE, HUDE) are lower in elevation compared to those at the mouths of the Napa River and Sonoma Creek, which cannot be physically real;
- A sensitivity test was performed by lowering the water level boundary at the Napa River by 0.2m (to simulate the case that the water level at Station M5 was too high) and the resulting flow direction in Napa Slough was reversed from the measured data.

Apart from the elevation shift, the tidal amplitudes and phases are reasonably reproduced at all the stations. The phase difference observed at the calibration stations during the second week of simulation is associated with the shift in the specified boundary conditions.

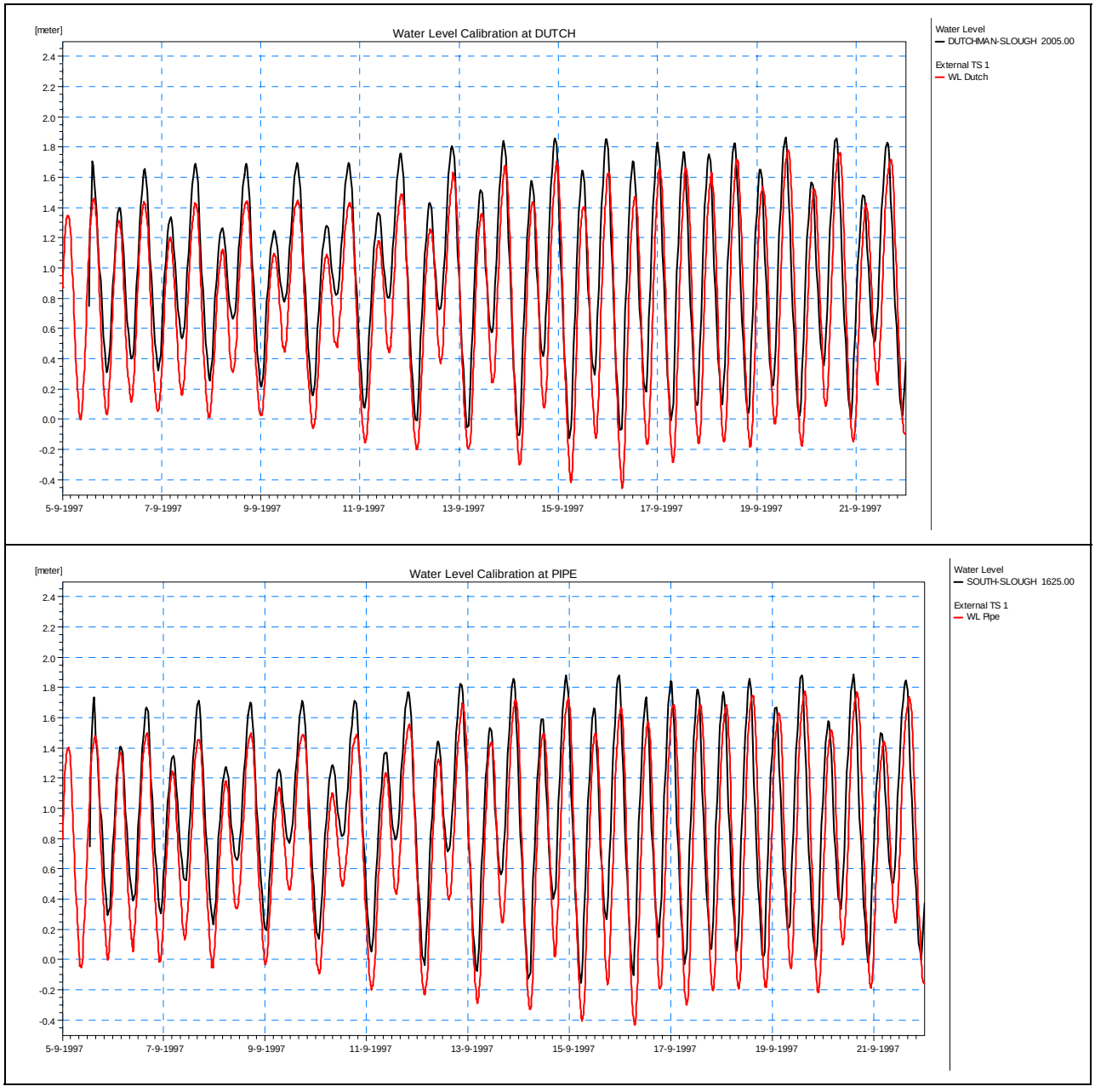

Figure 9a Water Level Calibration in September 1997 (Top to Bottom: DUTCH, PIPE)

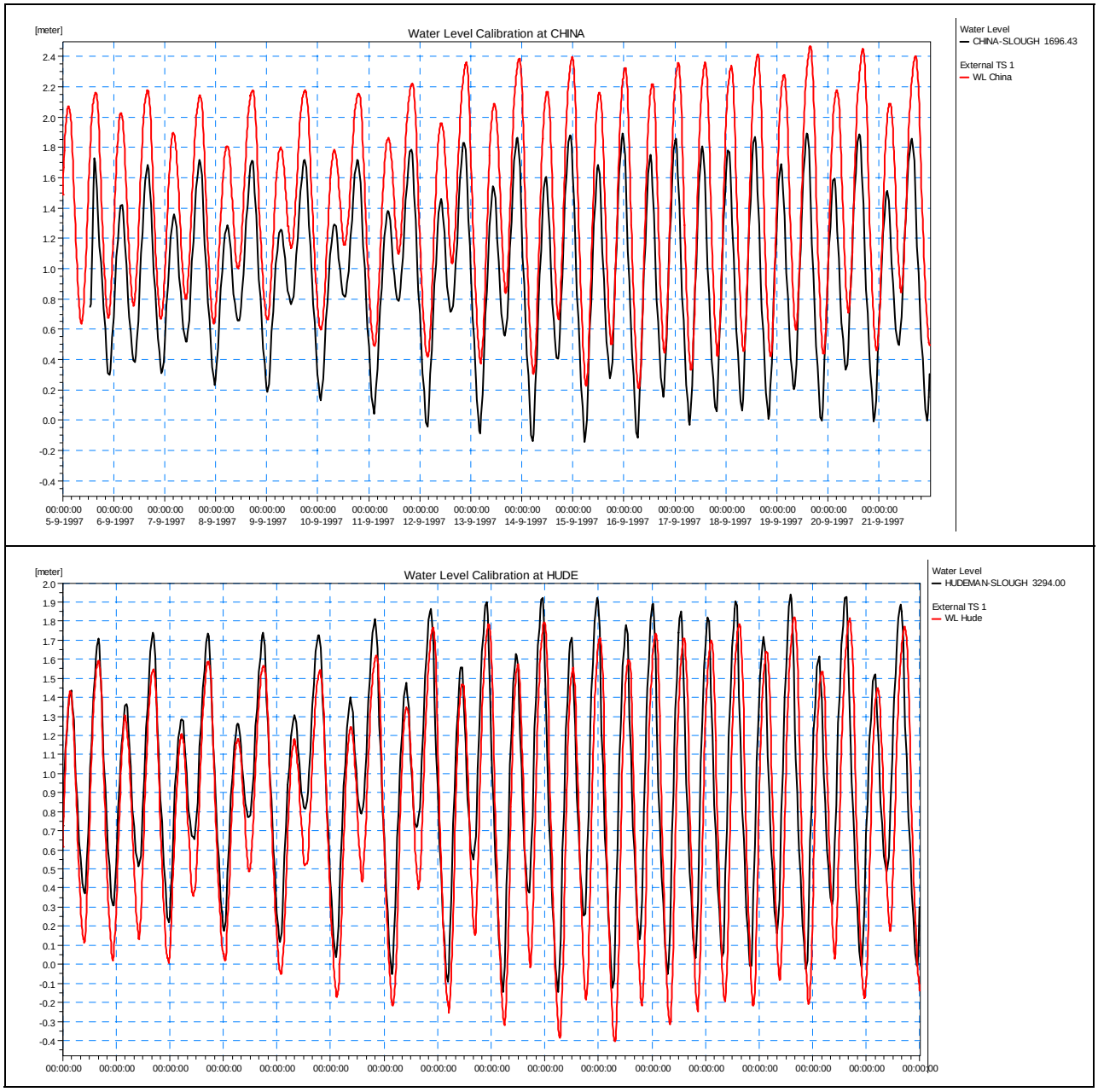

Figure 9b Water Level Calibration in September 1997 (Top to Bottom: CHINA, HUDE)

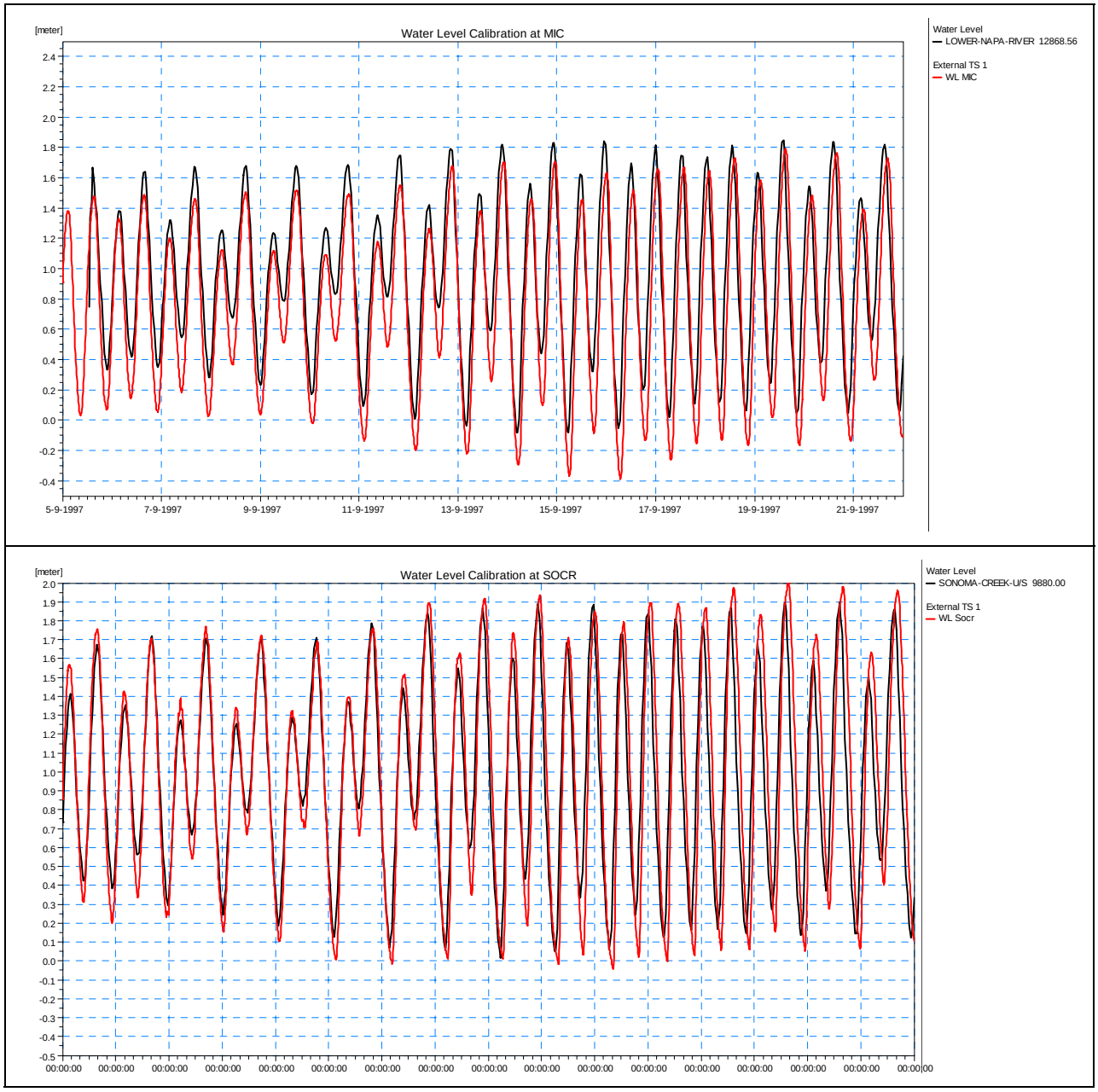

Figure 9c Water Level Calibration in September 1997 (Top to Bottom: MIC, SOCR)

A total of 11 stations have velocity measurements for the calibration period and provide a good spatial coverage in the major rivers and tidal sloughs. The predicted velocities are in good agreement with the measured data along the lower and upper Napa River, as exemplified in Figures 10a and 10b at stations M5 and M14. Close match between predicted and measured velocities is also achieved at stations NAPA, DEVIL and PABLO. In South Slough, the predicted and measured velocities are similar at station PIPE, though the model under-predicts the velocity during a falling spring tide. At Station SS, the predicted velocity tends to be greater than the measured velocity, but is within a 0.10 m/s. Likewise, the predicted velocities are within a 0.10 m/s at station CHINA. At Station SNS, the model under-predicts the velocity during the spring tide by about 0.2 m/s. Nonetheless, the time series plots illustrate that the timing of the turn of currents (flood and ebb) is well captured by the model. It should also be pointed out that the measured velocities are point velocities while the simulated velocities are cross sectionally averaged, and therefore the two are not expected to be identical.

The current velocity at Station HUDE exhibits the most irregular pattern in both the measured and predicted velocities and has the largest discrepancy between modeled and predicted values. This may be because the station is located near the null point where the tidal signal from the Sonoma Creek meets with that from the Napa River. Small errors in the model that do not show up at the other stations could be more pronounced near the null point since the resistance in the rivers and sloughs affects the travel time of the tidal signals through the slough network. This in turn alters the location of the null point. Therefore, the results are very sensitive at this location.

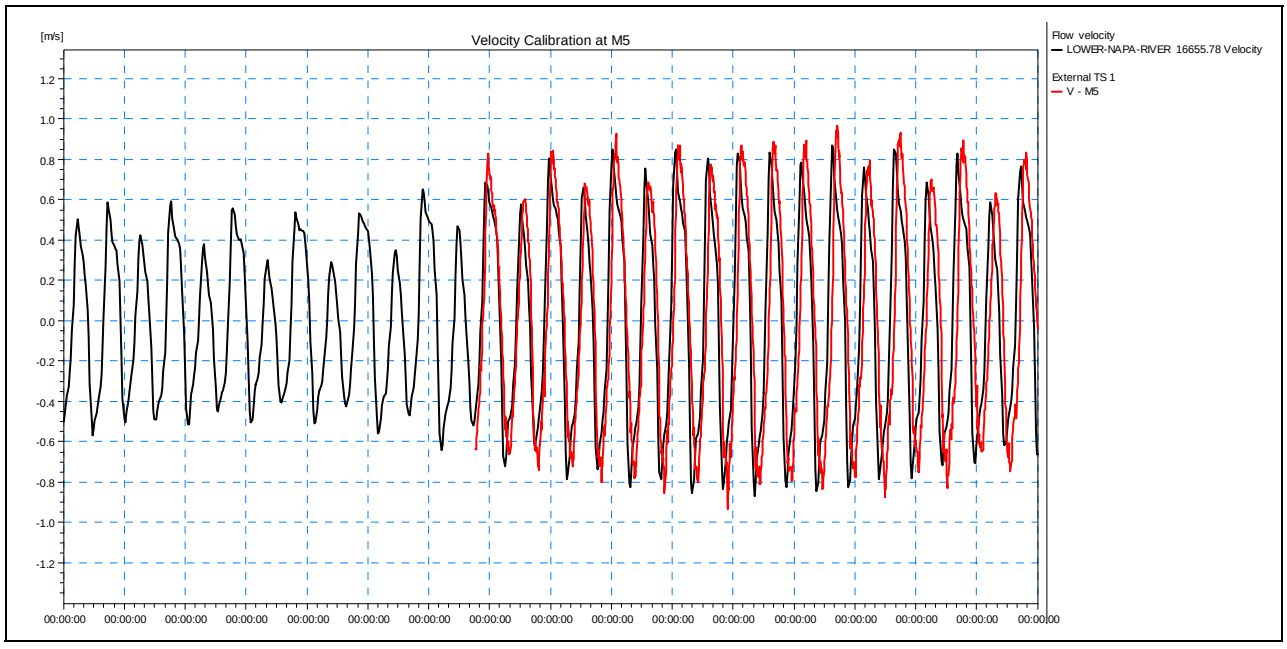

Figure 10a Velocity Calibration in September 1997 (M5)

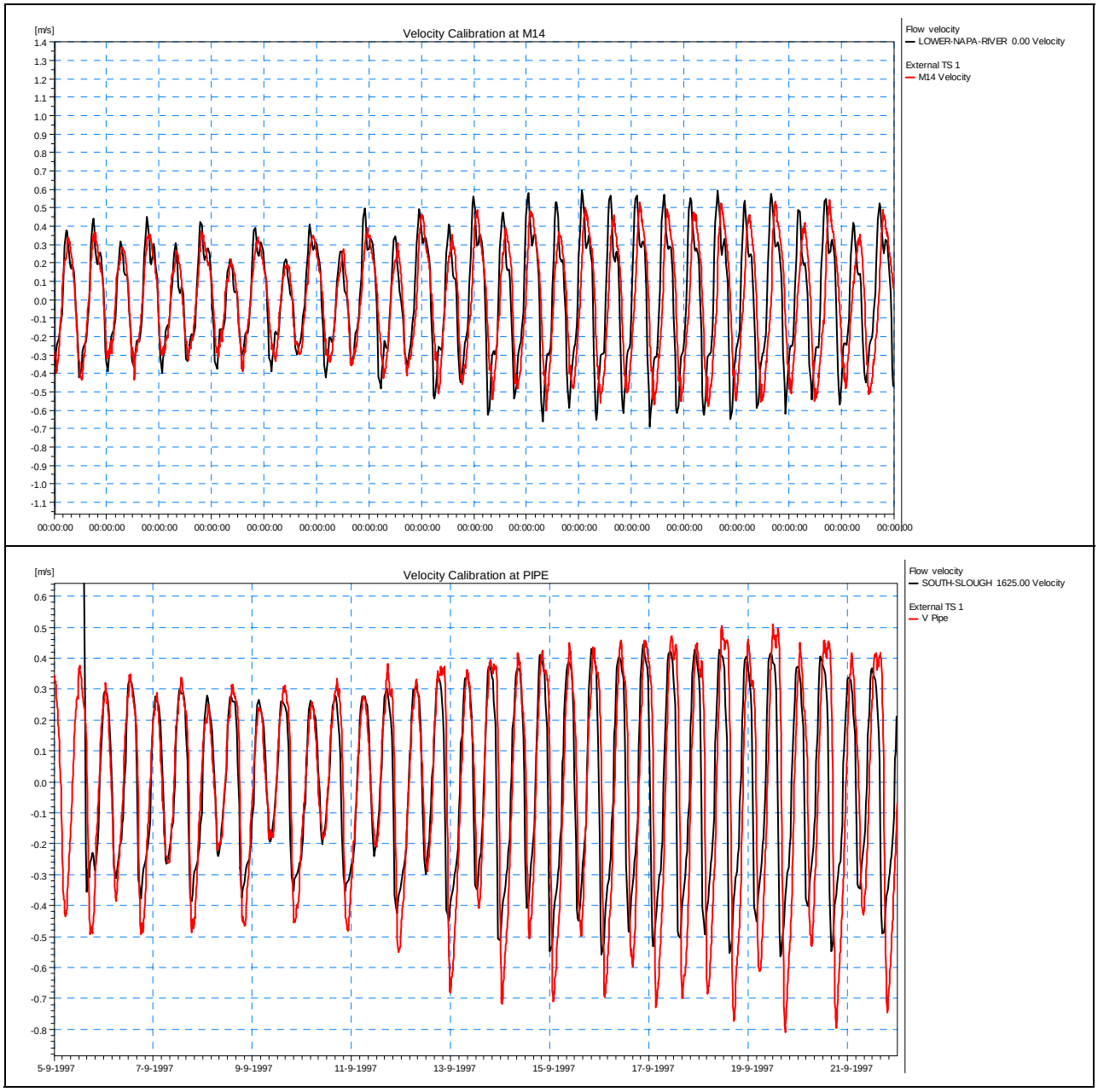

Figure 10b Velocity Calibration in September 1997 (M14, PIPE)

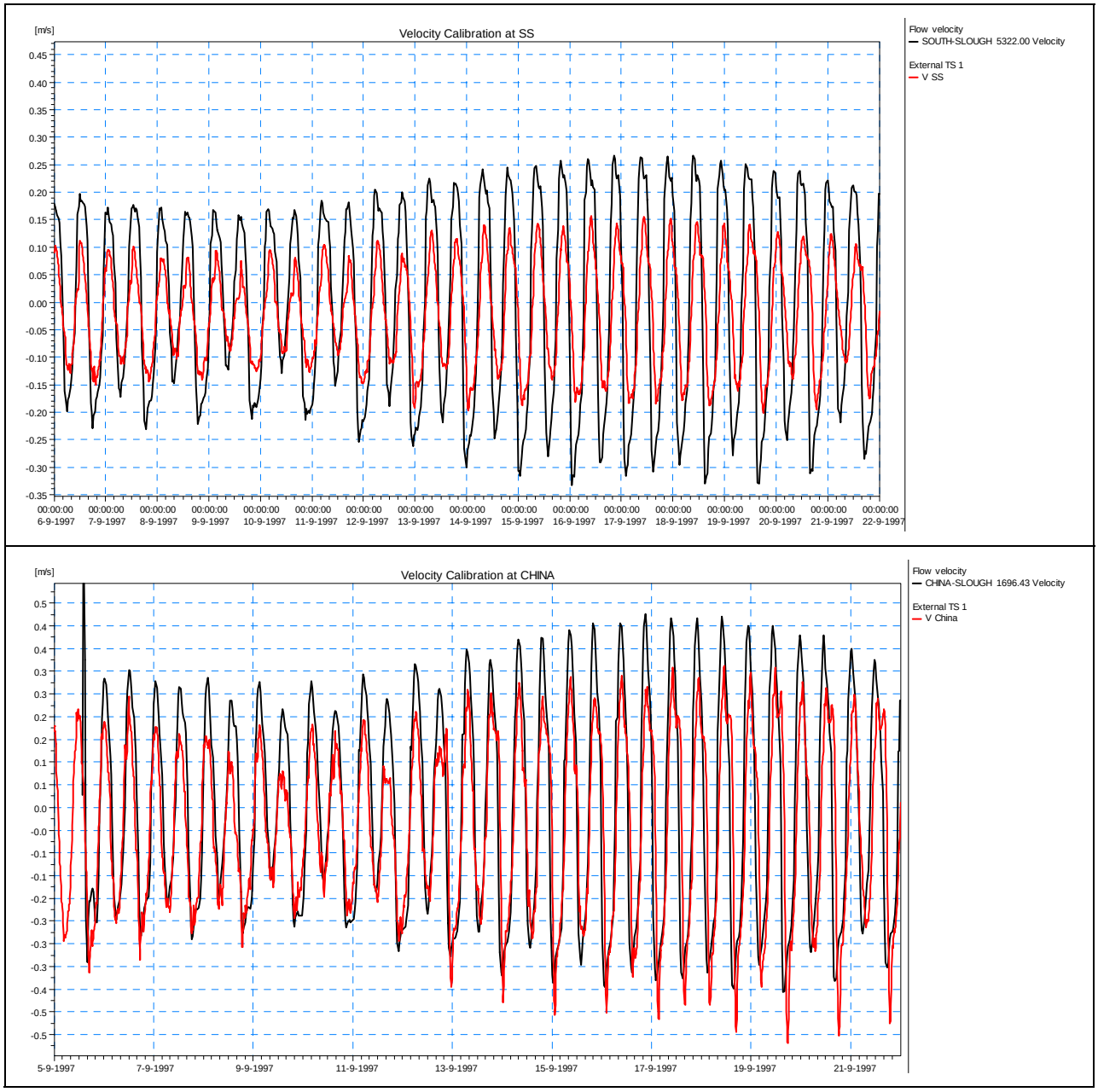

Figure 10c Velocity Calibration in September 1997 (Top to Bottom: SS, CHINA)

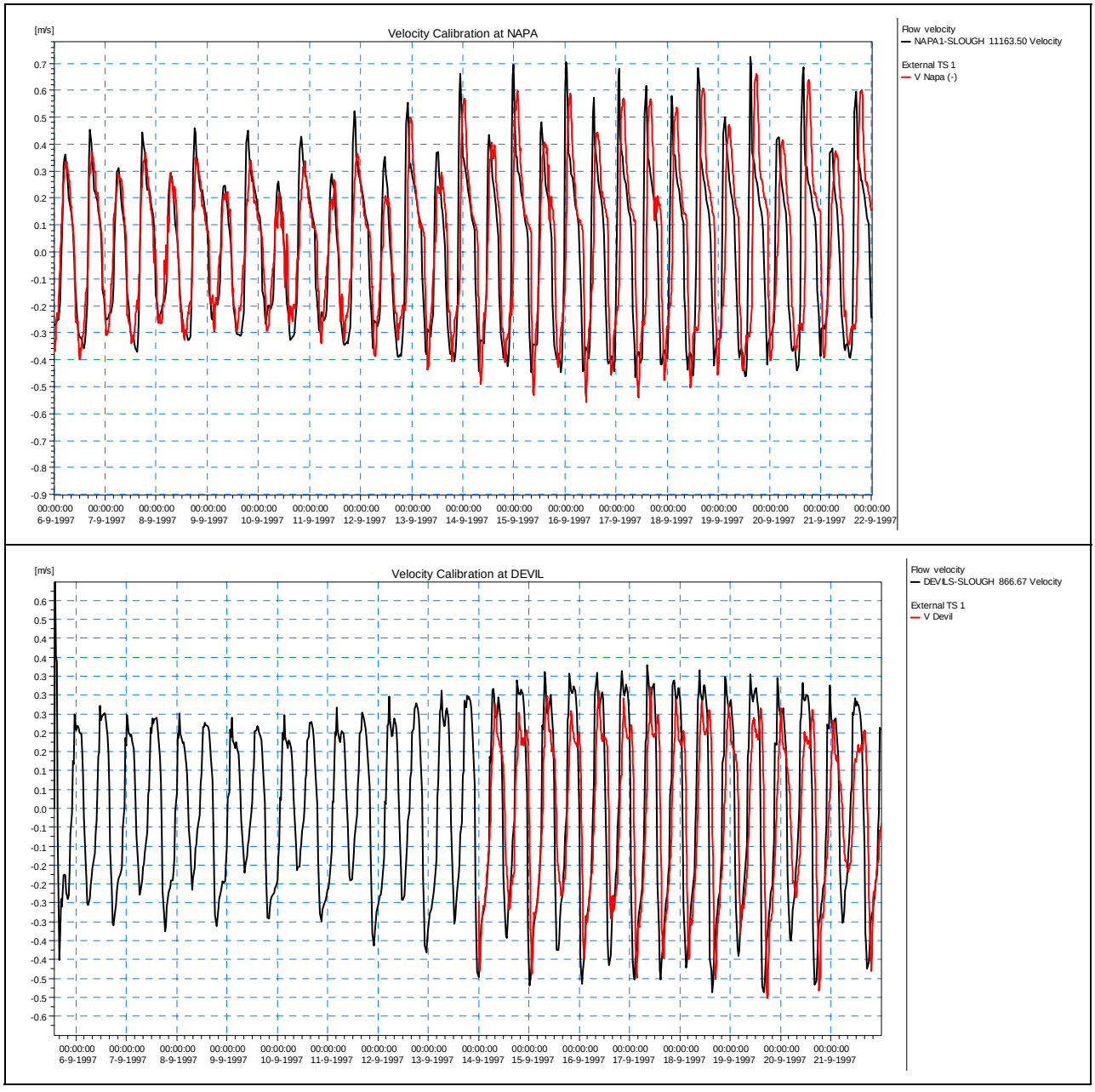

Figure 10d Velocity Calibration in September 1997 (Top to Bottom: NAPA, DEVIL)

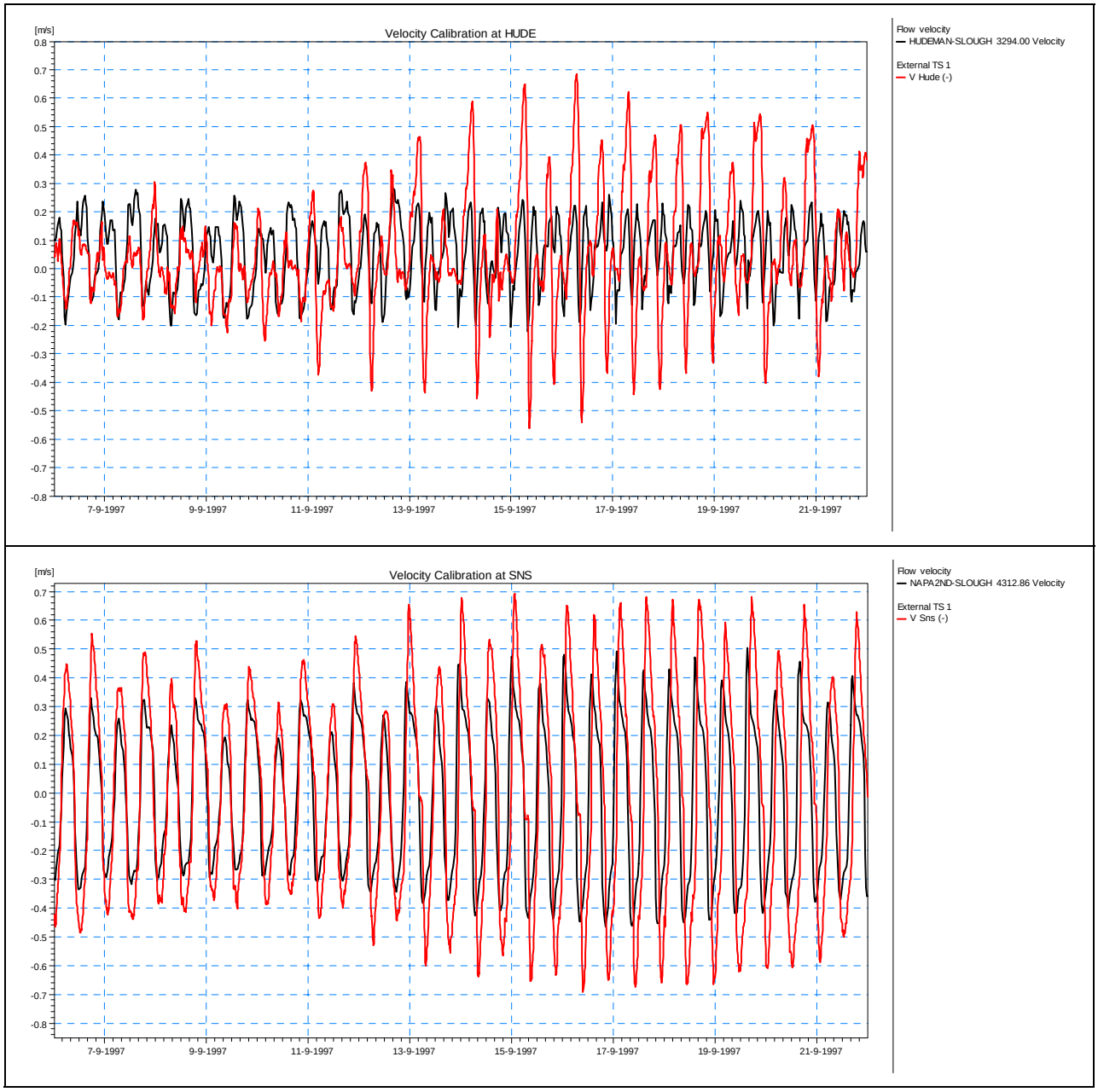

Figure 10e Velocity Calibration in September 1997 (Top to Bottom: HUDE, SNS)

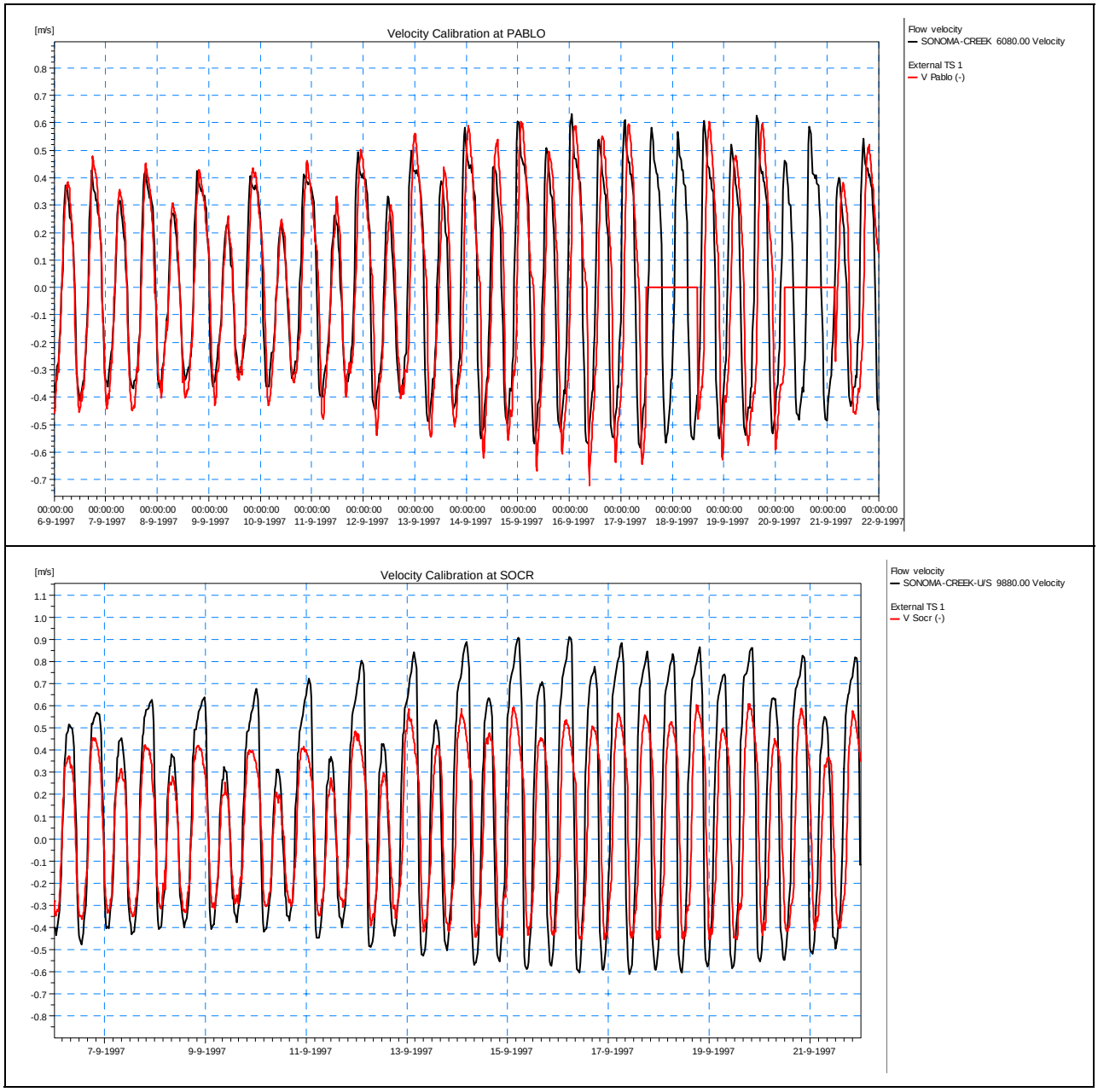

Figure 10f Velocity Calibration in September 1997 (Top to bottom: PABLO, SOCR)

9.1 BASE CASE FOR ALTERNATIVES EVALUATION

The Napa Plant Site project and the NSMR project will both affect the hydrodynamics in the Napa River; therefore, it is necessary to make an assumption on the implementation schedule of the two projects. NSMR Pond 2A is already breached and restored. Construction has begun (Fall 2005) on Ponds 3, 4, and 5 and they will probably be restored by the end of 2006. Breaches have already been introduced to Pond 3 at South Slough and Dutchman Slough, whereas NSMR ponds 6 to 8 are still in the planning phase (Susanne von Rosenberg, pers. comm.). Tidal restoration of Cullinan Ranch is also not expected to take place in the near future. Therefore, the base case condition assumed for this study includes the breached Ponds 2A, 3, 4 and 5 on the western side of the Napa River, represented as one-dimensional river branches as shown in Figure 11.

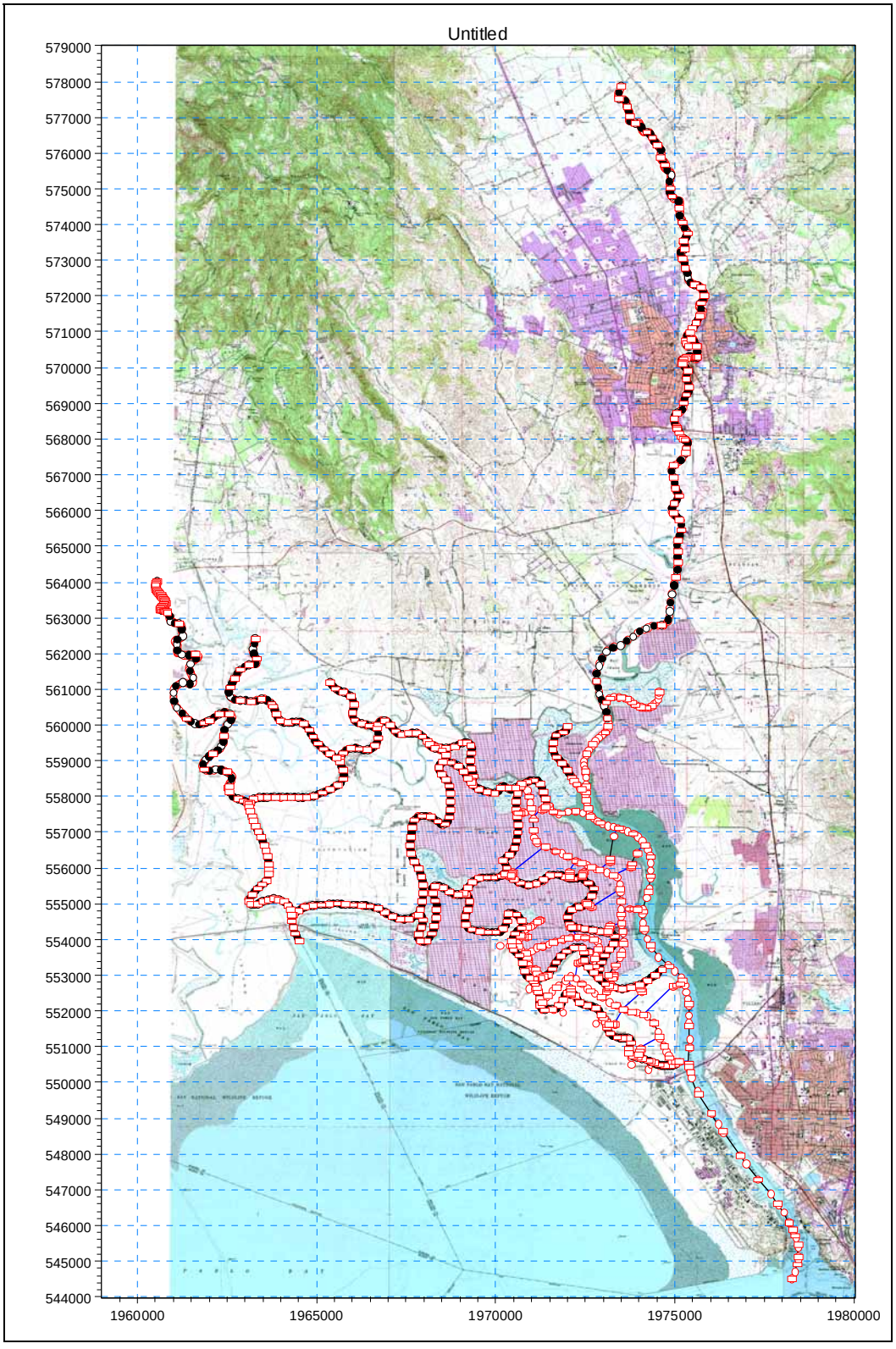

Figure 11 Model Setup for Base Case (Include Western Ponds 2A, 3, 4, and 5): Overview (Red squares indicating locations of cross-sections)

9.2 ALTERNATIVES SUMMARY

In addition to the "No Project" alternative, three project alternatives have been developed to evaluate costs, engineering feasibility and benefits associated with various potential project components and restoration strategies. Portions of the results from the modeling performed for each alternative will be used as selection criteria in the evaluation of the preferred alternative. Descriptions of the restoration alternatives are summarized below.[(1)]

- Alternative 1 – Full Tidal Restoration: This alternative would restore tidal action to all Napa Plant Site salt ponds. This alternative maximizes the potential for restoration of tidal marsh habitat. Figure 12 shows the proposed extent of the tidal boundary for Alternative 1.
- Alternative 2 – Tidal Restoration and Managed Ponds: This alternative would restore tidal action to a portion of the salt ponds and would maintain a managed pond. This alternative has the potential to restore large areas of tidal marsh habitat, and maintain a managed pond for waterfowl and shorebird habitat. Figure 13 shows the proposed extent of the tidal boundary and managed pond for Alternative 2.
- Alternative 3 – Tidal Restoration, Managed Ponds and Playa: This alternative would restore tidal action to a portion of the salt ponds, retain some managed pond, and allow some ponds to seasonally flood and dry as a function of natural hydrology and climate patterns (i.e., playa). This alternative has the potential to restore significant tidal marsh habitat, create seasonal wetland habitats that can be managed for waterfowl and shorebirds, and provide playa habitat for landscape diversity. Figure 14 shows the proposed extent of the tidal boundary, managed pond, and playa for Alternative 3.

Alternatives will be refined during the scoping and environmental permitting process.

[(1)] When using this document in conjunction with the project's environmental impact report (EIR) the reader should be advised that the alternatives are numbered differently in the EIR, as follows:

Alternative 1 in Modeling Tech Memo = Alternative 1 in EIR
Alternative 2 in Modeling Tech Memo = Proposed Project in EIR
Alternative 3 in Modeling Tech Memo = Alternative 2 in EIR

Figure 12 Alternative 1

Figure 13 Alternative 2

Figure 14 Alternative 3

Alternative 1 restores tidal conditions in all the ponds within the Napa Plant Site. Fagan Slough is one of the potential conveyances to bring tidal water to Ponds 9 and 10, which are located in the northern part of the Napa Plant Site (see Figure 12). Additional breaches along the Napa River are required to inundate the ponds south of the railroad. A two-dimensional model of the salt ponds was connected to the one-dimensional model of the River and Fagan Slough. This model was used to assist in designing the breach sizes and locations, and to predict the wetting and drying cycle for the wetland restoration areas. Using a two-dimensional approach provides flexibility for the design of internal channels and biological assessment.

For the two-dimensional model (MIKE21) used to simulate the ponds, the Manning's n values were assigned based on the anticipated future habitat types. Spatially variable Manning's n coefficients can be used to distinguish the different roughness in the internal slough, tidal marsh, and upland areas. In the case of tidal ponds, medium dense vegetation is anticipated to occur within a few years after the site is opened to tidal inundation. Since the vegetation height exceeds the water depth, high frictional loss is expected as the water moves through the wetland and hence a Manning's n of 0.04 to 0.08 is proposed. A lower roughness value of 0.025 is adopted for the internal sloughs.

10.1 BREACH SIZE ANALYSIS

The restoration of tidal conditions to the salt ponds relies on tidal characteristics and availability of tidal water from the Napa River and on the size of breach opening that will be created in the existing levees. The breach size has a critical role in the inundation characteristics of the ponds as it controls the amount of water entering the Site as well as the rate of water draining through it. On the other hand, the potential maximum volume of water that can be delivered to the Site is a function of the tidal prism.

Empirical relationships have been developed between the tidal prism and the size of the breach and/or channel (PWA, 1995, URS 2003) based on data collected from a number of wetlands. Figure 15 displays a correlation plot of diurnal tidal prism versus channel cross-sectional area with datasets compiled from wetlands in north San Francisco Bay and coastal wetlands in California. The diurnal tidal prism is the volume of water between Mean Higher High Water (MHHW) and Mean Lower Low Water (MLLW) in a marsh system, and is commonly used for systems with semidiurnal tides, such as those in California. In reality, the sizing of breach is also influenced by the sediment size, vegetation, and the marsh age. Nonetheless, these relationships can be used to obtain an estimate of the order of magnitude of the breach size.

Figure 15
Empirical Relationships between Potential Diurnal Tidal Prism and Breach Cross-Sectional Area

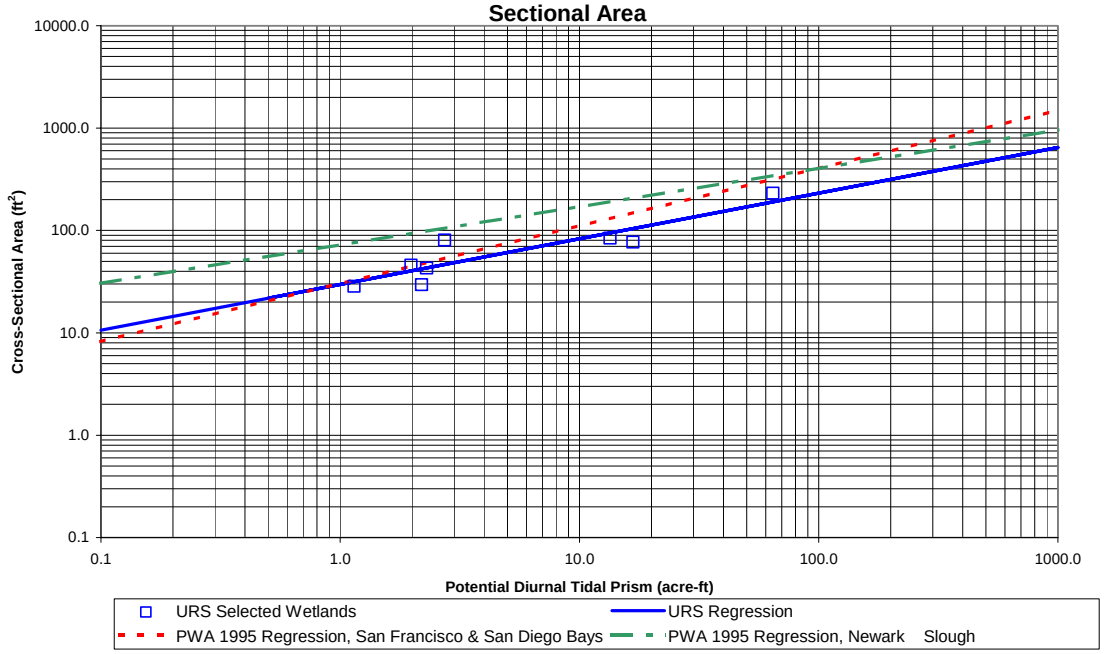

The Site was historically divided into a number of ponds for salt production through the construction of internal levees. Partial removal of these internal levees is required to allow free exchange of tidal water among individual ponds. On the other hand, connection of the ponds is constrained by the existing topography of the Site and the need to maintain the structural integrity and flood protection requirement of the railroad that traverses the northern part of the Site. Therefore, the Site is divided into three sub-areas for the evaluation and design of tidal restoration.

- Sub-area 1: ponds 9 and 10 (North Unit in EIR)
- Sub-area 2: ponds W1, W2 and W3 (Central Unit in EIR)
- Sub-area 3: all crystallizer beds 1 through 9, ponds B-1, B-2, B-3 and unit 3 (South Unit in EIR)

The external breach locations for these sub-areas are indicated by the schematic in Figure 16. Internal pond connection locations have been selected to match proposed internal slough alignments and connect other existing pond areas as required to meet the goals of each Alternative.

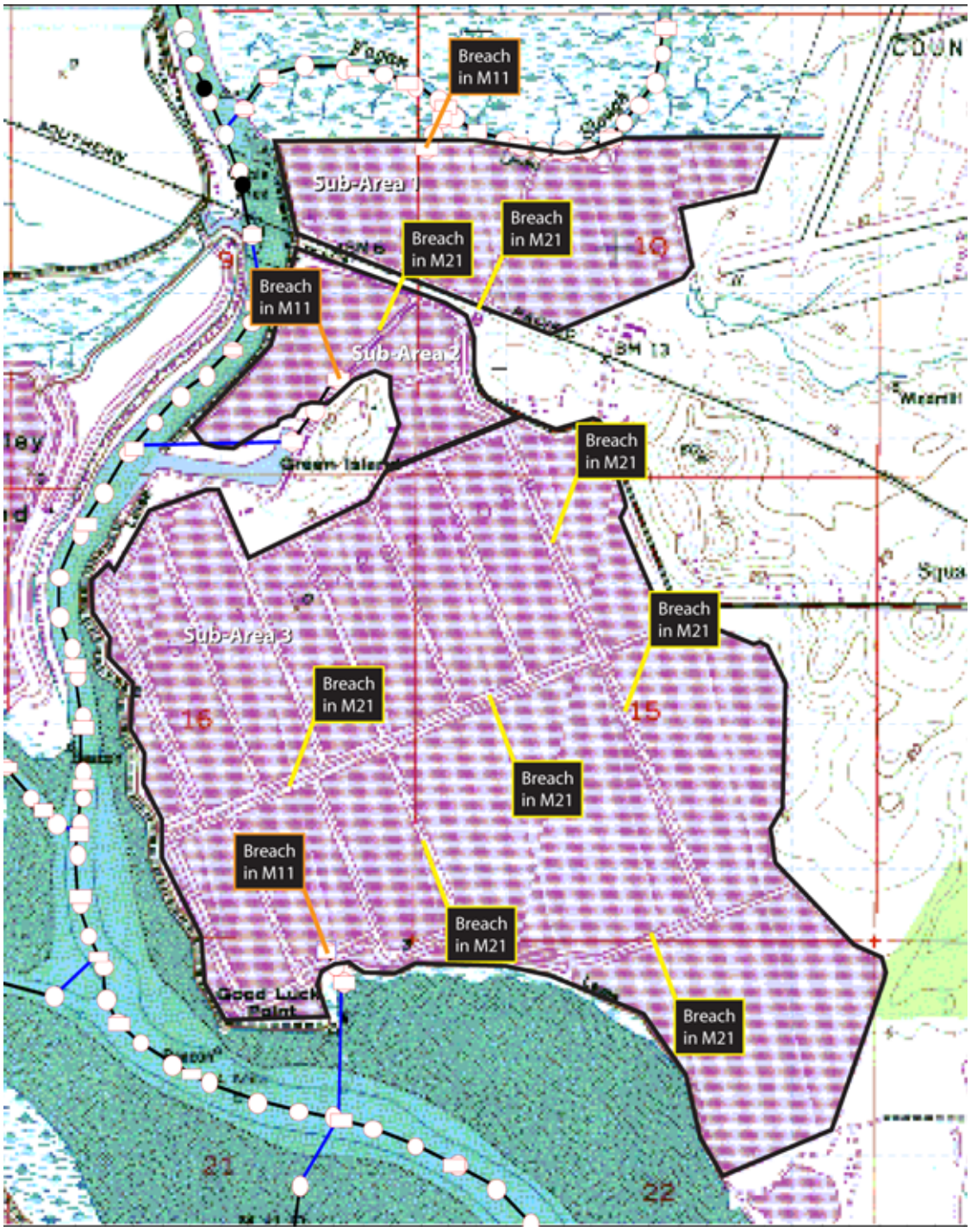

Figure 16 External Breach Locations for Alternative 1: All NPS Ponds Tidal (M11 refers to MIKE11 model and M21 refers to MIKE21 model)

The physical properties of these sub-areas are summarized in Table 2. The mean elevation of the marshplain was estimated using the DTM created for the Napa Plant Site. Area above MHHW is not inundated under normal tidal conditions, and as such is not included in the calculation of tidal prism.

There is an existing stockpile of sediments bordering the southern perimeter of sub-area 2. For the purpose of modeling, it was assumed that the sediments would remain in place so that a channel would need to be dredged from the barge channel to bring tidal water into the site. Accordingly, the area presented in Table 2 did not include this part of the upland area. If this upland area in pond W1 is to be excavated down to the marsh plain elevation of approximately 2.5 feet NAVD88, which involves a removal of approximately 185,000 CY of sediments, the inundation area would be larger than that indicated in Table 2, and the resulting increase in tidal prism in the Napa River would be correspondingly increased.

Table 2
Tidal Properties of Sub-Areas for Alternative 1

Sub-Area	Area below MHHW (acres)	Mean Elevation (ft, NAVD88)	Diurnal Tidal Prism (acre-feet)	Channel Area from Empirical Relationship (ft^2)
1	175	2.6	455	1,000
2	80*	3.5	136	500
3	925	2.7	2313	2,000

* Does not include W1 upland area that will most likely be graded down in proposed design

Initial breach locations were selected to approximate historic tidal channel locations. For sub-area 1, the breach location was selected on the southern levee of Fagan Slough bordering Ponds 9 and 10, while for sub-area 2, the breach location was selected along the southern edge of Pond W1, within the existing inlet area, to bring water into the Site. Two breaches were specified for sub-area 3. A breach was specified at the location of the historic channel opening into crystallizer bed 8 and into pond B-3.

To determine the optimum breach dimensions, the width and depth of the breaches were varied and the effects on the inundation extent and hydroperiod were evaluated. The different breach configurations considered are shown in Table 3 as options A, B and C. In sub-area 1, options A and B have the same breach dimensions. In view of the relatively small size of sub-area 2, the breach dimensions were kept constant under all three options. The maximum size of each breach was determined from the empirical relationships shown in Figure 15. The invert elevation of the breach in sub-area 3 under Option A was chosen to match the existing mudflat elevation bordering the southern perimeter of sub-area 3, whereas a deeper breach was assumed under Options B and C. It is assumed that a channel would naturally form through the mudflat to accommodate the flow from the deeper breach.

Table 3
Analysis of Breach Size for Alternative 1

Breach Configuration Option	Sub-Area 1 breach			Sub-Area 2 breach			Sub-Area 3 primary breach		
	Width (ft)	Depth[a] (ft)	Area (ft^2)	Width (ft)	Depth[a] (ft)	Area (ft^2)	Width (ft)	Depth[a] (ft)	Area (ft^2)
A	200	2.3	450	200	3	600	200	3.6	700
B	200	2.3	450	200	3	600	330	4.3	1400
C	330	3.3	1100	200	3	600	660	4.3	2800

a = depth below existing grade

The areas inundated at Mean High Water (MHW) for the three options are shown in Figures 17a through 17c. The whole Site is essentially inundated daily during the flood tides for all three options regardless of the size of the breaches since the pond bottom elevations are fairly low as a consequence of land subsidence over the years. Also, the bathymetry is relatively uniform with the exception of sub-area 2, which includes some upland areas. The average depth of water within the Site is approximately 2 feet at MHW and it increases slightly with the larger breach size. In the absence of defined flow paths within the Site, the water could not completely recede before the next tide came in and thus a significant portion of the Site remained submerged over the tide cycle, as illustrated in Figures 17a through 17c.

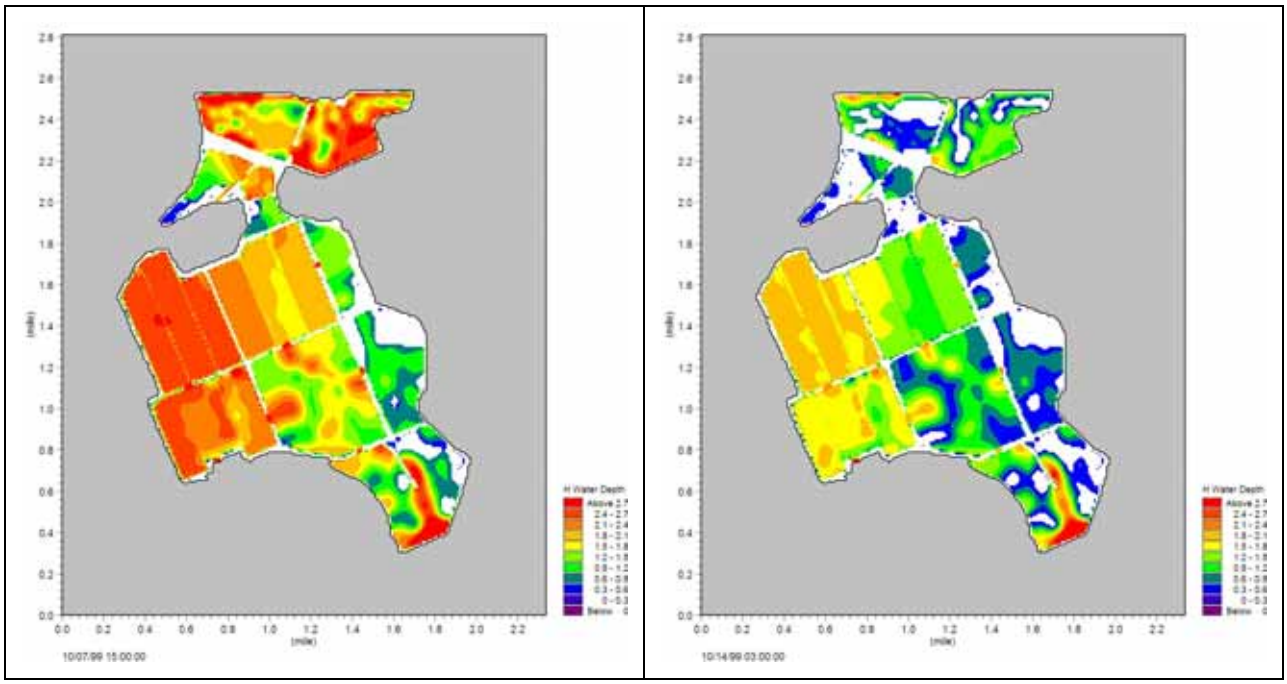

Figure 17a Inundation Depths for Breach Configuration Option A under MHW (left) and MLLW (right)

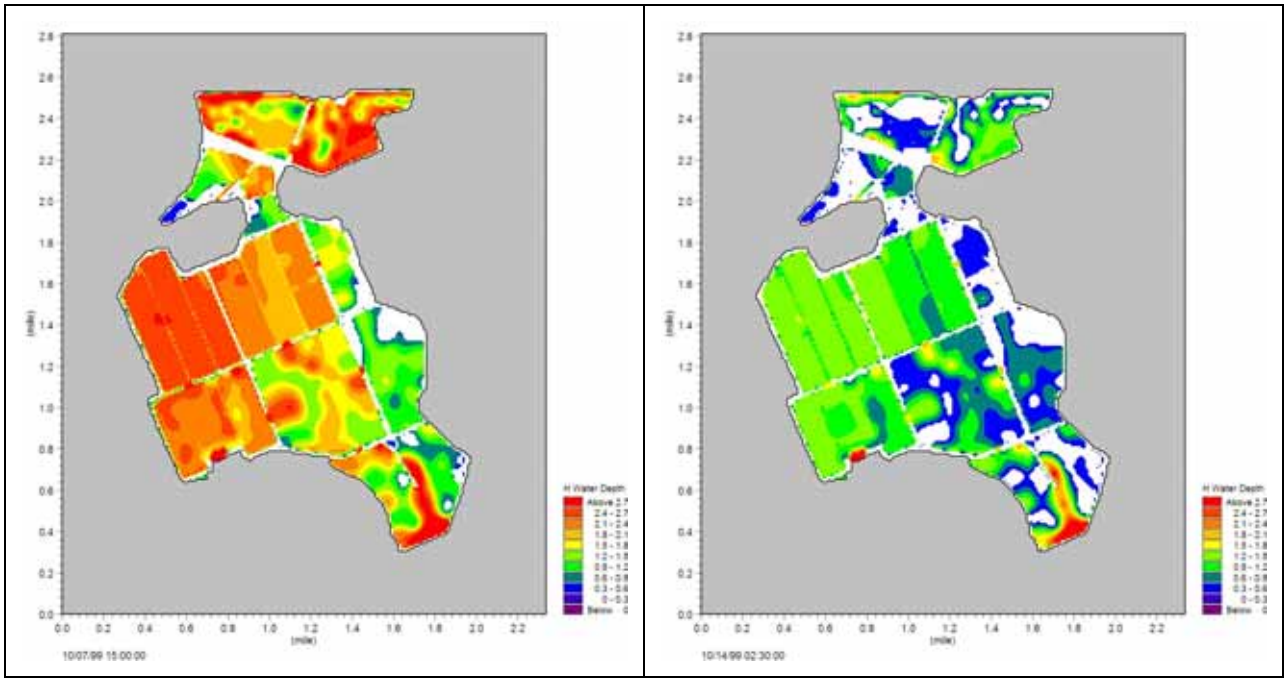

Figure 17b Inundation Depths for Breach Configuration Option B under MHW (left) and MLLW (right)

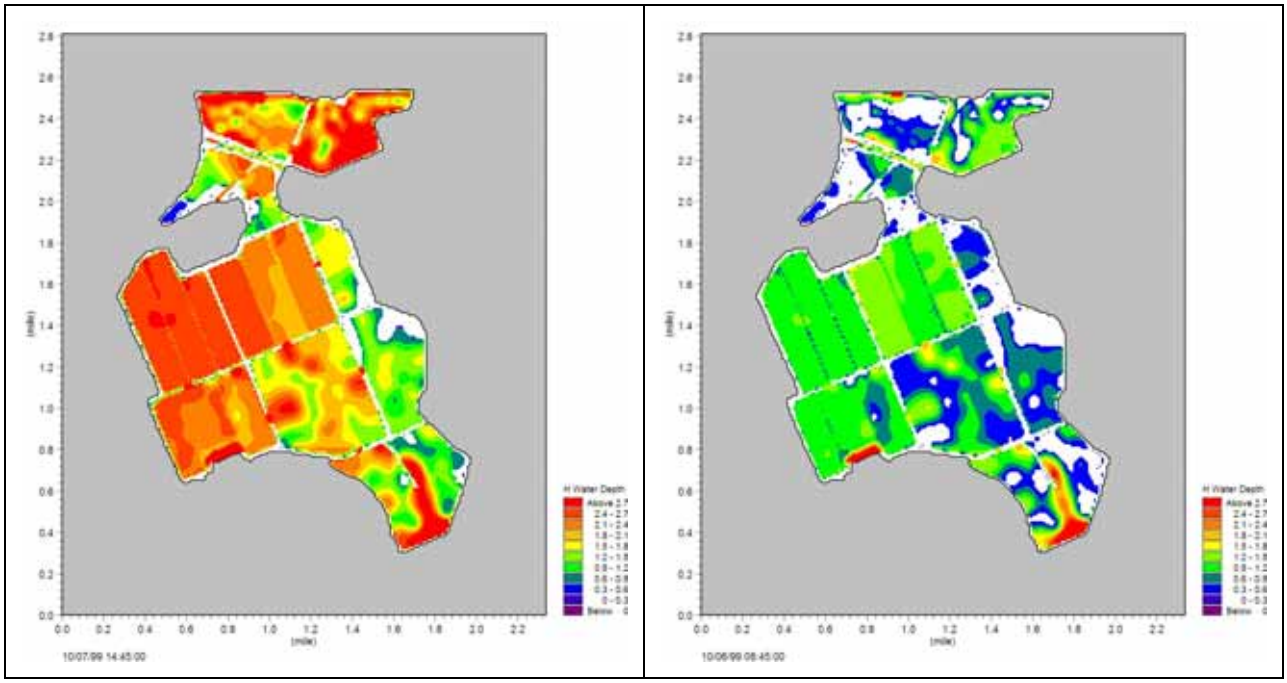

Figure 17c Inundation Depths for Breach Configuration Option C under MHW (left) and MLLW (right)

The ponding phenomenon is most prominent in sub-area 3 due to its large size. The time elapsed between the ebb tide and the succeeding flood tide is not sufficient for the water to travel through the Site owing to the large distance from the interior point to the outlet, as well as the high frictional losses on the marshplain. In contrast, the ponding water in sub-areas 1 and 2 primarily

occurs in the low-lying areas, which become disconnected as the water recedes. Therefore, the drainage in sub-area 1 exhibits no notable improvement when the breach cross-sectional area is more than doubled.

Alternatively, sub-area 3 drainage does improve with the larger breaches. The effect of the breach size on tidal flows through the opening of each sub-area is also assessed. As shown in Figure 18 (bottom), the discharge through the breach of sub-area 3 exhibits almost a two-fold increase as the breach area is doubled from 700 (Option A) to 1400 ft^2 (Option B). However, as the breach area increases further to 2800 ft^2 (Option C), it only leads to a slightly larger inflow (positive discharge in Figure 18) during the flood tides while the outflow during the ebb tides (negative discharge in Figure 18) shows a moderate increase. The discharge for Option C during both the flood and ebb tides is about 4500 cfs, similar to the average inflow/outflow estimated from the potential diurnal tidal prism. The results therefore indicate that the breach area provided in Option C is not a constraint in the drainage efficacy, and that internal sloughs are necessary to enhance the drainage through the ponds.

In the case of sub-area 1, the increase in breach cross-sectional area from 450 to 1100 ft^2 has a negligible impact on the discharge during either the flood or ebb tides (as can be seen where the three discharge time series align with one another on Figure 18 (top), with the discharge being approximately 900 cfs, similar to that estimated from the potential diurnal tidal prism. Hence, in order to achieve better wetting and draining, internal sloughs would be required to drain the low-lying areas.

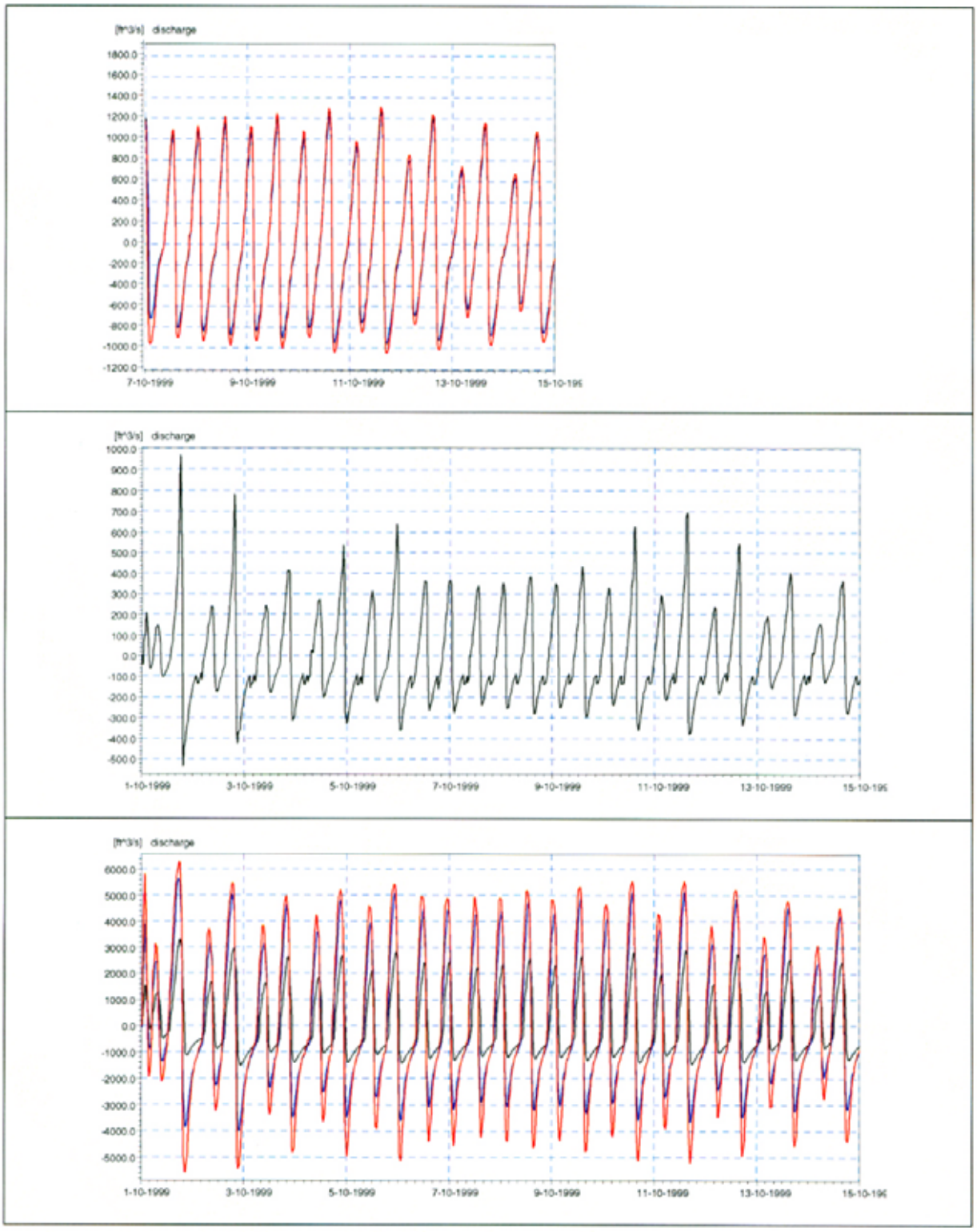

Figure 18 Tidal Flows through the Breaches in Sub-area 1 (top), Sub-area 2 (middle) and Sub-area 3 (bottom) for Options A (black line), B (blue line) and C (red line)

For sub-area 2, where the breach size was not increased for the various options, all discharge time series are in alignment with one another.

10.2 INTERNAL CHANNEL EVALUATION

The design of an internal channel network within the restored wetland requires the following considerations: channel cross-sectional geometry, branching or the order of channels, density of channels, as well as the length and sinuosity of individual channel segments. These parameters, with the exception of cross-sectional geometry, are collectively known as the planform of the channel system.

The cross-sectional shape of the channel is dependent on the physical properties of the bottom sediment and the marsh vegetation, and the hydraulic properties of tidal flows in the channel which govern the bed shear stress and in turn the sedimentation process. The detailed geometry (e.g. trapezoidal cross section) of the internal sloughs cannot be resolved by the 20-m grid used for the two-dimensional model, therefore a nominal channel width is adopted for specifying the channel dimensions in MIKE21. In practice, trapezoidal channels can be constructed with side slopes as determined by the shear strength of the sediments. Total wetland area influences the density and order of the channel network. In general, the larger the area, the denser the network with higher order channels that will be required to provide adequate drainage. The length and sinuosity of a channel usually increase with the order of the channel as the system develops over time (PWA, 1995).

Although the geomorphology of the channel system is expected to self-evolve under the influence of nature, the potential for success for the restoration project will be higher if the system is designed to function as closely as possible to that of a natural system under the particular tidal regime. Therefore, the historic sloughs that existed on the site prior to diking were identified and adopted as the guide for the design of the channel network for Alternative 1. It is also believed that the bottom sediments along the historic sloughs would be less consolidated than the surrounding marshplain and hence there would be a better chance for the channel system to evolve to its quasi-equilibrium form by excavating along the pre-existing alignment. The in-situ shear vane tests undertaken at the NSMR ponds 3,4 and 5 indicate that the shear strength is generally below 8kPa at the historic slough channels, substantially weaker than the marshplain's shear strength of 15 kPa. These tests also indicate that the surface sediments are very soft and mud-like (PWA 2002b). Laboratory analysis results of the sediment cores further confirm that the sediments in the historic slough channels have lower dry densities, which in turn lead to lower critical shear stress, facilitating erosion.

Two internal channel options were evaluated, as shown on Figure 19a and 19b: option D includes two channel systems in sub-area 3 (with an additional breach in pond B3), and option E extends the channel in sub-area 3 further and also incorporates a channel network in sub-area 1. The modeled width of the channel ranges from 60 feet to over 300 feet for the higher order sloughs, near the mouth. The inundation plots for the two channel options under MHW and MLLW are presented in Figure 19.

As in the previous options, the entire Site is inundated during the flood tides. The inclusion of internal channels in sub-area 3 under Option D drastically improves the drainage characteristics, with ponds B1, B2, B3 and unit 3 almost completely drained under MLLW. This means these ponds will be intertidal with cyclical wetting and draining on a daily basis. The addition of

bifurcations and lower order channels to the primary channel in sub-area 3 enlarges the intertidal area and reduces the depth of water in the ponds that remain submerged during the ebb tides. The area that becomes exposed in sub-area 3 under MLLW increases from 15% of the total marsh area for Option C to almost 50% for Option E. Significant improvement in drainage is also achieved in sub-area 1 in the presence of the internal sloughs, with the exposed area under low tides increased from 32% to 54% between Options C and E.

With regard to tidal flows, the discharge through the breach at sub-area 1 is not altered by the internal channels. In contrast, the tidal exchange is increased by about 40-50% from earlier options (A, B and C) in sub-area 3 in the presence of a channel network such as the one modeled in Option E, suggesting that the channel system increases the ability to drain the ponds.

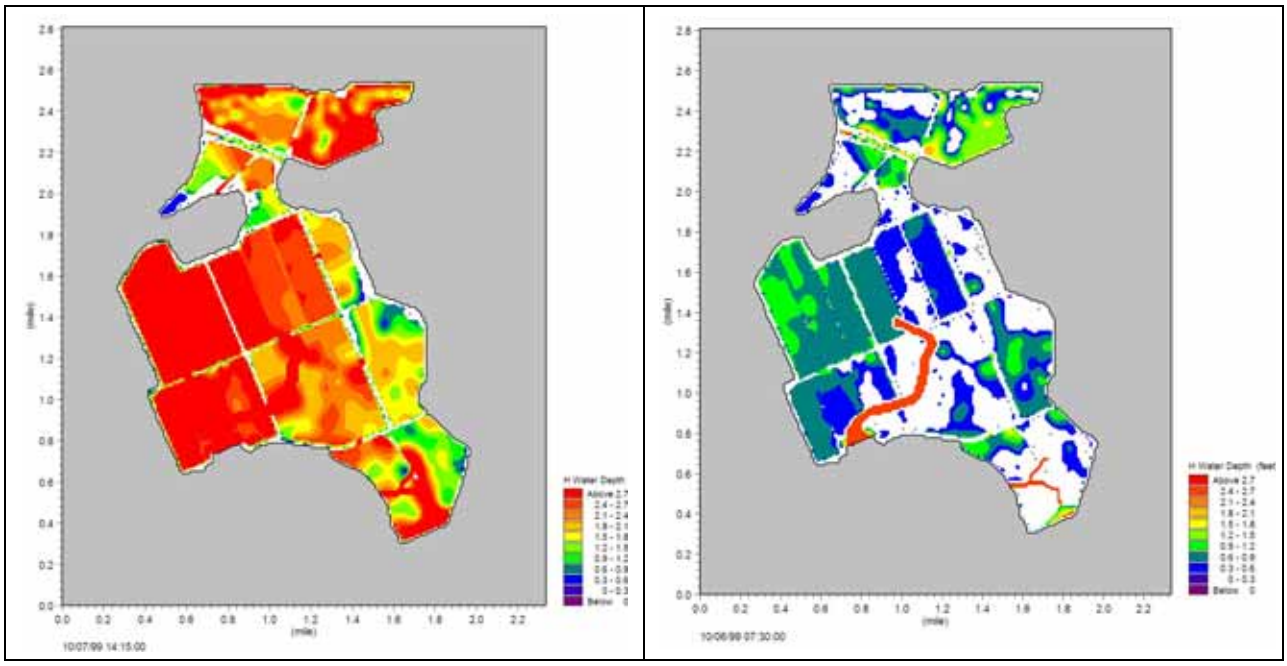

Figure 19a Inundation Areas for Option D under MHW (left) and MLLW (right)

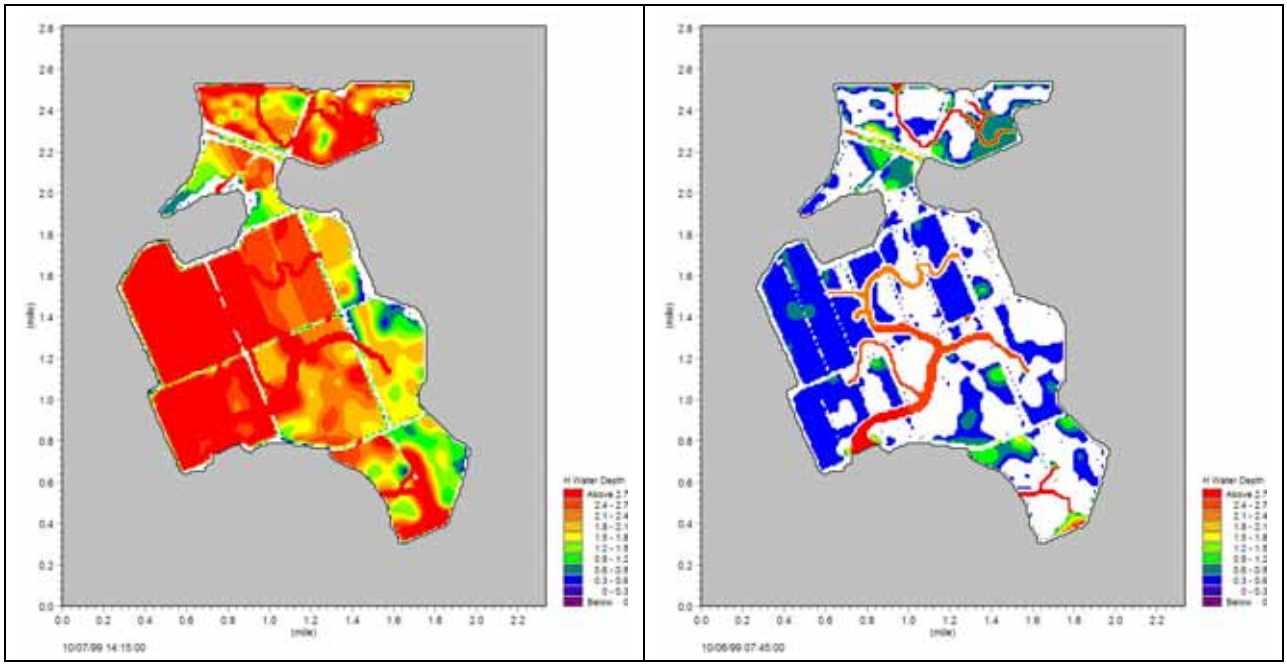

Figure 19b Inundation Areas for Option E under MHW (left) and MLLW (right)

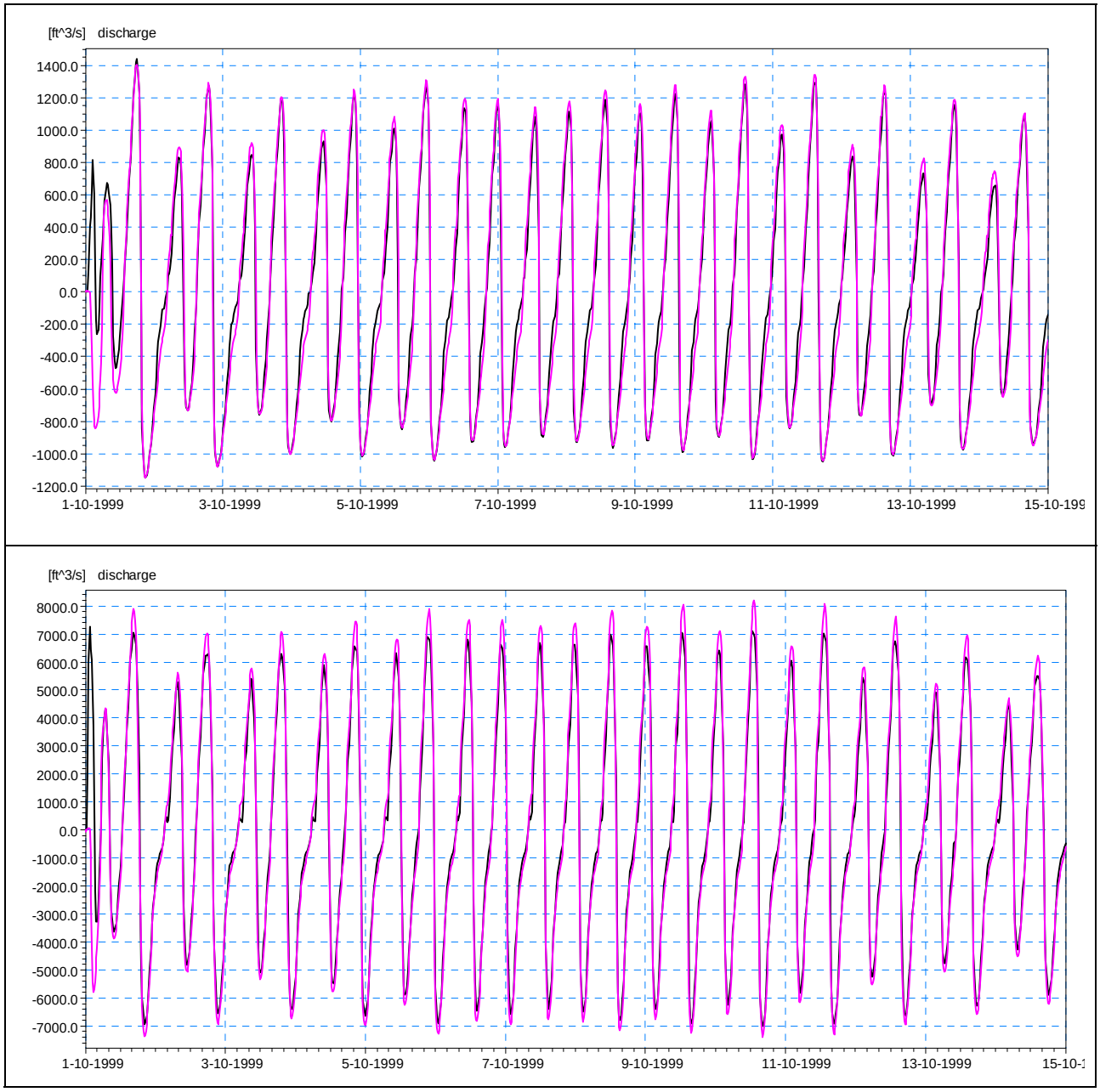

Figure 20 Tidal Flows through the Breaches in Sub-area 1 (top) and Sub-area 3 (bottom) for Options D (black line) and E (pink line)

10.3 RESULTS FOR NORMAL TIDAL CONDITIONS

This section describes the results from the dynamic modeling of normal tidal conditions for Alternative 1. Modeling normal tidal conditions (non-flood flows) uses input data from October 1999, as explained below. Based on the analysis of the breach size and evaluation of the channel configuration, Option E will be adopted for the subsequent modeling. The model grid is displayed in Figure 21.

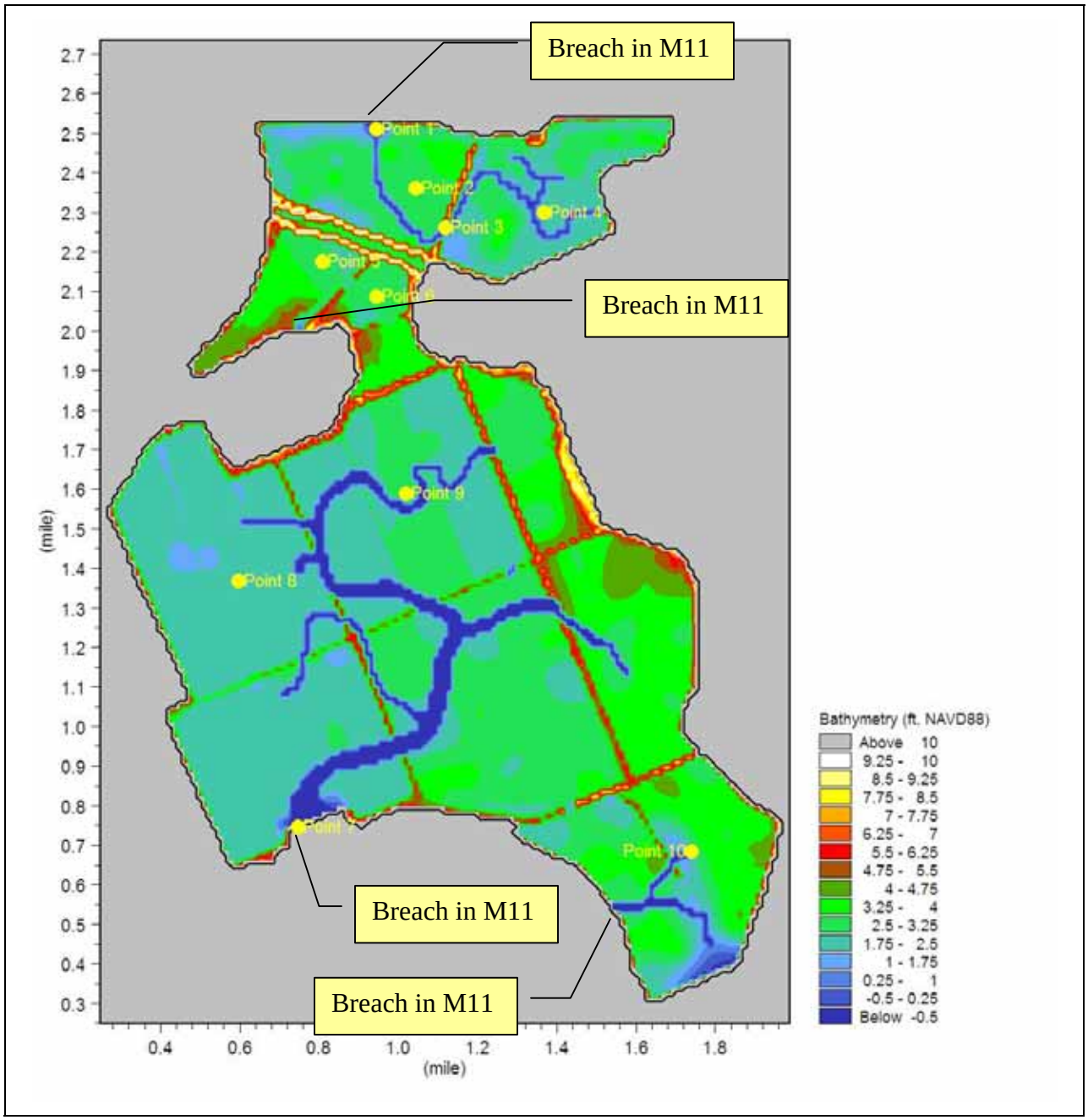

Figure 21 Model Bathymetric Grid for Alternative 1 (M11 refers to MIKE11 model)

Simulation was performed for normal tidal conditions since the resulting hydraulic regime within the Site will exert a dominating effect on the ecological system. A 2-week period covering a

complete spring-neap cycle in October 1999 was selected. The Napa River discharge was typical of the dry weather flow during this time of the year, ranging from 3 to 10 cfs (CDEC, Station ID: NAP). The results show that the entire Site is inundated twice daily by the two high tides (MHW and MHHW), and about half of the area is drained at least once a day under MLLW, as described in the previous section.

In addition to the inundation extent, the hydroperiod is also of interest for habitat assessment. The predicted tidal elevations at selected points (as shown in Figure 21) in each sub-area are plotted in Figure 22, along with the average elevation in the respective sub-area. There is negligible attenuation in the high tides in all 3 sub-areas, suggesting that the head is sufficient to move the water into the Site. In sub-area 1, there is also no marked attenuation in the low tide and the sub-tidal zone (as exemplified by Point 2), which is probably a reflection of the undulations in the pond's bottom elevation. On the other hand, the ebb tide lags the River in sub-area 2 because the tide is dampened due to frictional losses as they propagate through the higher marshplains. The low tide is also dampened in sub-area 3, but the dampening is much less pronounced than in sub-area 2. The tidal signal varies with the elevation, proximity to the breach or channel, and the local topography, resulting in different inundation characteristics within each sub-area. For instance, point 10 exhibits intertidal behavior essentially on every tide, while point 8 drains only once a day during certain periods of the simulation (during neap tides). On the other hand, point 9 is always submerged. These results indicate that the restored Site is likely to support a variety of habitats that will experience different tidal conditions.

The channel network is anticipated to continually evolve after the ponds are opened to tidal action. To simulate the potential tidal regime in the Site years after the restoration is complete, the internal channel network was assumed to expand with the emergence of more first order channels. Although the channel geometry would probably change over time as a result of erosion and accretion, it was not modified in the model run for the "future scenario" in view of the uncertainty in the geomorphological changes. Medium to dense vegetation would likely be established, leading to an increased surface roughness of the Site. Based on these premises, the 2-week normal tidal simulation was performed on the evolved bathymetry coupled with a higher Manning's n value of 0.08 in the marshplain. The inundation surface under MLLW is displayed in Figure 23, overlain by an image depicting both the present and historic landforms of the Site. The results indicate that the evolution of channels will gradually enhance drainage in the long term, and a larger portion of the Site will become intertidal.

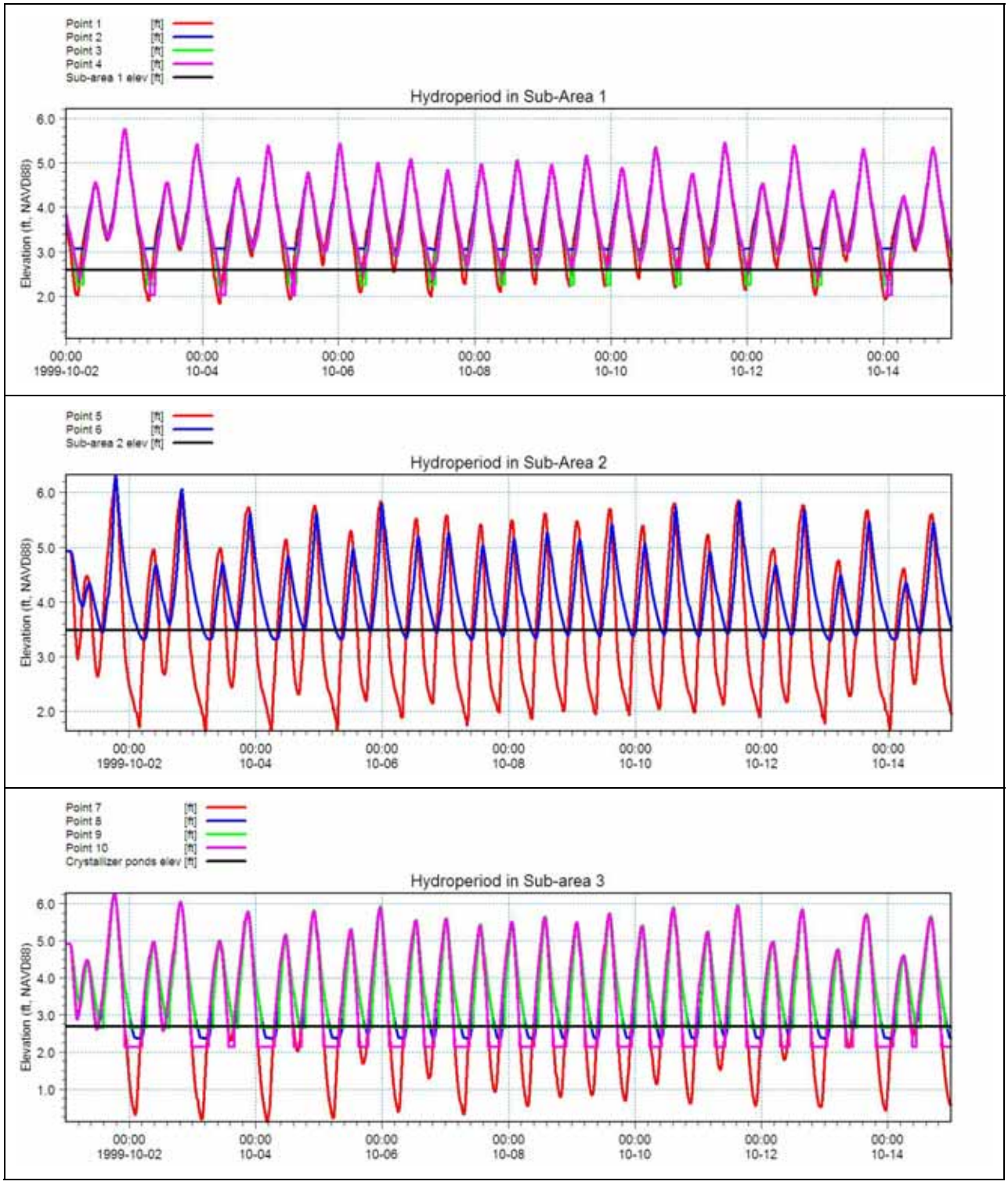

Figure 22 Predicted Water Surface Elevation for Alternative 1 Under Normal Tidal Conditions

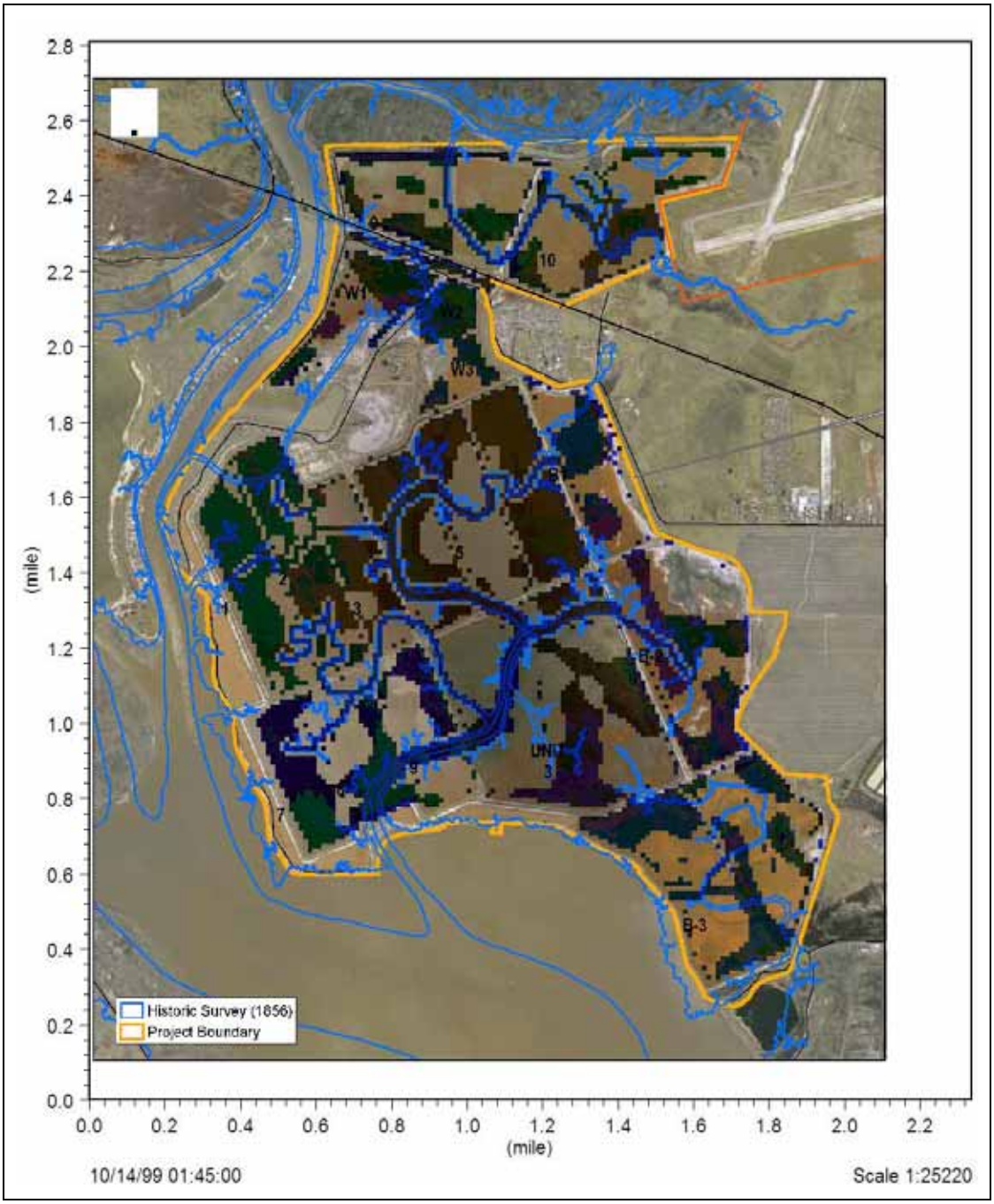

Figure 23 Postulated Inundation Surface under MLLW for Alternative 1 - Years After Restoration

Besides water level, current speed is also important to wetland restoration because it is strongly correlated with the rate of erosion and deposition and hence the sediment dynamics. The magnitude of the current will also affect the design of erosion control measures at the breaches. Depending on the nature of the tides, the current can be in phase with the tide (progressive wave) or out of phase (standing wave). Two maxima occur in a day. The current speed is dependent on the tidal prism as well as the bottom friction of the wetland. In general, the shallower the water, the greater the drag on the movement of water, and the lower the velocity. Figure 24 shows the average current speed inside the Site for Alternative 1, calculated as the root-mean-square (RMS)

velocity. RMS speed is presented rather than maximum speed since the tidally averaged speed has a more persistent influence on the sediment dynamics over the long term, as opposed to a one-time maximum value which may occur only once due to wind gusts, etc.

As expected, the current speed is highest at the breaches, and is on the order of 2 ft/s for the main breach of sub-area 3 where the discharge is largest. The current speed remains high along the internal channels, which convey the water in and out of the Site. On the marshplain, the speed ranges from 0.8 to 0.2 ft/s, and decreases with increasing distance from the channel. The lower velocity encourages the deposition of sediment as the tidal water spreads through the Site, thereby allowing gradual accretion over time. On the other hand, the higher velocity in the internal channels may lead to erosion and the subsequent deepening and widening of the sloughs.

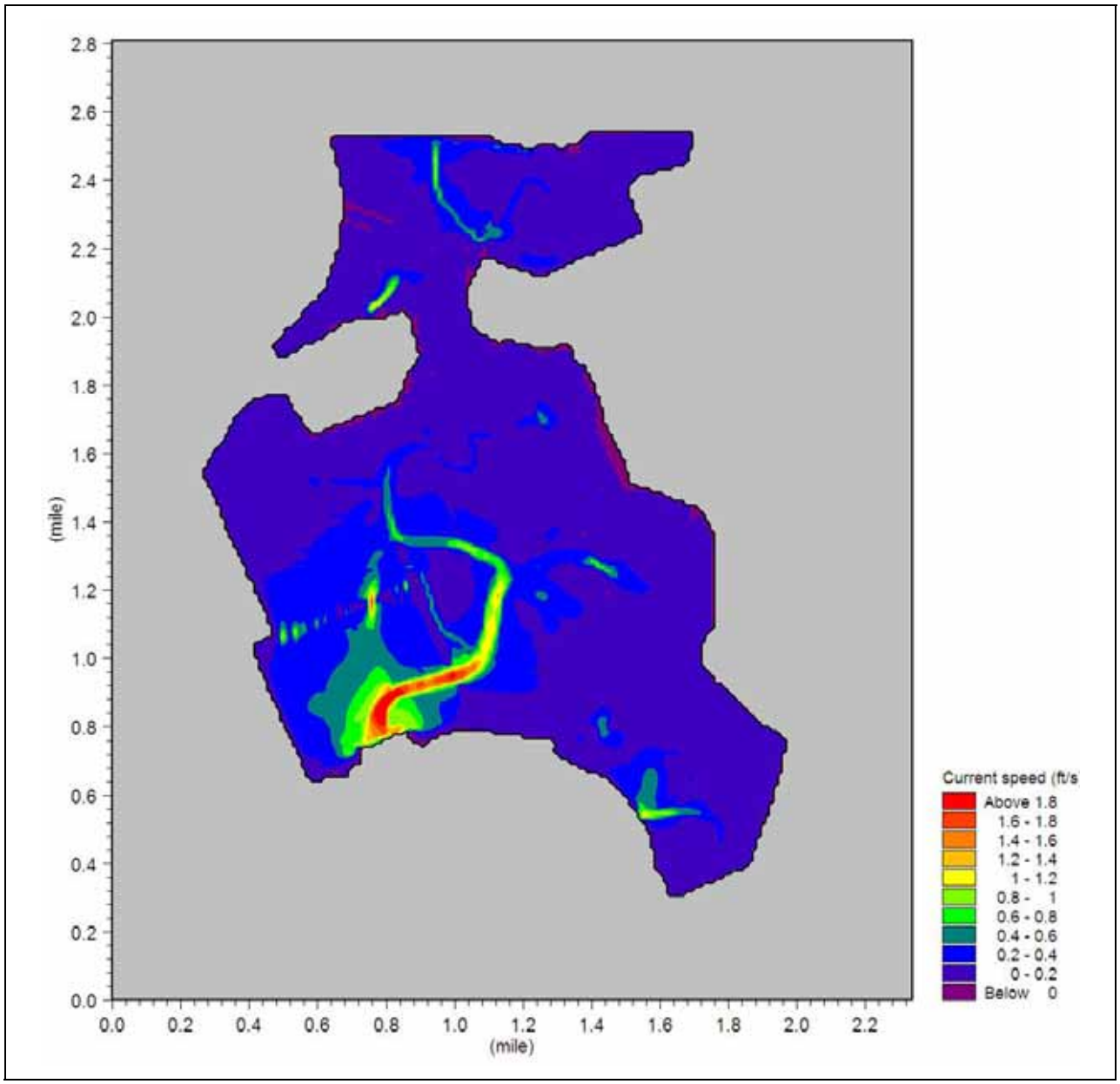

Figure 24 RMS Current Speed for Alternative 1

The tidal flows introduced to the Site will be accompanied by increased velocities in the Napa River at the breach locations. Comparison of current speed between Alternative 1 and the base case as presented in Figure 25 indicates that the velocities are increased to varying degrees in the river outside each of the breaches. The impact on velocity is greatest in Fagan Slough because there is only nominal flow in the slough prior to the restoration of ponds 9 and 10. After restoration of Ponds 9 and 10 the peak velocities in Fagan Slough will be about 8 to 10 times the pre-restoration velocities. On the other hand, the pre-project flow in the Napa River is already of appreciable magnitude, and thus the incremental tidal flows associated with the opening of the ponds only cause a 10% and 25% increase in root-mean-squared velocity in the Napa River at the breaches in sub-area 2 and sub-area 3, respectively. Among all the breaches, the current speed is highest in Fagan Slough because of its smaller cross-sectional area.

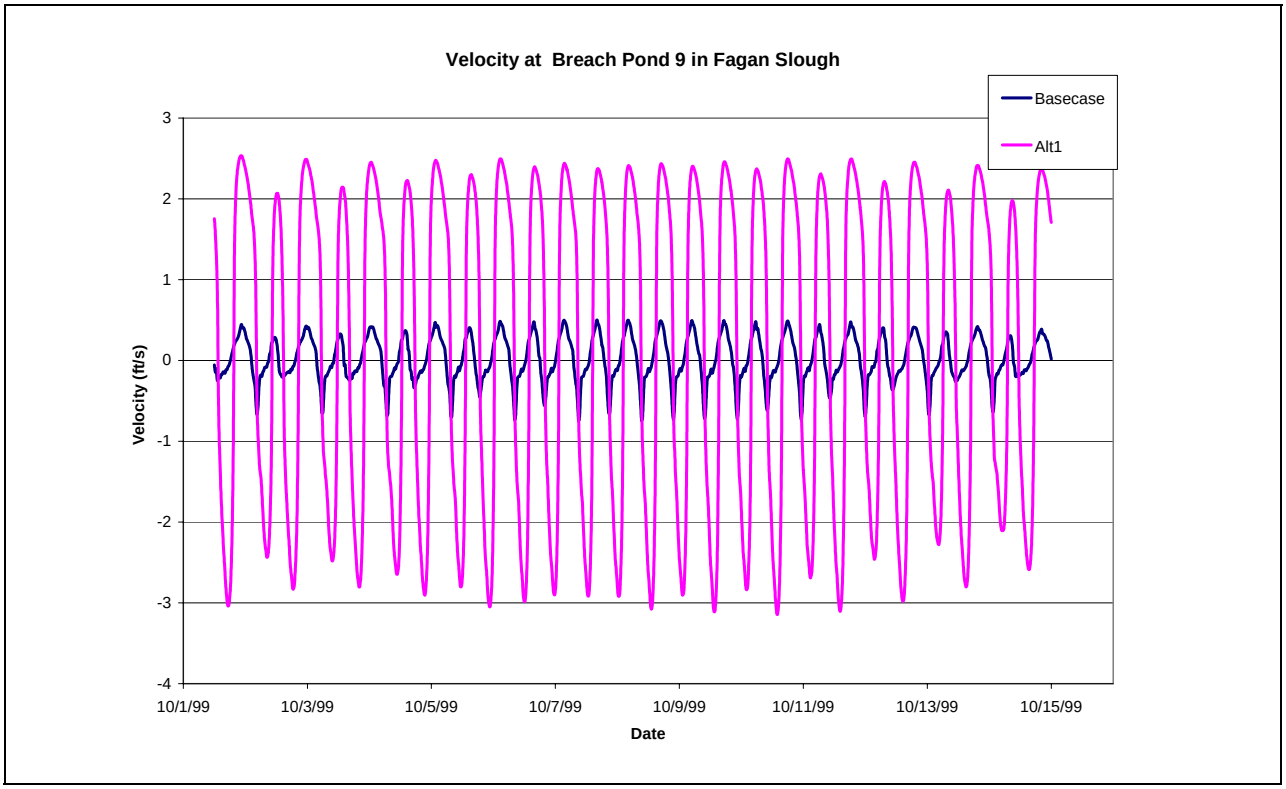

Figure 25 Comparison of Current Speed in Napa River and Fagan Slough between Alternative 1 and Base Case (continued on following pages)

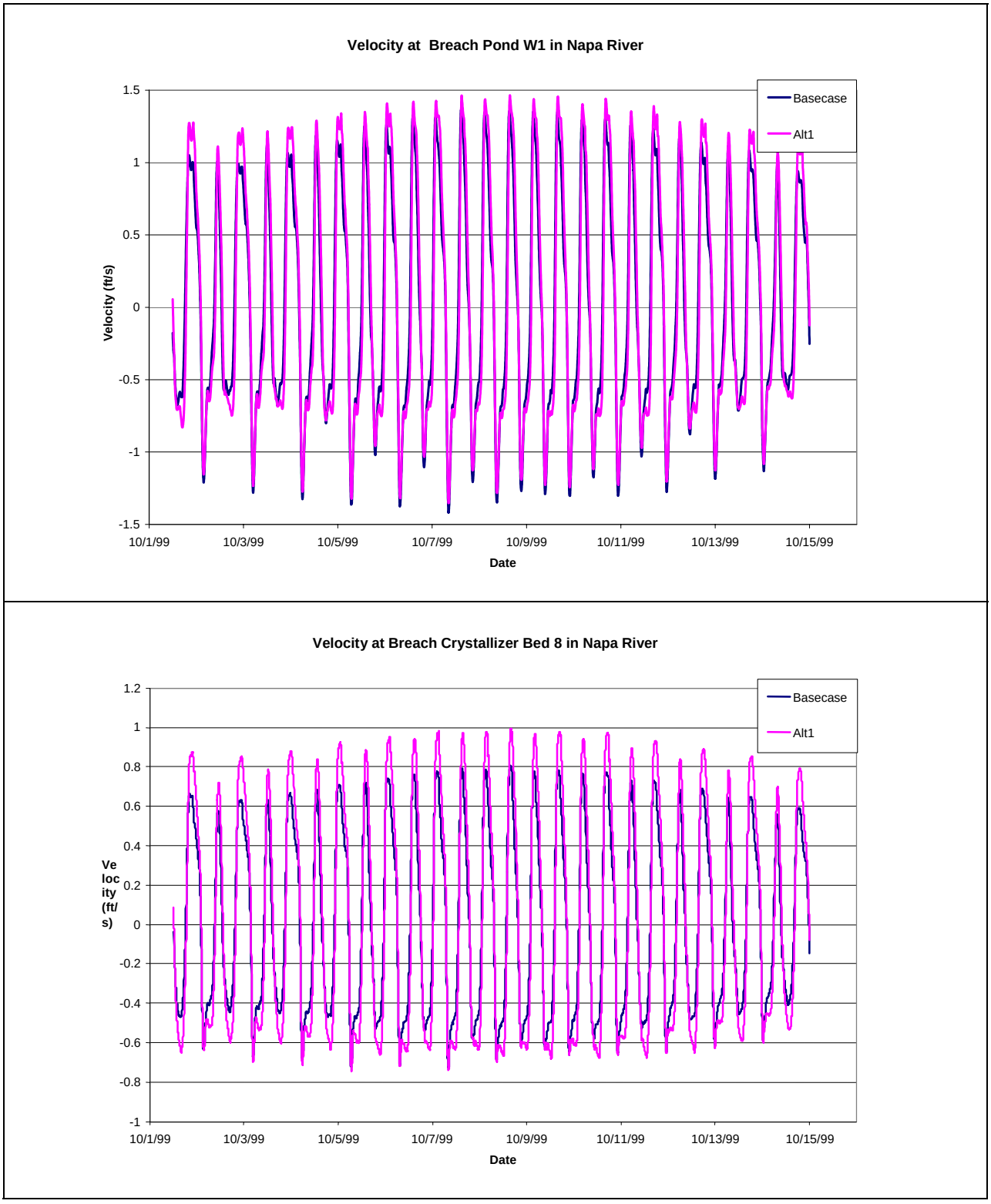

Figure 25 Comparison of Current Speed in Napa River and Fagan Slough between Alternative 1 and Base Case (continued on following page)

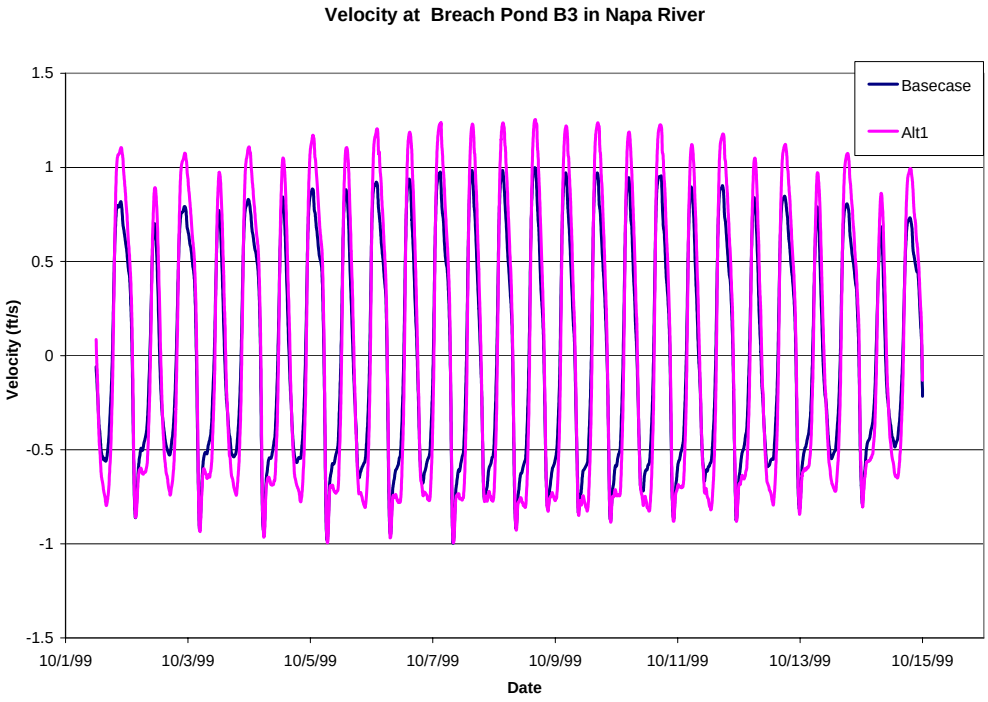

Figure 25 Comparison of Current Speed in Napa River and Fagan Slough between Alternative 1 and Base Case

When the Site is open to tidal action, it will draw in water from the Bay through the Napa River. Consequently, the tidal prism entering the Napa River will be enlarged to provide the additional volume of water to fill the Site. However, since the tidal exchange between the Site and the river is small compared to the existing tidal prism in the Napa River, the effect is expected to be negligible, as exemplified by Figure 26. The total diurnal tidal prism of sub-areas 1, 2, and 3 is about 2,900 acre-feet, equivalent to an average discharge of 5,860 cfs over a 6-hour filling period. This leads to a 7% increase in discharge in the Napa River as compared to the base case of typical dry weather flow.

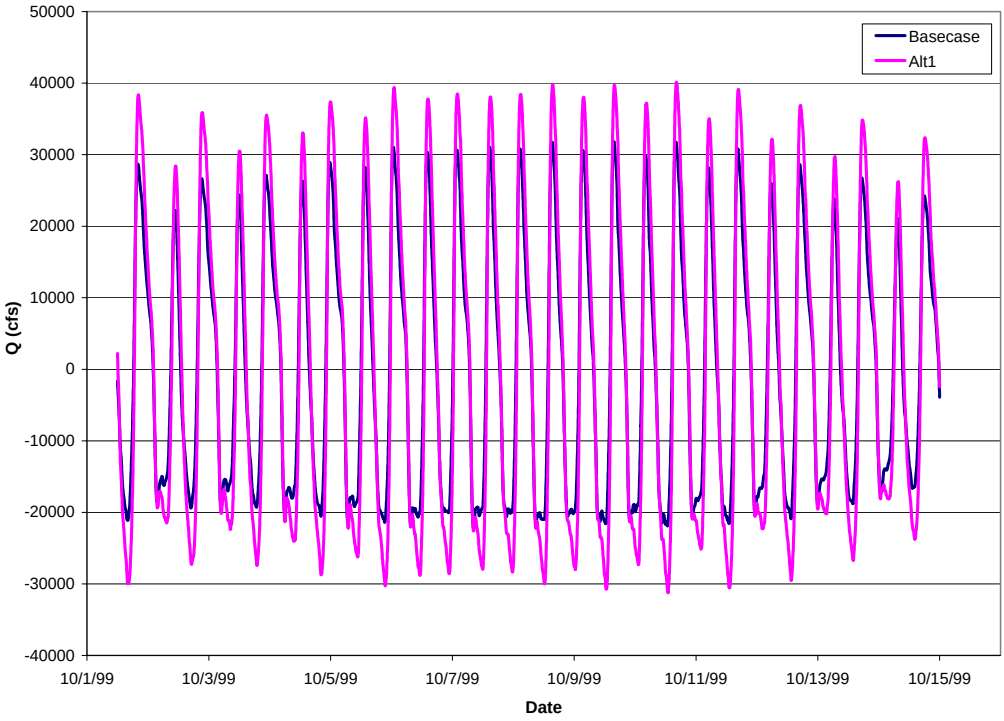

Figure 26 Change in Tidal Flow Downstream of Breaches in Napa River for Alternative 1

10.4 RESULTS FOR FLOOD FLOW CONDITIONS

One of the restoration objectives is to maintain the existing level of flood protection along the project reach of the Napa River. Therefore, simulations were performed for flooding scenarios to determine the maximum water surface elevation in the Site so that any modifications to levees having a flood control function can be designed accordingly. The model predictions will also be used to assess the impact on the flood levels along the Napa River. The effect of the restoration project on flooding at the nearby Napa Airport, however, requires a detailed hydraulic analysis of the area between Fagan Slough and the airport, as well as the functionality of the existing culvert located at the upstream end of Fagan Slough. Therefore, it will be addressed at a later stage in the modeling for the preferred alternative.

10.4.1 Dynamic Analysis

Dynamic simulation was conducted for a 2-week period beginning from February 1, 1998 to assess the hydraulic performance of the restored ponds under extreme flood flow conditions, and to determine the effect the restoration may have on flood elevations in the River. During this period, there was a substantial amount of freshwater inflow from the Napa River with a peak discharge of 21,200 cfs (slightly less than the 10-year peak flow as shown in Section 10.4.2, Table 4). Concurrently, the bay experienced an exceedingly high tide on February 6, 1998, with an elevation of 8.5 ft NAVD88 at the Point Reyes Station at the ocean, which was the highest on record at that station. Therefore, the combined effect of freshwater flow and tide is anticipated to produce a conservative (worst case) estimate of the maximum water surface elevation in the Site.

As a result of tidal amplification as the tides propagate into the Bay, coupled with the effect of the flood flows, the predicted water surface elevation in the Site reached a level of 9.84 ft NAVD88, as shown in Figure 27. It took several days for the tide to resume its normal level and consequently the model shows that the Site would have remained submerged over an extended period. On the other hand, the results indicate that the restoration of the Site under Alternative 1 has no bearing on the water level at the Napa River because the incremental tidal prism associated with the ponds is negligible compared with the existing tidal flows in the river. A comparison of the water level in the Napa River immediately downstream of the breaches to sub-area 3 is presented in Figure 28.

The predicted velocity at the breaches under flood flow conditions is shown in Figure 29. The predicted velocity estimates of the upper bound of velocity adopted for designing of erosion control protection at the breaches. For the breaches at sub-areas 1 and 2, the maximum speed is about 1 to 1.5 ft/s, whereas both breaches at sub-area 3 exhibit a higher maximum speed of 3 ft/s. These velocities are not considered substantial, and reasonable erosion control can be placed around the breach opening to prevent excessive scour.

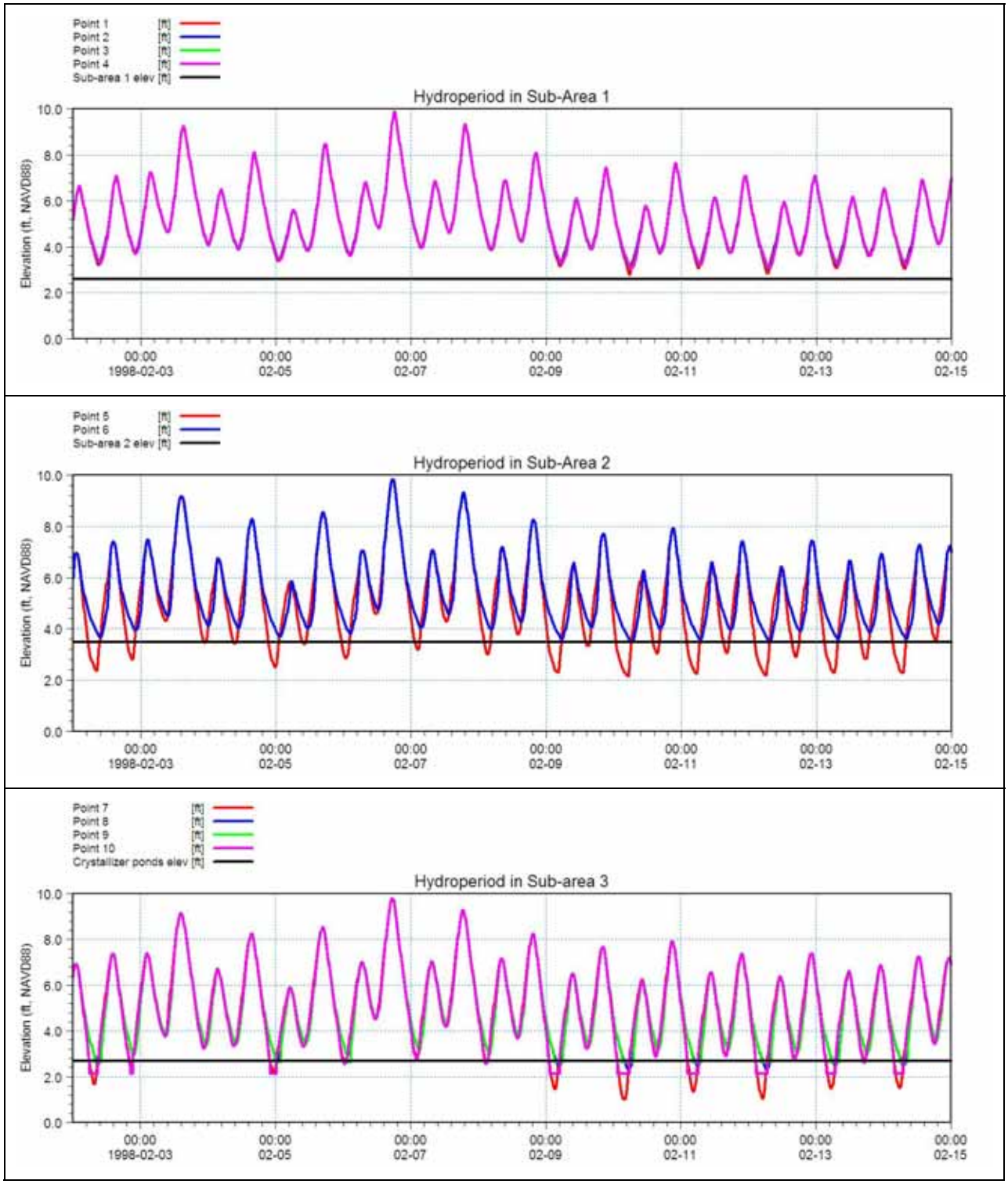

Figure 27 Predicted Water Surface Elevation for Alternative 1 Under Flood Flow Conditions

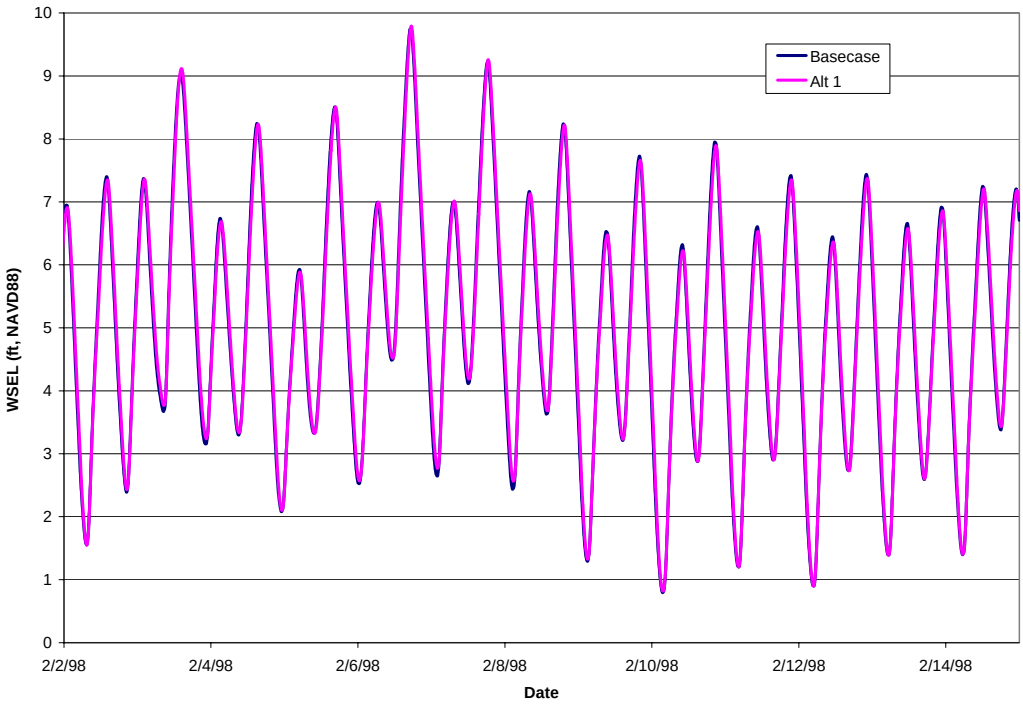

Figure 28 Change in Water Level Downstream of Breach at Napa River for Alternative 1

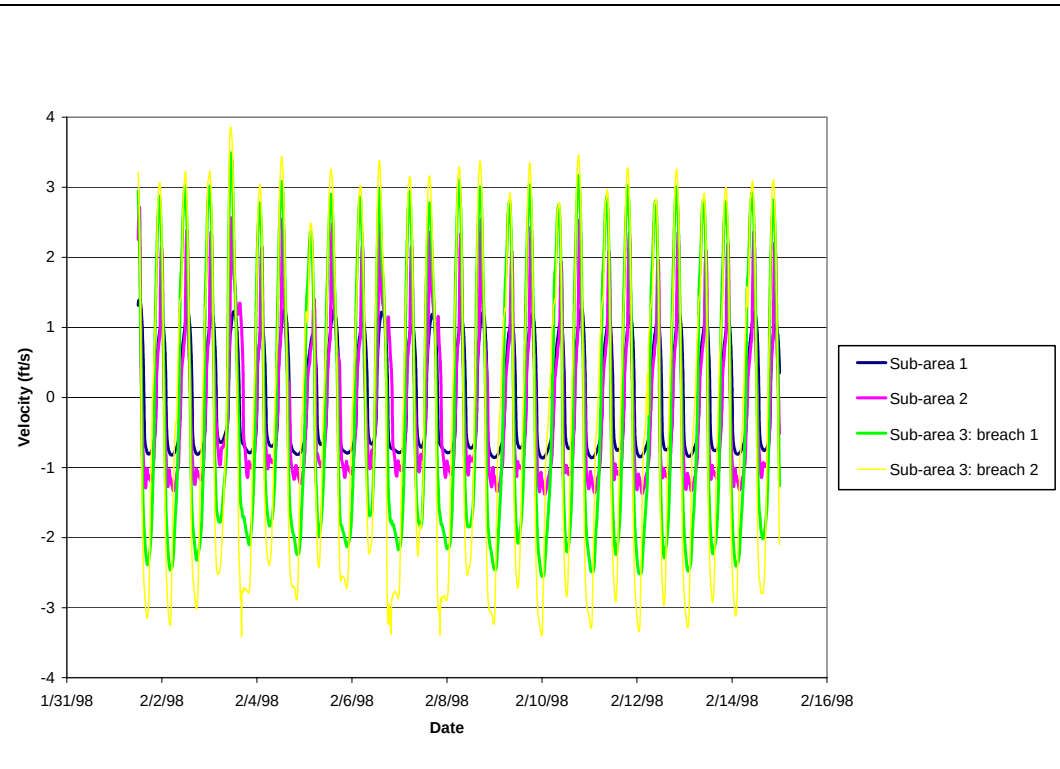

Figure 29 Velocity at Breaches during Flood Flow Conditions for Alternative 1

10.4.2 Steady-State Analysis

Steady-state simulations were undertaken to provide a basis for the design of flood protection measures. The effects of upstream flood flows and downstream tidal levels were investigated for different combinations of the boundary conditions as listed in Table 4. The flows at the Napa River near the confluence with Fagan Slough for the different return periods were obtained from the FEMA Flood Insurance Study (1990). The mean flow was taken as the mean annual runoff measured at the gage at Napa City (USGS 11458000), and proportioned for the tributaries. Due to the lack of hydrologic data for Sonoma Creek, the mean flow was estimated based on the ratio of drainage areas between Sonoma Creek and the Napa River, whereas the flood flows for different return periods were computed using the correlation factor developed by PWA as described in Section 7.3. The same water level was prescribed at the mouth of Sonoma Creek and the Napa River, with values obtained from the FEMA study (1990).

Table 4
Steady-State Analyses of Flood Flow Conditions

	Upstream Flow Boundary		Downstream Tidal Boundary	
Run	Return-Period	Napa River flow (cfs)	Tidal Datum/ Return-Period	Water Level at Mouth of Napa River (ft NAVD88)
1	Mean Q	204	10-year tide	8.56
2	Mean Q	204	100-year tide	9.06
3	10-year Q	25,500	MHHW	6.21
4	50-year Q	38,900	MHHW	6.21
5	100-year Q	45,200	MHHW	6.21
6	100-year Q	45,200	100-year tide	9.06

Note: Q = flow

The results from the steady-state simulations are summarized in Table 5. During average or low flow conditions, the water level in the Site is controlled solely by the tides in the Bay. During flood flow conditions, the water surface elevation increased above the tide level along the Napa River. This causes a difference in water level across the Site with the highest level attained in sub-area 1, as reflected in runs 3 through 6.

Table 5
Results from Steady-State Simulations for Alternative 1

Run	Water level in sub-area 1 (ft NAVD88)	Water level in sub-area 2 (ft NAVD88)	Water level in sub-area 3 (ft NAVD88)
1	8.56	8.56	8.56
2	9.06	9.06	9.06
3	6.51	6.43	6.27
4	6.94	6.74	6.35
5	7.20	6.93	6.40
6	9.54	9.22	9.17

Under Alternative 2, crystallizer beds 1, 2, and 3 will be retained as a managed pond while the remainder of the Site will be restored to tidal wetland. Although the managed pond is represented in the model setup, it is only included as inactive cells in the 2-dimensional model and has no effect on the hydrodynamics of the Site.

11.1 INTERNAL CHANNEL EVALUATION

The findings from the breach size and channel configuration analyses conducted for Alternative 1 were applied here for the design of the layout. Sub-areas 1 and 2 are identical to that of Alternative 1. With respect to sub-area 3, the internal channel network was modified around crystallizer beds 1, 2, and 3, and the existing levee bordering these 3 ponds were assumed to be above the normal tidal levels so that the managed pond was isolated from the rest of sub-area 3. Since crystallizer beds 1, 2, and 3 are excluded from tidal exchange, the marsh area is reduced to 760 acres, and the potential diurnal tidal prism is reduced to 1,976 acre-feet. Two options were considered to determine the optimum size of the breach at pond 8 of sub-area 3. One option adopts the same breach opening as in Alternative 1, and the second option reduces the cross-sectional area by 50% by decreasing the width of the breach to 330 feet.

Results from the model show drainage from the ponds is similar between the two options. A smaller breach size can be considered in Alternative 2 because the tidal prism is reduced due to the creation of the managed pond in the northwest corner of sub-area 3. The model grid adopted for Alternative 2 is presented in Figure 30.

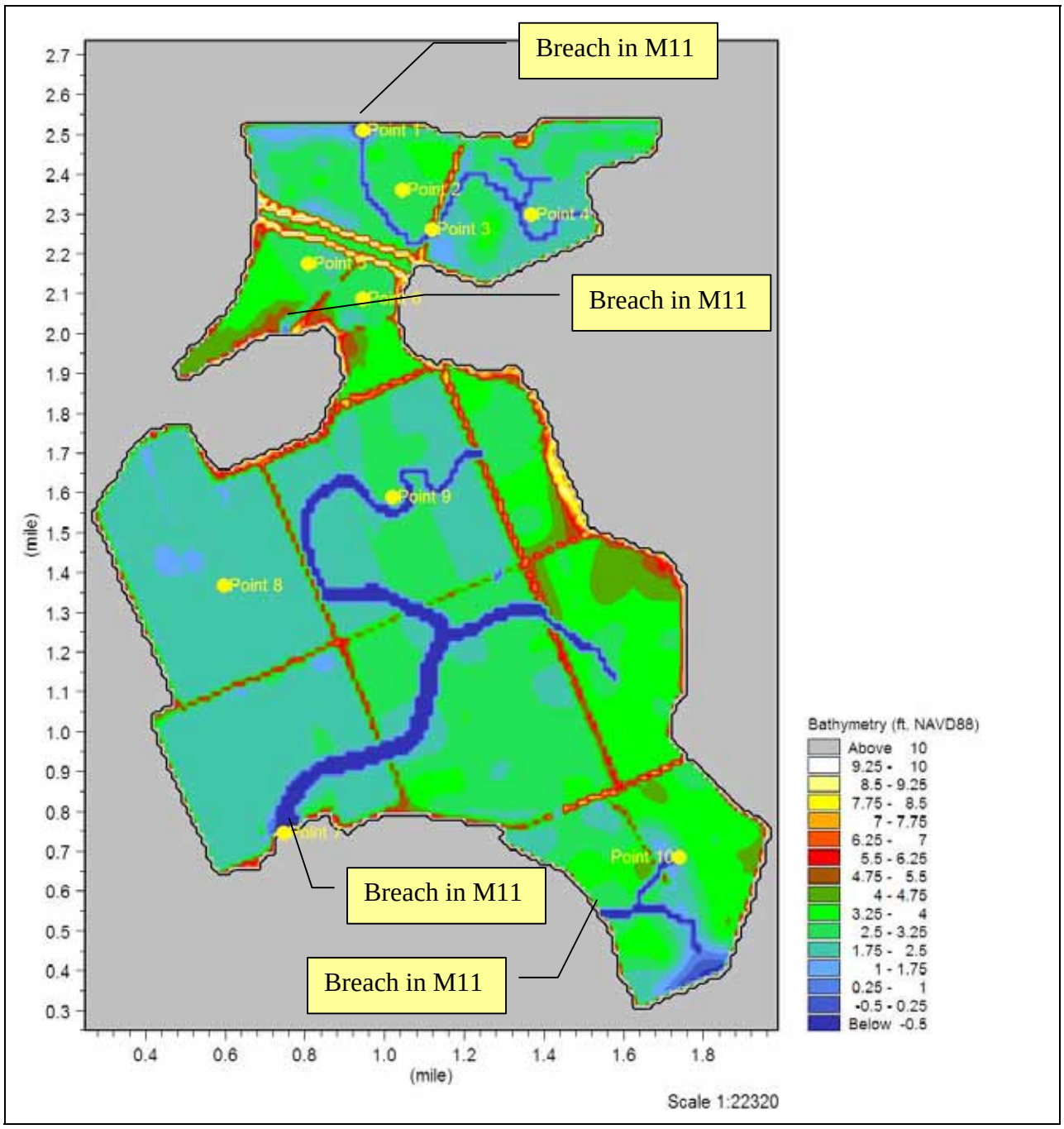

Figure 30 Model Bathymetric Grid for Alternative 2 (M11 refers to MIKE11 model)

11.2 RESULTS FOR NORMAL TIDAL CONDITIONS

Simulation was performed for normal tidal conditions using a 2-week period in October 1999, covering a complete spring-neap cycle. The results show that the entire Site is inundated twice daily by the two high tides (MHW and MHHW). Approximately 54% and 53% of sub-area 1 and sub-area 3 (excluding crystallizer beds 1, 2, and 3) is drained at least once a day under MLLW, respectively (as shown in Figure 31).

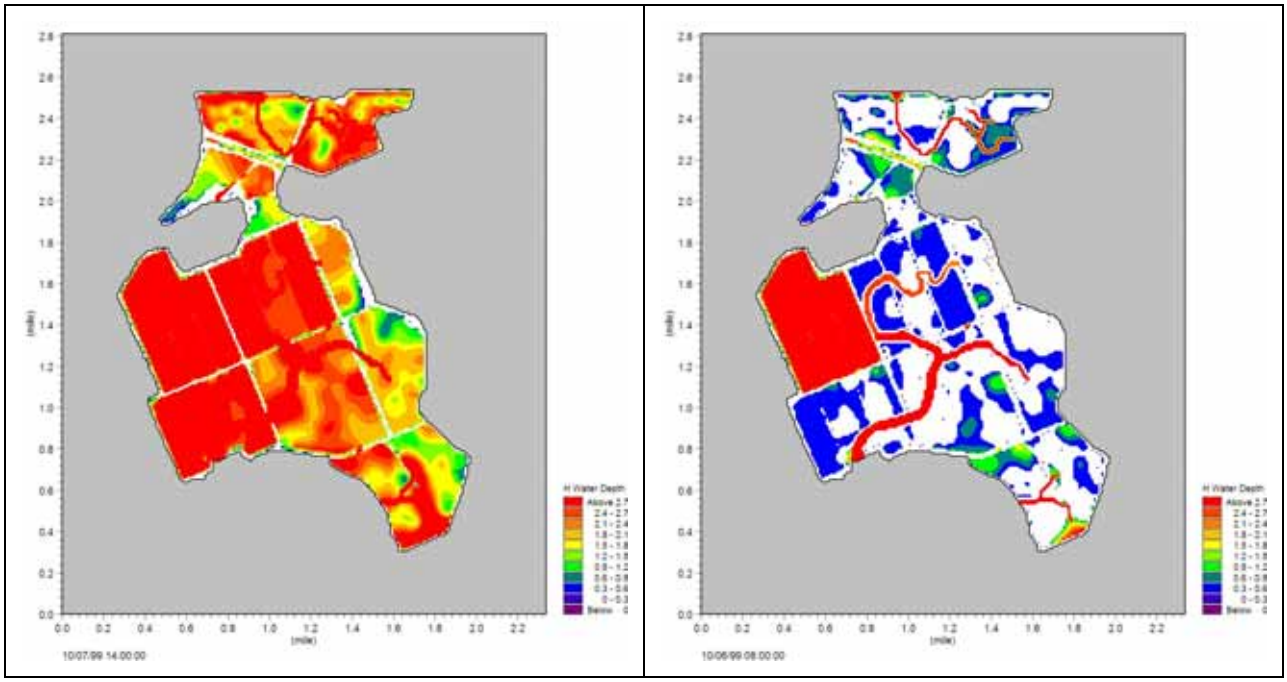

Figure 31 Inundation Areas for Alternative 2 under MHW (left) and MLLW (right)

The predicted water surface elevation at selected points (as shown in Figure 30) in sub-area 3 is plotted in Figure 32, along with the average elevation of the sub-area to examine the hydroperiod resulted in different parts of the sub-area. The hydrodynamics in sub-areas 1 and 2 have not been modified from Alternative 1 and therefore the predicted water levels are not repeated here. As in Alternative 1, there is negligible attenuation in the high tides, while the low tides are slightly dampened. The hydroperiod in areas outside the managed pond is also similar to that of Alternative 1.

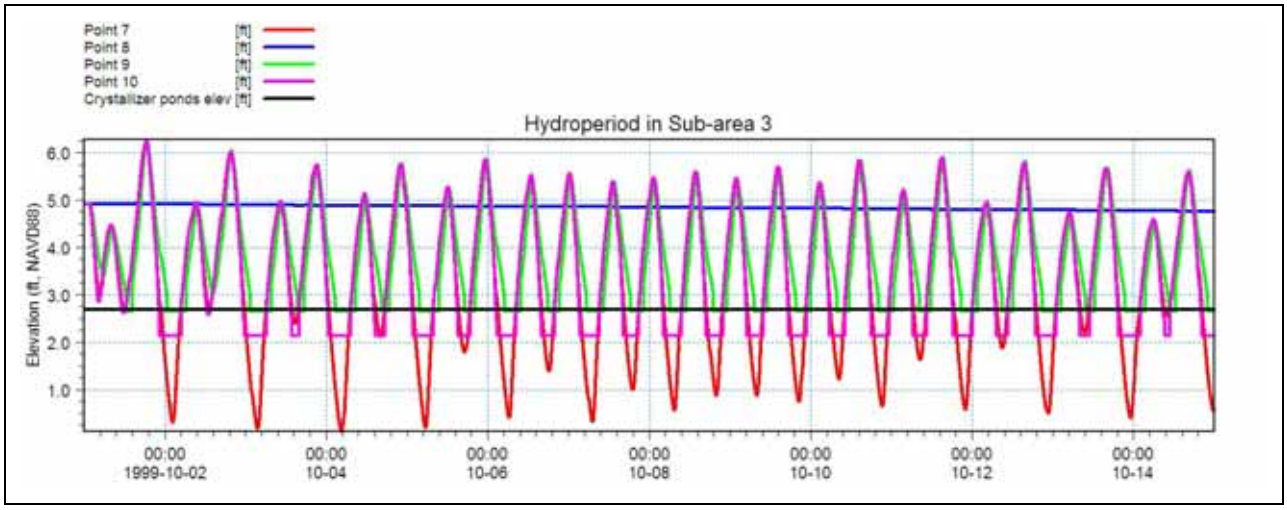

Figure 32 Predicted Water Surface Elevation in Sub-area 3 for Alternative 2 Under Normal Tidal Conditions

The root-mean-square current speed for Alternative 2 is displayed in Figure 33. The maximum speed at the main breach of sub-area 3 is similar to that of Alternative 1, and is on the order 2 ft/s. The current speed remains high along the internal channels, which convey the water in and out of the Site. On the marshplain, the speed drops quickly to 0.2 ft/s. The lower velocity encourages the deposition of sediment as the tidal water spreads through the Site, thereby allowing gradual accretion over time. On the other hand, the higher velocity in the internal channels may lead to erosion and the subsequent deepening and widening of the sloughs.

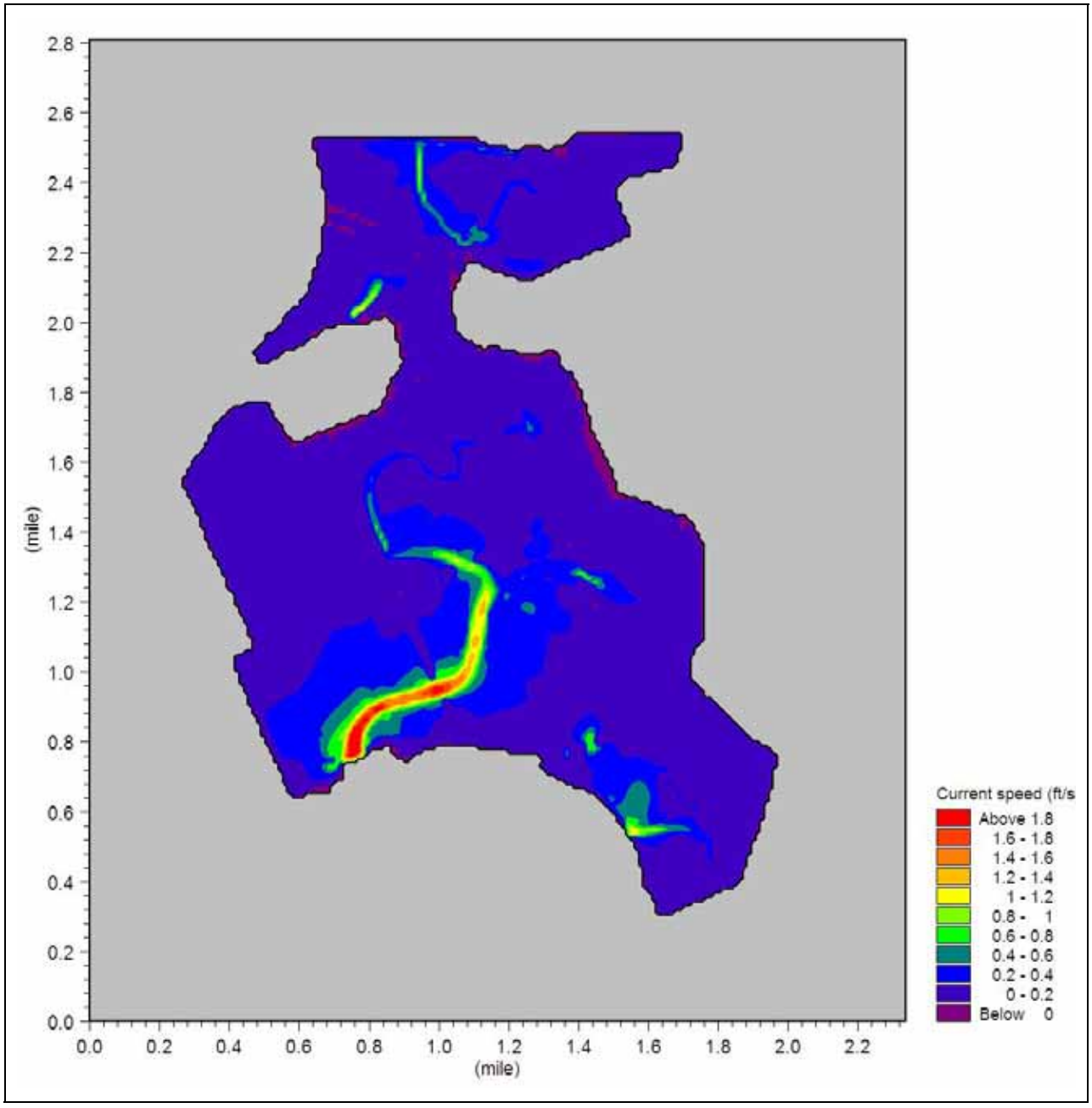

Figure 33 RMS Current Speed for Alternative 2

The impact on velocity in the Napa River outside the breaches of sub-area 3 is expected to be slightly smaller for Alternative 2 because the tidal flow going through sub-area 3 is less. Hence, the increase in tidal current is about 20%, as illustrated in Figure 34. The velocity in the Napa River and Fagan Slough outside the breaches of sub-area 1 and 2 is the same as Alternative 1 and therefore is not reproduced here.

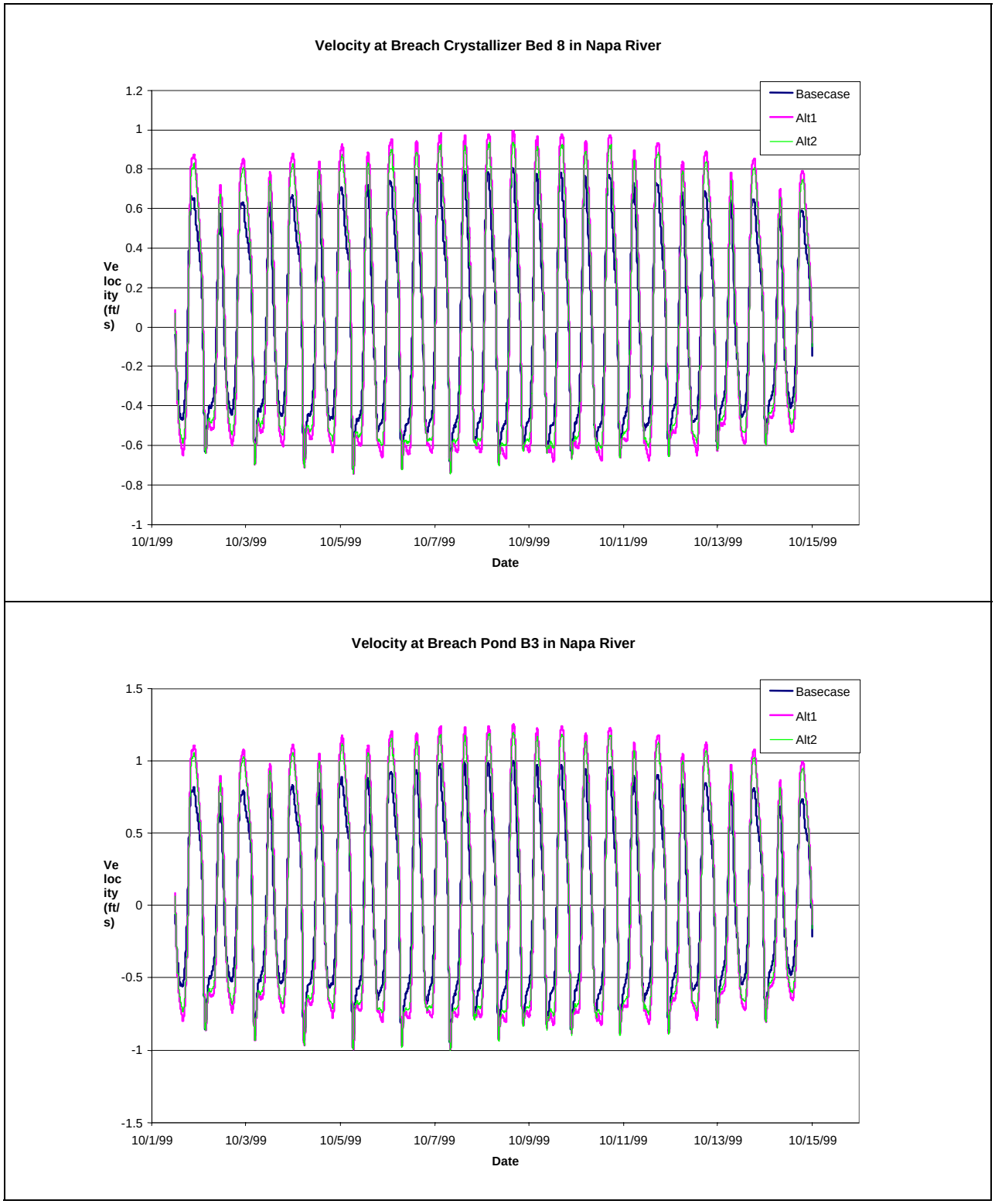

Figure 34 Comparison of Current Speed in Napa River Outside Breaches in Sub-area 3 Between Alternative 2 and Base Case

The smaller restored area for Alternative 2 results in an increase in tidal prism in the Napa River from the base case is about 5%, smaller than that of Alternative 1, as shown in Figure 35. The total diurnal tidal prism of Alternative 2 is about 2,567 acre-feet, equivalent to an average discharge of 5,180 cfs over a 6-hour filling period.

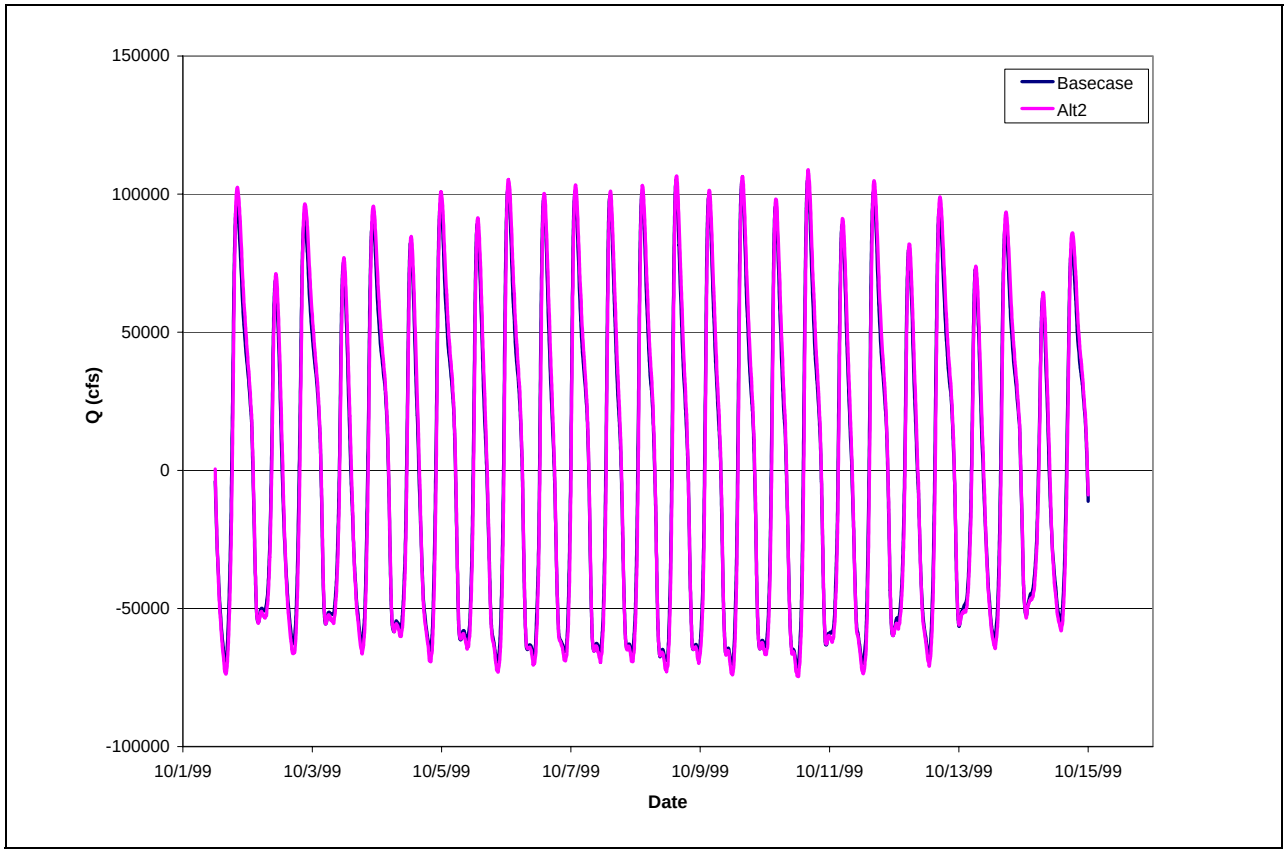

Figure 35 Change in Tidal Flow at Mouth of Napa River for Alternative 2

11.3 RESULTS FOR FLOOD FLOW CONDITIONS

11.3.1 Dynamic Analysis

The predicted water surface elevation for selected points in sub-area 3 during a flood flow period in February 1998 is presented in Figure 36. As in Alternative 1, the water level in the Site reached a maximum of 9.84 ft NAVD88, thereafter the tide gradually resumed its normal level over the next several days. The model shows that the extraordinarily high tide would have caused an overtopping of the existing internal levees bordering the managed pond, as reflected in the abrupt rise in water level at Point 8.

On the other hand, in view of the smaller increase in tidal flows, Alternative 2 will have a smaller impact on the water level in the Napa River than Alternative 1.

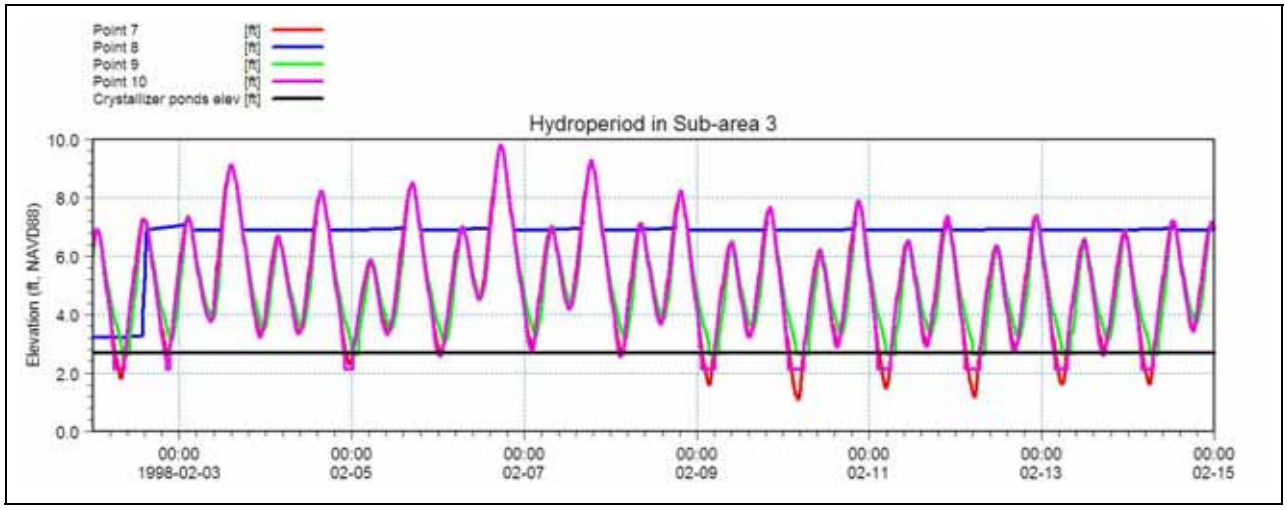

Figure 36 Predicted Water Surface Elevation in Sub-area 3 for Alternative 2 Under Flood Flow Conditions

The predicted velocity at the breaches under flood flow conditions is shown in Figure 37 to provide an estimate of the upper bound of velocity to be adopted for the design of erosion control protection at the breaches. The maximum speeds at the breaches of sub-areas 1 and 2 are the same as in Alternative 1, at about 1 to 1.5 ft/s, respectively. On the other hand, the velocity at the breach of crystallizer bed 8 is higher than that of Alternative 1 due to the smaller breach size, which causes the flow to be more concentrated. Therefore, the velocity at that breach reaches a maximum value of approximately 4 ft/s. Nonetheless, these velocities are not considered substantial, and reasonable erosion control measures can be placed around the breach opening to prevent excessive scour if judged necessary. This decision can be made following further analyses at the final design stage.

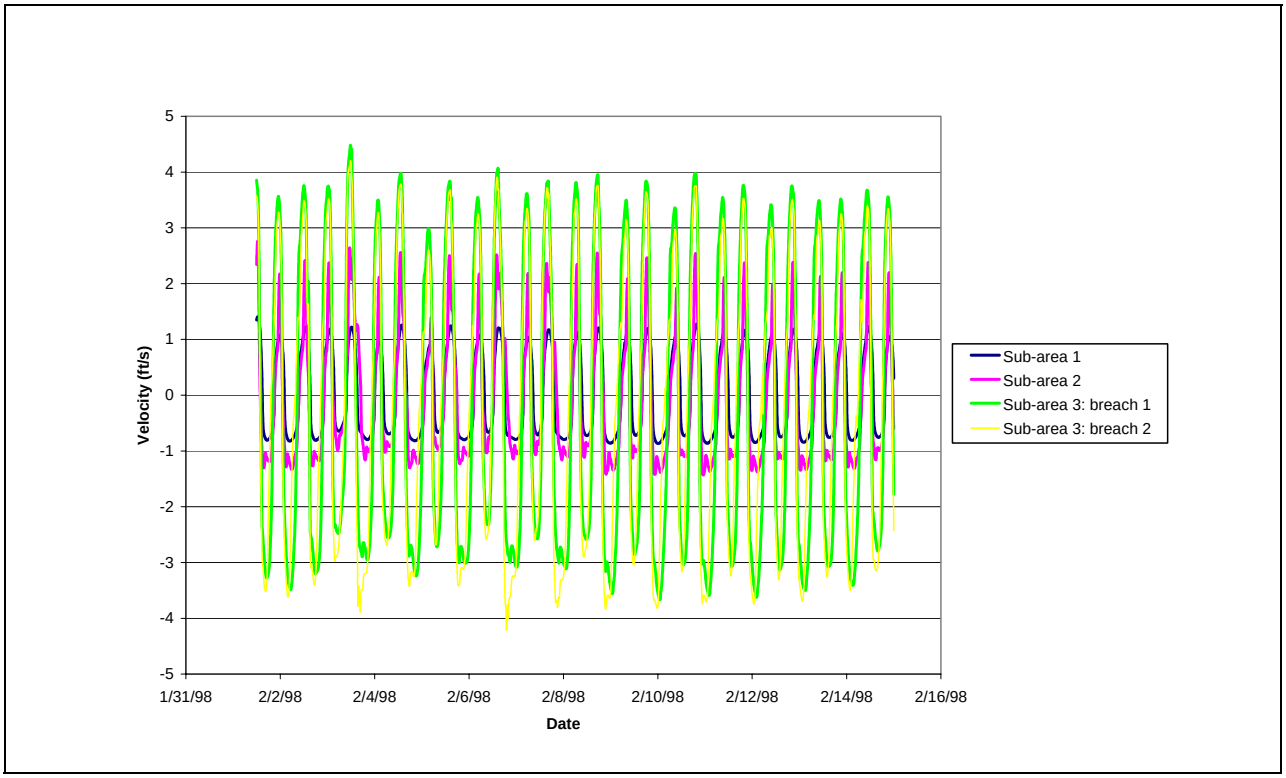

Figure 37 Velocity at Breaches During Flood Flow Conditions for Alternative 2

11.3.2 Steady-State Analysis

The results from the steady-state simulations for Alternative 2 are summarized in Table 6. The predicted water level in the Site is exactly the same as in Alternative 1 for runs 1 and 2 because the water level is controlled solely by the tides in the Bay during average or low flow conditions. However, the water level in all three sub-areas is marginally higher for Alternative 2 under flood flow conditions because the flood retention volume provided by the Site is slightly decreased with crystallizer beds 1, 2, and 3 functioning as a managed pond.

Table 6
Results from Steady-State Simulations for Alternative 2

Run[(a)]	Water level in sub-area 1 (ft NAVD88)	Water level in sub-area 2 (ft NAVD88)	Water level in sub-area 3 (ft NAVD88)
1	8.56	8.56	8.56
2	9.06	9.06	9.06
3	6.55	6.46	6.29
4	7.00	6.81	6.42
5	7.28	7.01	6.49
6	9.60	9.28	9.22

(a) The runs are defined in Table 4.

Alternative 3 differs from Alternative 2 in that ponds W1, W2 and W3 will not be restored to tidal action. In terms of modeling, the cells in sub-area 2 will remain inactive because no hydraulic connection is established into the area. The model grid for Alternative 3 is shown in Figure 38.

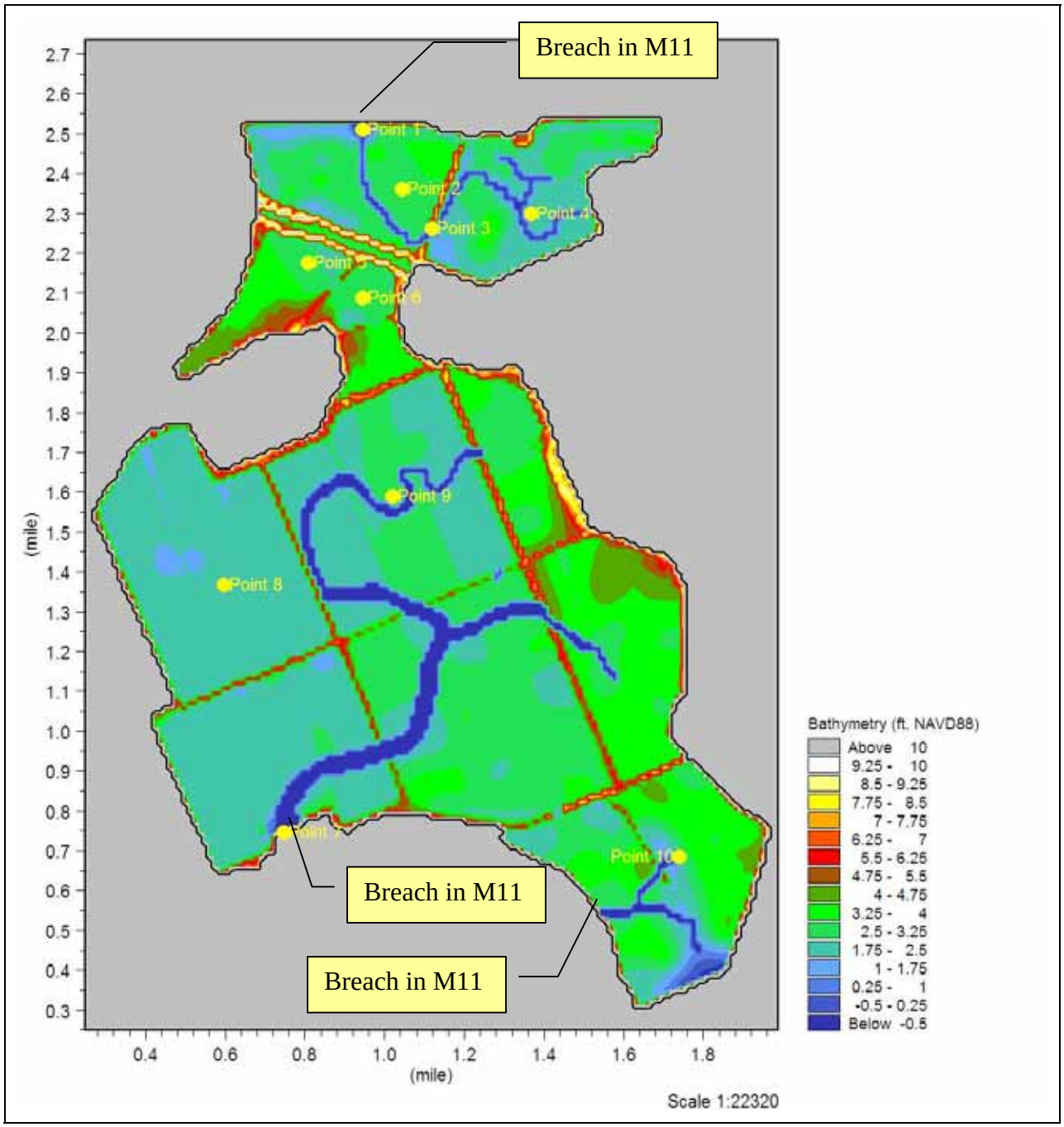

Figure 38 Model Bathymetric Grid for Alternative 3 (M11 mean in model MIKE 11)

12.1 RESULTS FOR NORMAL TIDAL CONDITIONS

Simulation was performed for normal tidal conditions using a 2-week period in October 1999, covering a complete spring-neap cycle. The inundation depths as presented on Figure 39 are identical to that of Alternative 2 in sub-areas 1 and 3 because: (1) the three sub-areas are served by independent breaches, and (2) the tidal prism entering the Napa River is not constrained by the capacity of the river. Therefore, the exclusion of sub-area 2 from tidal action has no impact on the inundation characteristics in the rest of the Site. The variation in water depth within sub-area 2 reflects the existing bottom elevation variation. In comparison, crystallizer beds 1, 2, and 3 have a more uniform bathymetry.

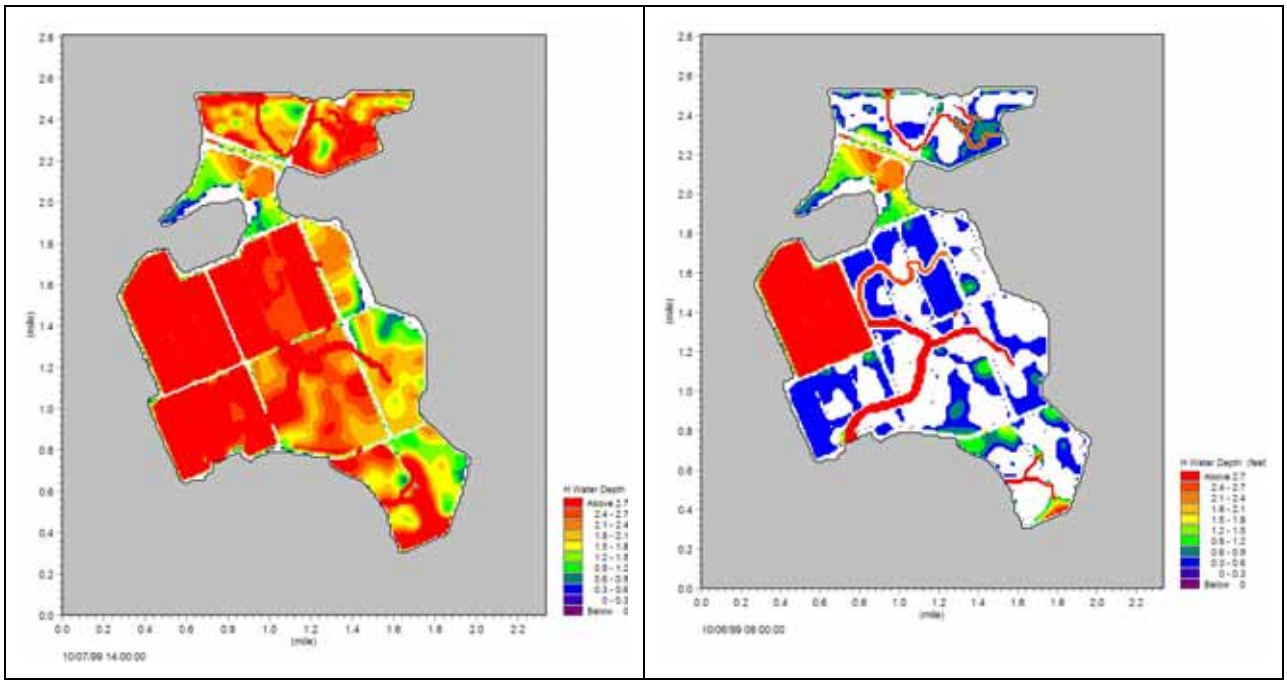

Figure 39 Inundation Areas for Alternative 3 under MHW (left) and MLLW (right)

Since the tidal flows in sub-areas 1 and 3 are unaffected by the hydraulic regime in sub-area 2, the root-mean-square current speed for Alternative 3 is also the same as in Alternative 2, as displayed in Figure 40. The maximum speed at the main breach of sub-area 3 is on the order of 2 ft/s, and the speed decreases to 0.2 ft/s on the marshplain.

The changes in velocity in Fagan Slough and the Napa River outside the breaches are the same as Alternative 2, even though there is no longer a breach at sub-area 2 for Alternative 3. This suggests that the increase in velocity in the river is not due to the localized outflow at the individual breach, but a consequence of the cumulative increase in tidal prism along the river.

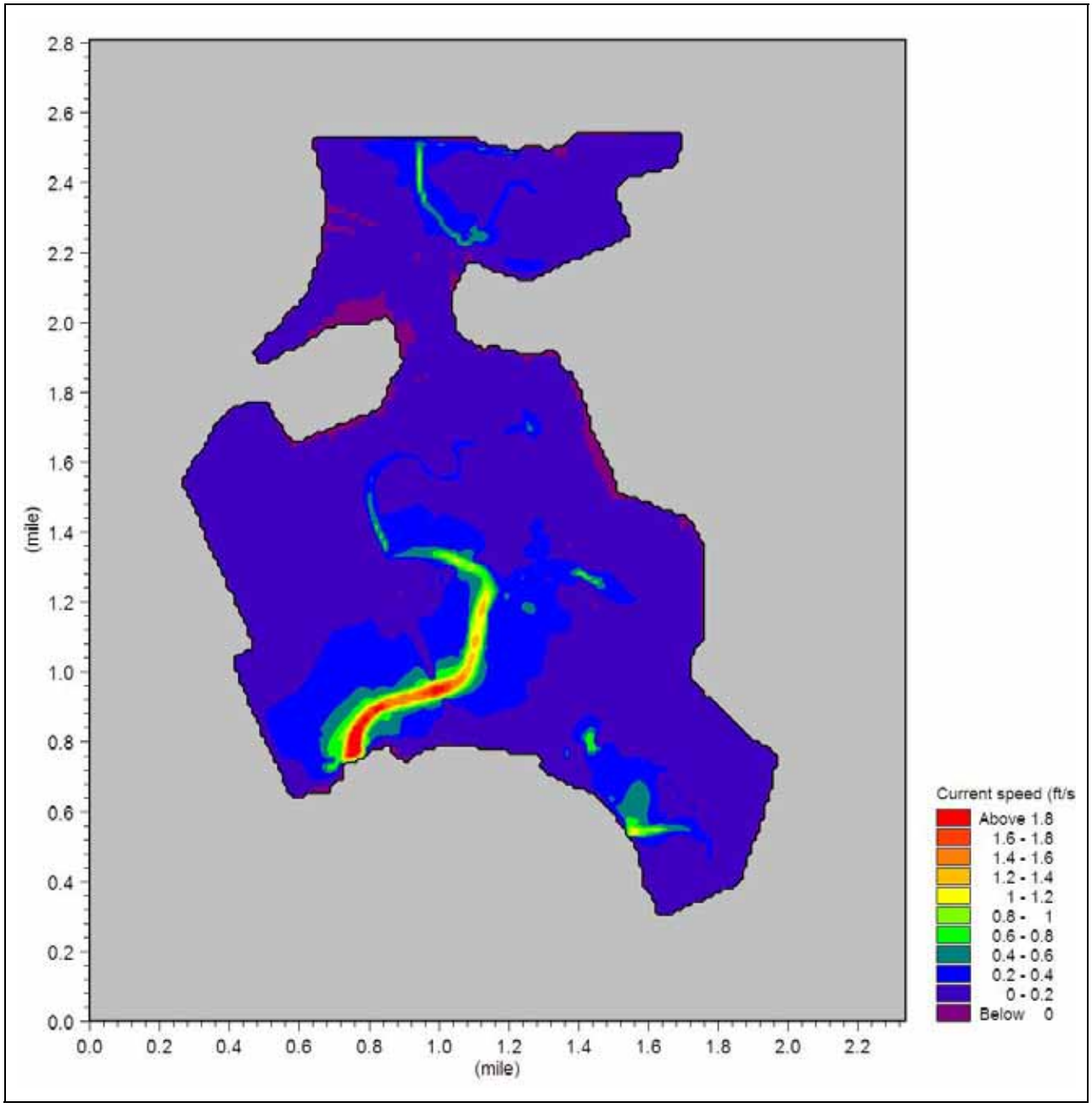

Figure 40 RMS Current Speed for Alternative 3

Since sub-area 2 only contributes a small percentage of the total tidal prism of the Site, the difference in tidal discharge in the Napa River between Alternatives 2 and 3 is insignificant. Hence, the increase in tidal prism in the Napa River from the base case is also about 5%, as demonstrated in Figure 41. The potential diurnal prism for Alternative 3 is 2,431 acre-feet, or 5% smaller than that of Alternative 2.

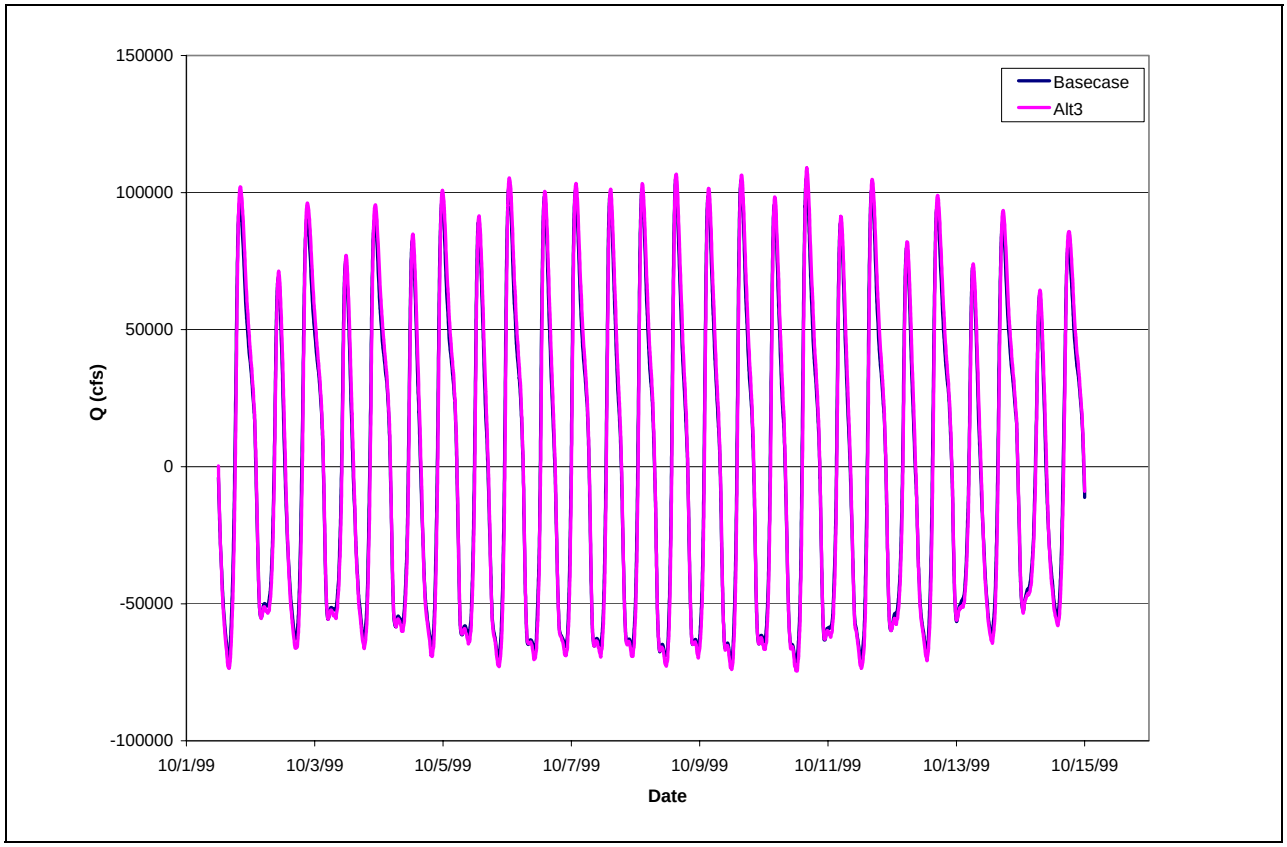

Figure 41 Change in Tidal Flow at Mouth of Napa River for Alternative 3

12.2 RESULTS FOR FLOOD FLOW CONDITIONS

12.2.1 Dynamic Analysis

The predicted water surface elevation for Alternative 3 in sub-areas 1 and 3 during the flood flow period in February 1998 is essentially the same as for Alternative 2. Although there is no breach made to sub-area 2, the model shows that the water level in that sub-area would still have reached a maximum of 9.84 ft NAVD88 (Figure 42) as a consequence of overtopping of the existing levees along the southern perimeter of pond W3. The extreme high tides propagate to the far end of sub-area 3 in crystallizer beds 5 and 6, where the water spills over the existing levees separating pond W3 and ponds 5 and 6, and enters ponds W1, W2, and W3. This would flood the Plant Site access road. When the water recedes during the ebb tides, the model shows that the water level in sub-area 2 drops back to a lower level corresponding to the crest elevation of the levee along the southern perimeter of pond W3.

The maximum velocities for designing erosion control protection at the breaches will be the same as that of Alternative 2 at the corresponding openings.

As in the case of Alternative 2, Alternative 3 is not expected to effect the water level in the Napa River.

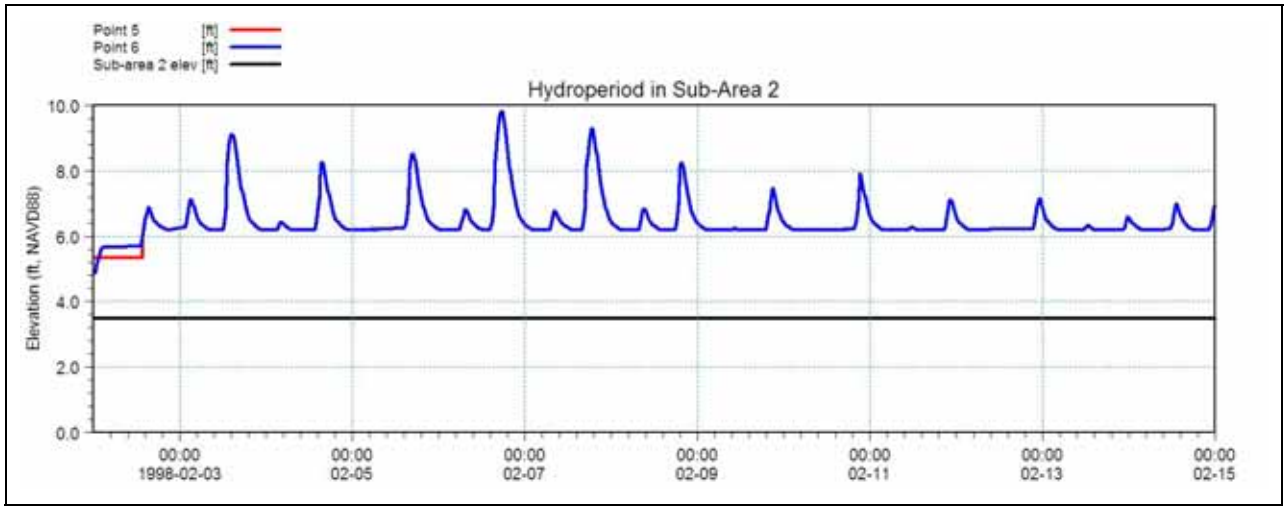

Figure 42 Predicted Water Surface Elevation in Sub-area 2 for Alternative 3 Under Flood Flow Conditions

12.2.2 Steady-State Analysis

The results from the steady-state simulations for Alternative 3 are summarized in Table 7. The predicted water level in the Site is exactly the same as in the other alternatives for runs 1 and 2 because the water level is controlled solely by the tides in the Bay during average or low flow conditions. Although there is no direct hydraulic connection between sub-area 2 and the Bay, the high tides would overtop the existing levees and hence the same water level prevails over the entire Site. Since the flood retention volume associated with sub-area 2 is negligible, the water levels in sub-areas 1 and 3 are the same as in Alternative 2 for runs 3 through 6. On the other hand, the water levels in sub-area 2 are lower compared to Alternative 2 for the corresponding flows because the water levels in sub-area 2 are in equilibrium with the levels in sub-area 3.

Table 7
Results from Steady-State Simulations for Alternative 3

Run[(a)]	Water level in sub-area 1 (ft NAVD88)	Water level in sub-area 2 (ft NAVD88)	Water level in sub-area 3 (ft NAVD88)
1	8.56	8.56	8.56
2	9.06	9.06	9.06
3	6.55	6.30	6.30
4	7.01	6.42	6.42
5	7.28	6.49	6.49
6	9.63	9.22	9.22

(a) The runs are defined in Table 4.

The impact of the Restoration Project on the Napa River has been analyzed for three alternatives using the one-dimensional model of the river network. The results indicate that there will be minimal change in the water surface elevation in the Napa River at the breach locations, and only a minor increase in cross-sectionally averaged velocity in the river because of the substantial tidal flows through the river under the base case. Since there are sensitive users located along the west bank of the Napa River near its confluence with Fagan Slough, a more detailed analysis of the velocity distribution across the river and how it may be altered by the increased flows through Fagan Slough was undertaken. In addition an analysis of the Barge channel and discussions on marsh evolution and of salt diffusion from the soil are included in this section.

13.1 FAGAN SLOUGH ANALYSIS

A 25m grid was developed for the reach of Napa River spanning approximately 0.5 miles and 1 mile north and south of its confluence with Fagan Slough, respectively, as illustrated in Figure 44. The bathymetric data was based on the fine grid developed for the NSMR project, and extended to the limits of the model domain through interpolation of the one-dimensional river cross-sections available at discrete transects. The average elevation in this reach of the Napa River is about -11 feet NAVD88, with the lowest elevation at approximately -25.5 feet NAVD88. The northern and southern ends of the grid were hydrodynamically coupled to the upper and lower Napa River branches in the MIKE11 model. To reduce the computation run time for the simulation of the restored ponds, the flows at the breaches of the ponds were extracted from the model outputs of the standard setup for Alternative 2 (presented in Section 11), and prescribed as lateral flows for the two-dimensional Napa River model. A spatially uniform Manning's n value of 0.03 was specified.

A two-week simulation from 1st to 15th October 1999 was performed for the normal tidal conditions. Figure 45 presents the change in RMS speed between the base case and Alternative 2. The maximum change in velocity occurs along the central axis of the Napa River where the velocity and flow are the highest. At the mouth of Fagan Slough, the incremental speed is locally higher where the water enters from the east bank of the Napa River and it rapidly dissipates to less than 0.05 ft/s above the base case as the increased flow spreads across the river.

The current speed and direction at three different locations across the Napa River near the mouth of Fagan Slough are shown in Figure 46. The velocity is almost unchanged at the western bank of the river where the residential units and docks are located (bottom figure in Figure 45). This indicates that the restoration of Ponds 9 and 10 will cause an insignificant impact on the sedimentation or erosion process along the western bank of the Napa River. On the other hand, the flow properties at the eastern river bank are substantially modified because of the phase difference between the breach flows and the tides. Since the draining of the site is not completed before the next tide comes in, the flow reversal pattern at slack tide is not as distinct as under the base case.

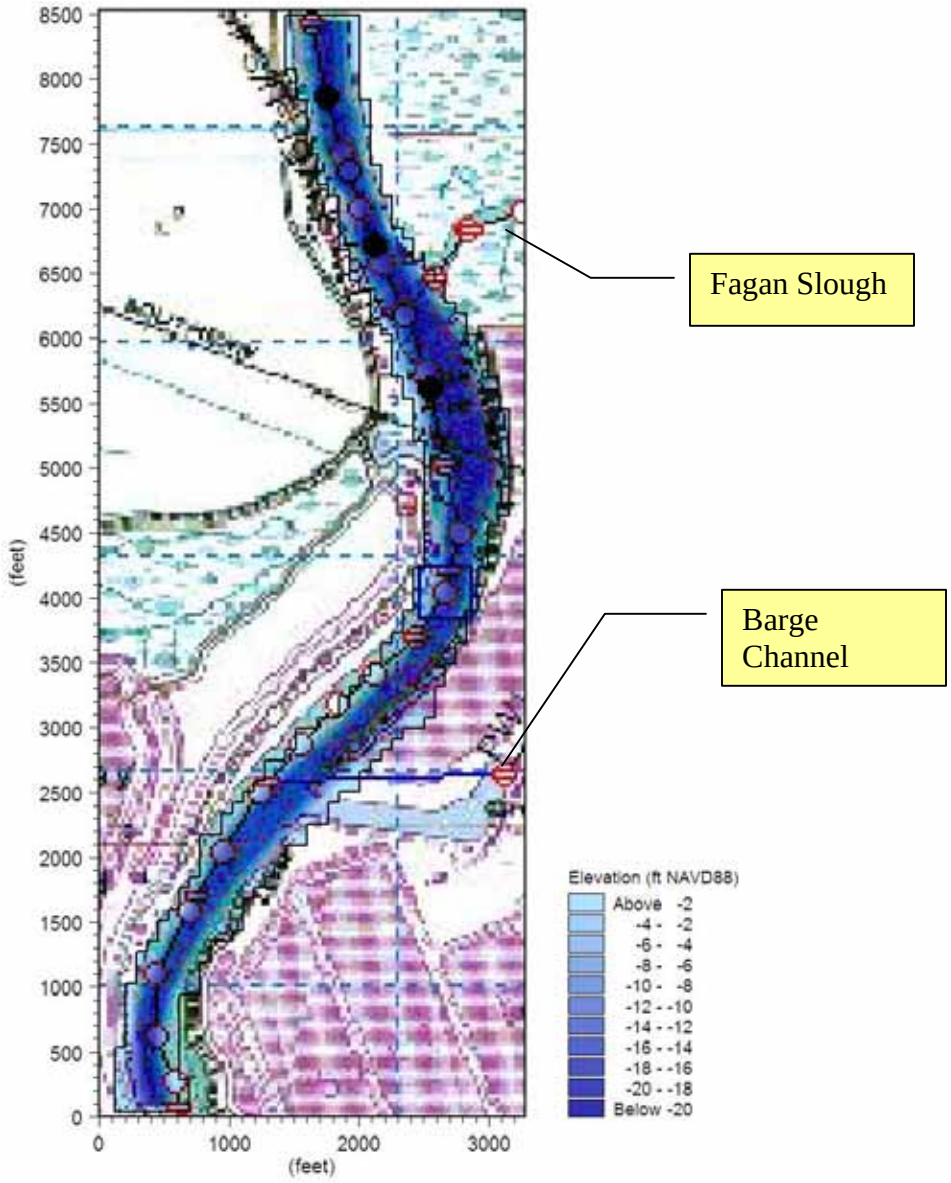

Figure 44 Two-dimensional Grid of Napa River for Detailed Modeling of Preferred Alternative

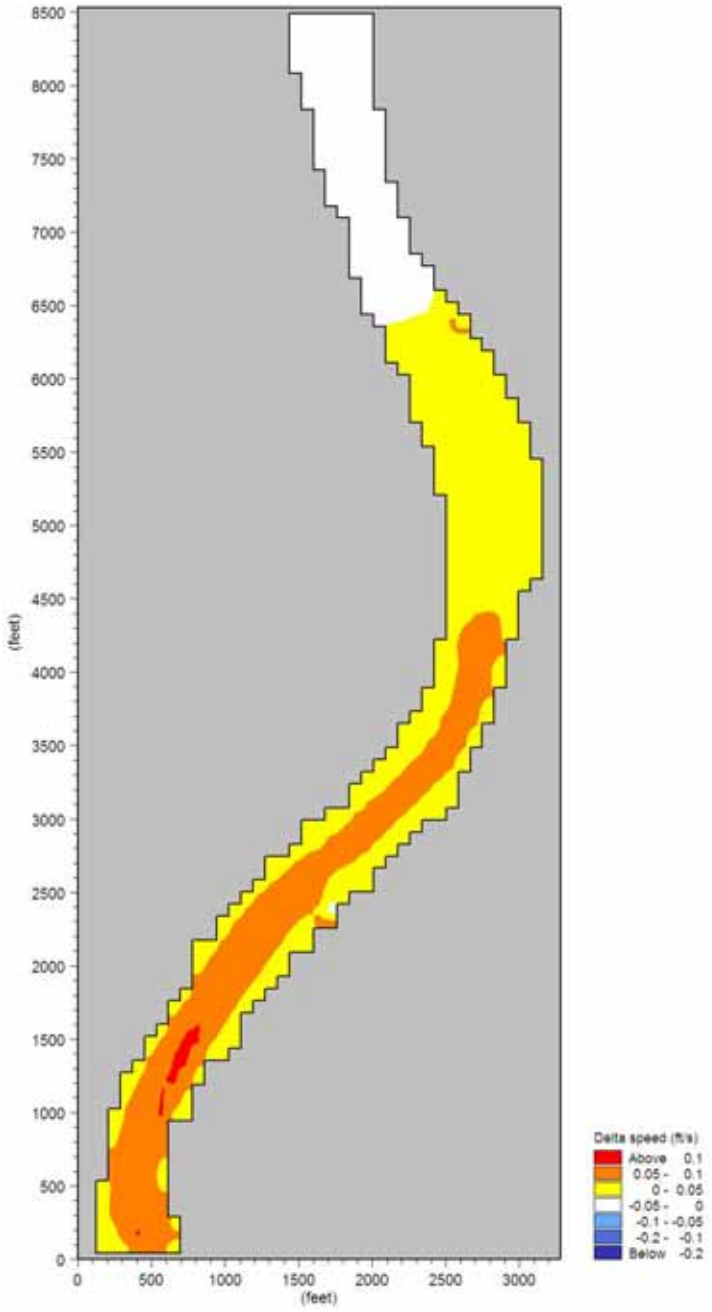

Figure 45 Change in RMS Speed for Alternative 2 under Normal Tidal Conditions

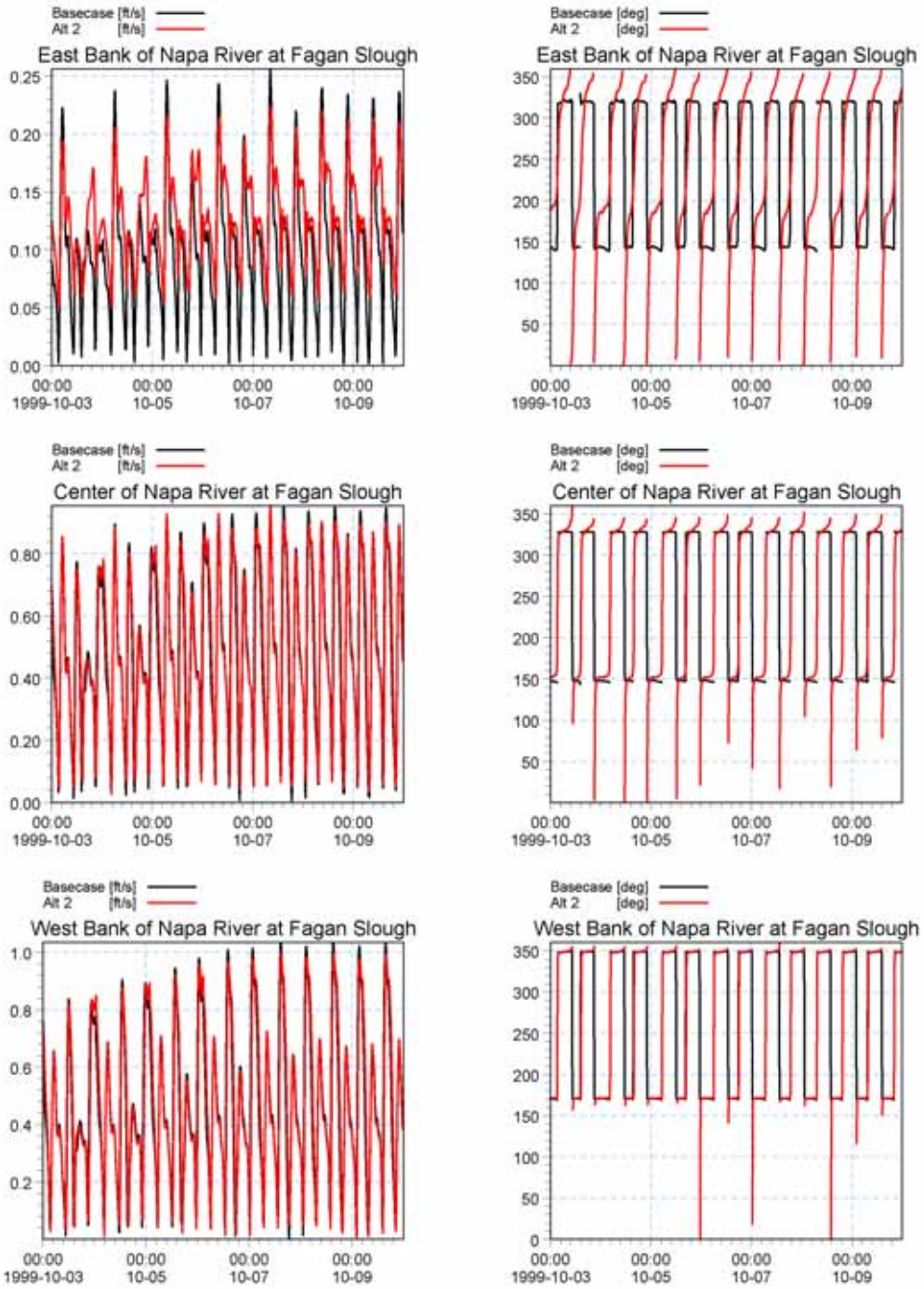

Figure 46 Comparison of Current Speed and Direction Across the Napa River

13.2 BARGE CHANNEL ANALYSIS

Presently, the barge channel is a dead end slough that requires periodic maintenance dredging to prevent it from filling with sediment. Cargill uses the channel for loading barges that transport salt generated at the Napa Plant Site. Opening the wash ponds to tidal action would increase the flow in the barge channel; however, the tidal prism generated by opening the wash ponds would not be large enough to maintain the barge channel at its existing size of over 200 feet. Hydraulic geometry relationships developed for San Francisco Bay estuary tidal marshes (Williams et al. 2002) suggest that opening the wash ponds (approximately 90 acres) to tidal action would result in a channel that is about 70 feet wide and likely less than 10 feet deep (at MLLW). Initially, the channel may be wider until the wash ponds fill with sediment and the tidal prism reduces. To maintain a boat launching facility, the launch ramp would need to be located near the breach location or possibly at the end of a dock that extends into the main part of the channel.

13.3 TIDAL HABITAT EVOLUTION

A sediment mass balance model was developed to predict and quantify the geomorphic evolution of the salt ponds after they have been opened to the Napa River. After the levees are breached the salt ponds may act as sediment sinks and sediment in the Napa River will accumulate in the salt ponds. The sediment mass balance model is similar to that described in Appendix D of the Napa Salt Marsh Feasibility Study (US Army Corps of Engineers 2004) for the Napa Sonoma Marsh Restoration (NSMR) project. For this analysis the rate of change in the marsh elevation was assumed to be a function of the sediment concentration in the flood tide waters (i.e., in the Napa River) and the settling rate of the sediment in the wetland. Figure 47 below shows the variables used in the analysis.

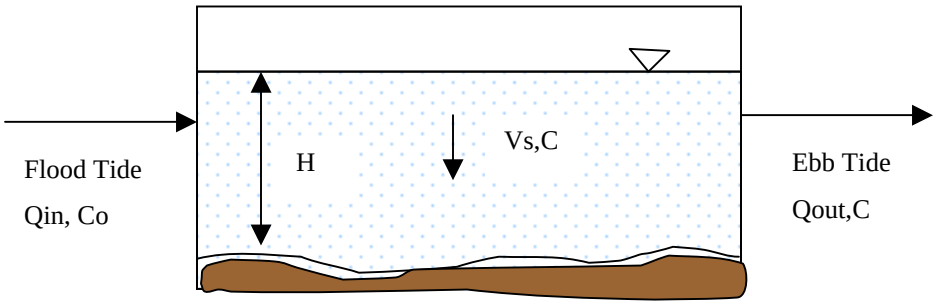

Figure 47. Schematic Showing the Parameters Used in the Calculation of Habitat Evolution

The following assumptions were used in the analysis:

- USGS sediment data collected at Mare Island was analyzed to determine an average suspended sediment concentration (SCC) to use in the analysis. The SSC ("Co" in Figure 47) in the flood tide waters was 125 mg/l (the same as used in the Napa Salt Pond feasibility study).
- A "typical" tide was used in the analysis.

- Sediment was assumed not to be resuspended once settled.
- The settling velocity was assumed equal to:

  $Vs = kC^{4/3,}$

  Where:

  Vs = the settling velocity (m/s)

  k = 0.00011 for SI units,

  C = sediment concentration in the wetland.

  This is the same relationship used in the Napa Salt Ponds Feasibility Study.

  - Dry density of inorganic sediment when deposited = 400 kg/m3
  - Only marsh rise through sedimentation was included. The increase in marsh elevation due to sediment trapping by vegetation and organic deposition was not included. These processes will become important as the marsh develops.
  - Sea level rise was assumed to be 0.0036 m/yr, the same as used in the Napa Salt Pond Feasibility Study.
  - An average elevation, derived from the topographic survey, for each pond was used as the initial elevation. No additional fill in the ponds was considered.
  - Only existing internal pond dimensions were considered. Internal pond levees and ecotone areas to be constructed are not included in the analysis.

With the above assumes the equation for the change in concentration of sediment in the salt pond during a flood tide is:

$$(h-z)\frac{dC}{dt} = (C_o - C)\frac{dh}{dt} - v_s C \qquad (1)$$

and for and ebb tide:

$$(h-z)\frac{dC}{dt} = -v_s C \qquad (2)$$

Equations 1 and 2 can be used to calculate the concentration of sediment in the salt ponds at all times. The change in elevation of the salt pond bottom can then be calculated using Equation 3:

$$\Delta z = \frac{v_s C \Delta t}{\rho_d} \qquad (3)$$

where ρ_d is the dry density of the salt pond sediment.

The results of the marsh evolution are shown in Figures 48a through 48c, which show the predicted development of tidal marsh for each planning unit. The analysis is based on average elevations and internal dimensions (i.e., levees are not included) of each pond, and does not consider the placement of additional fill in the North Unit or creation of ecotone. Additionally, the analysis does not consider the area that would be occupied by tidal channels (both constructed and those that would develop through natural processes).

The rate of marsh plain accretion starts out high because the duration of flooding is high. As the wetland increases in elevation the duration of flooding decreases so the rate of marsh plain growth also decreases. It was assumed that vegetation would start to colonize the ponds when the pond bottom elevation approaches sea level. For all the alternatives the elevation of the ponds will start to reach sea level starting in about years 3 to 5, and would continue for about another 10 years, by which time all the ponds should be at sea level or higher. Mature marsh was assumed to start developing when the pond bottom elevation is equal to Mean High Water (MHW). It is expected to take 50 years or more for tidal areas in all alternatives to develop into high marsh. However, variations in topography and depositional patterns will cause this to occur sooner in some locations.

Figure 48a. Predicted Tidal Wetland Development in North Unit

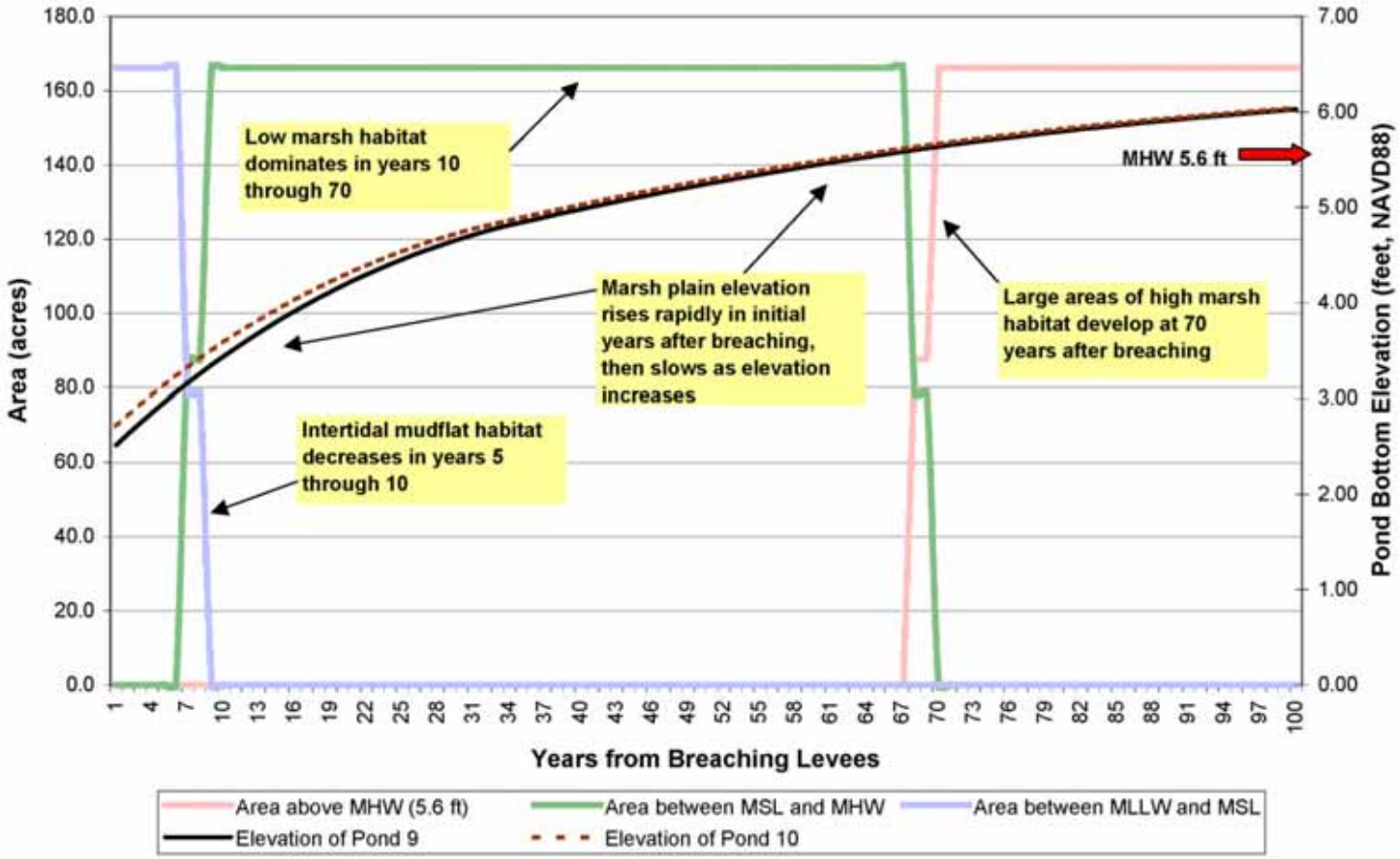

Figure 48b. Predicted Tidal Wetland Development in Central Unit

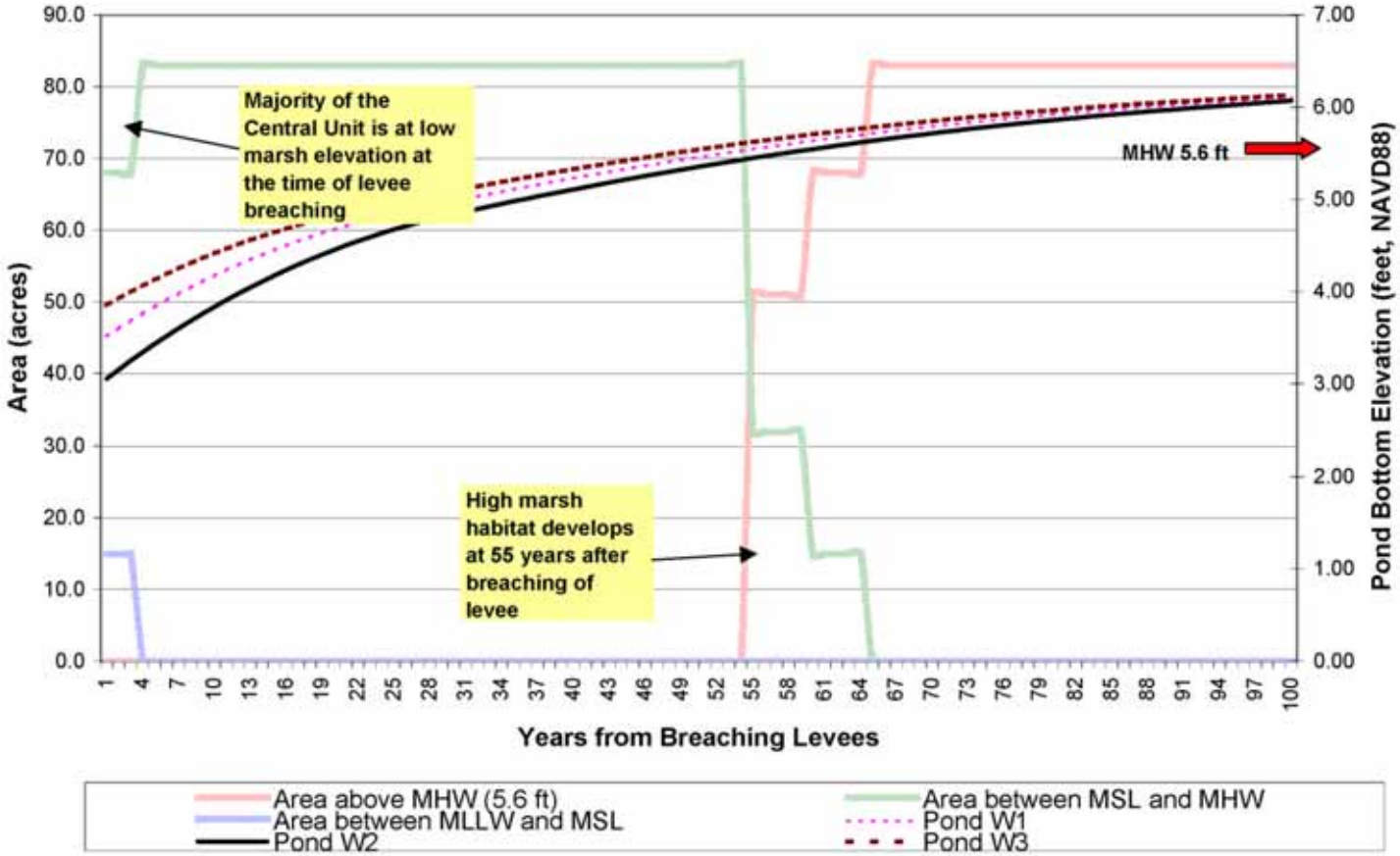

Figure 48c. Predicted Tidal Wetland Development in South Unit

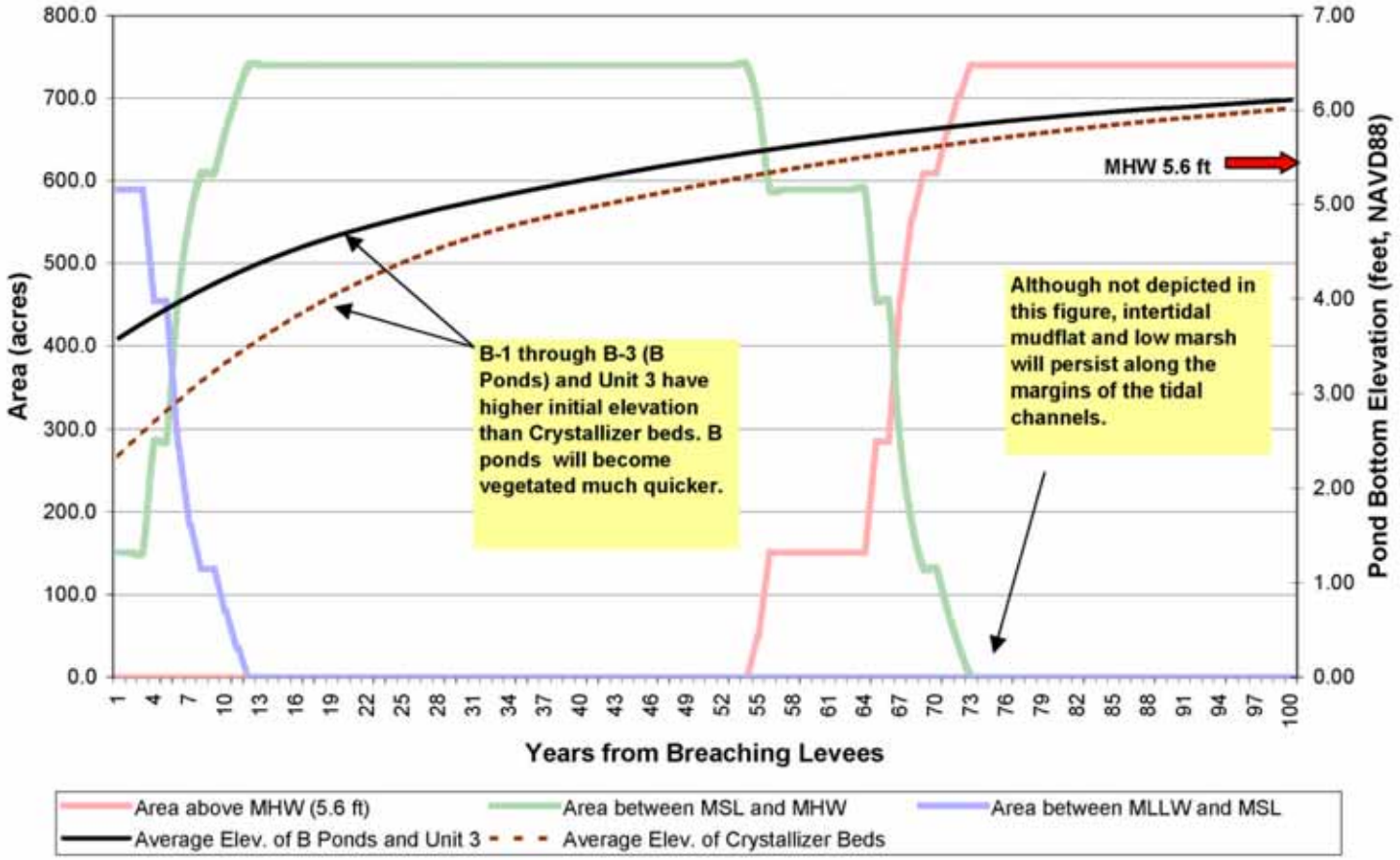

13.4 SALT DIFFUSION FROM POND SOILS

13.4.1 Analysis of Salt Diffusion from Pond Soils

During normal operations of the restored non-managed salt ponds water from the Napa River will enter the ponds where it will be exposed to the saline soils on the pond bottoms. Salt from these soils can diffuse into the tidal waters and increase the salinity of the water that leaves the ponds on a falling tide. Soil and water samples were collected from Ponds 9 and 10 to estimate the potential to increase the salinity of water discharging from the salt ponds after they are breached.

The salt in the soil will diffuse slowly through the soil into the water at a rate on the order of the molecular diffusion rate. It will also diffuse slowly through a thin layer of water adjacent to the soil. Once in the main body of the water the rate of diffusion will increase greatly due to turbulence generated by wind and heating and cooling of the water.

A simple diffusion model was developed to simulate the diffusion of salt into the tidal waters. The model is based on Fickian diffusion, which simply states that the flux of salt is proportional to the concentration gradient of salt. The constant of proportionality is the diffusion coefficient (Fisher et al. 1979). For diffusion in one-dimension with a constant source concentration the concentration profile at any time is:

$$C(x,t) = C_o(1 - erf(\frac{x}{\sqrt{4Dt}})) \qquad \text{for x>0} \qquad (1)$$

where:

C = concentration of salt at distance x at time t

C_o = concentration at x=0, assumed to be constant.

x = distance from source

D = diffusion coefficient

t = time

erf = error function

Equation 1 is valid for the case where there is no salt in the water entering the wetland. In this case C(x,t) represents the increase in salt concentration in the tidal water. For the case where there already is salt in the water entering the wetland the increase would be less than predicted by Equation 1. For the extreme case of when the salt concentration in the tidal waters equals or exceeds the soil salt concentration there would be no increase in concentration.

For this analysis it was assumed that the water column can be divided into two layers and that Equation 1 can be applied to each layer separately. The source concentration (C_o in Equation 1) for the upper layer was assumed to equal the concentration at the top of the lower layer (the layer

that directly mixes with soil water). This assumption should be valid since the upper layer mixes at a rate that is several orders of magnitude greater than the lower layer so that the concentration is essentially constant in the lower layer relative to the upper layer. Two diffusion coefficients are used in applying Equation 1. In most of the water column diffusion will be generated by turbulence in the water from wind and differential heating and cooling. The mixing due to winds and other surface phenomena does not necessarily extend to the bottom of the water column. Near the bottom there will often be a layer of more quiescent water that mixes only slowly. For this thin layer above the soil it was assumed that the diffusion coefficient was on the order of the molecular diffusion coefficient. The diffusion coefficient can be calculated from the Nernst Equation (Hines and Maddox 1985) or obtained from the CRC Handbook of Chemistry and Physics (Weast, 1980). For salt this is on the order of $1x10^{-9}$ m^2/s.

The diffusion coefficient due to the winds can be estimated as (Fisher et al., 1979):

$$E_v = 0.067du^* \qquad (2)$$

Where:

E_v = vertical diffusion coefficient (m^2/s)

D = depth of water (meters)

u* = shear velocity (m/s).

The shear velocity is a measure of the shear or force on the water column. For the existing case this shear is due to the wind.blowing across the water's surface. This value cane be estimated using Equation 3 (Fisher et al., 1979):

$$u^* = \sqrt{1.3x10^{-3}\frac{\rho_a}{\rho_w}U^2} \qquad (3)$$

where:

ρ_a = density of air (kg/m^3)

ρ_w = density of water (kg/m^3)

U = wind speed (m/s)

After the ponds are opened to the tides the currents in the wetland will also induce mixing. In this case the shear velocity is more difficult to estimate. A reasonable assumption is to assume it

is about 10% of the average velocity in the wetland (Fisher et al., 1979). The average flow rate in the wetland during a tide is equal to the tidal prism divided by the half the tidal period. The tidal prism is defined as the difference between the Mean High Water (MHW) and the average pond bottom elevation times the surface area of the pond. This results in Equation 4 below for shear velocity during a tide cycle:

$$u^* = 0.1 * \frac{A}{W\frac{T}{2}} \qquad (4)$$

A = area of pond (m^2)

W = average width of pond (m)

T = tidal period (s)

Since none of the ponds are presently open to tidal action it was not possible to calibrate or validate Equation 1 for tidal conditions. However, Equations 1, 2 and 3 were used to test the model for existing conditions. Data used in the analysis are described in Section 13.4.2

Figure 49 shows the rainfall pattern at the Napa Salt Ponds from October 2005 through January 17th 2006. Salinity data were collected from the ponds on January 10th, 2006. This is about 41 days after the first significant rainfall (Dec. 1) that started to fill the ponds with water. Table 8 shows the data used in the analysis. The distance above the bottom of the lowest measured salinity value was not known exactly. It was as close to the bottom as the instrument would allow which was usually within 2 inches. This was assumed to be near the top of the bottom layer used in the analysis. Different locations were assumed and the answer was found not to be sensitive to its exact location. Changing its assumed location changed the calibration of the molecular diffusion coefficient by less than an order of magnitude. The upper layer diffusion coefficient was unchanged from the calculated value. Figure 50 shows the modeled and measured salinity values.

The results shown in Figure 50 indicate that the model provides a reasonable estimate of the distribution of salt in the salt ponds due to the diffusion of salt from the soil into the water column.

When the ponds are opened up to tidal flow the changes from the existing condition simulated above will be:

- The flow of water in the wetland will induce addition mixing of water in the wetland.
- The water will be exposed to the soil for a shorter duration of time. Under the existing condition simulation the observed salt concentrations were observed after water had been in the ponds for more than a month. After breaching the ponds most of the water will only be in the ponds at most about 12 hours. This allows for less time for salt to diffuse out of the soil into the water column.

- The thin layer of water near the bottom where salt directly diffuses into the water will be thinner since there will be mixing at the bottom of the pond as well as the top.

Table 8 shows the vertical dispersion coefficient due to tidal flows. It is on the same order of magnitude as the mixing due to the winds, therefore mixing should be about the same as in the existing conditions (when the wind is blowing). In general this mixing is rapid and near uniform conditions will existing in the tidal waters. Assuming that the lower mixing layer (the thin layer of water above the soil where molecular diffusion governs) is on the order of one-third of an inch (it may be larger once vegetation starts to grow) the increase in salinity will be less then 1 ppt assuming the tidal waters are fresh. For salty tidal waters the diffusion of salt into the water column will be even less.

These results are consistent with the measured results from the laboratory analysis presented in Section 13.4.2. In the laboratory experiments the increase in salinity after about 6 hours of exposure to pond soils was on the order of about 0.5 ppt. The bottom measurement was higher but the top measurement would be more indicative of what would exist in most of the water column.

Figure 49 Precipitation near Napa for 2005-2006 Water Year

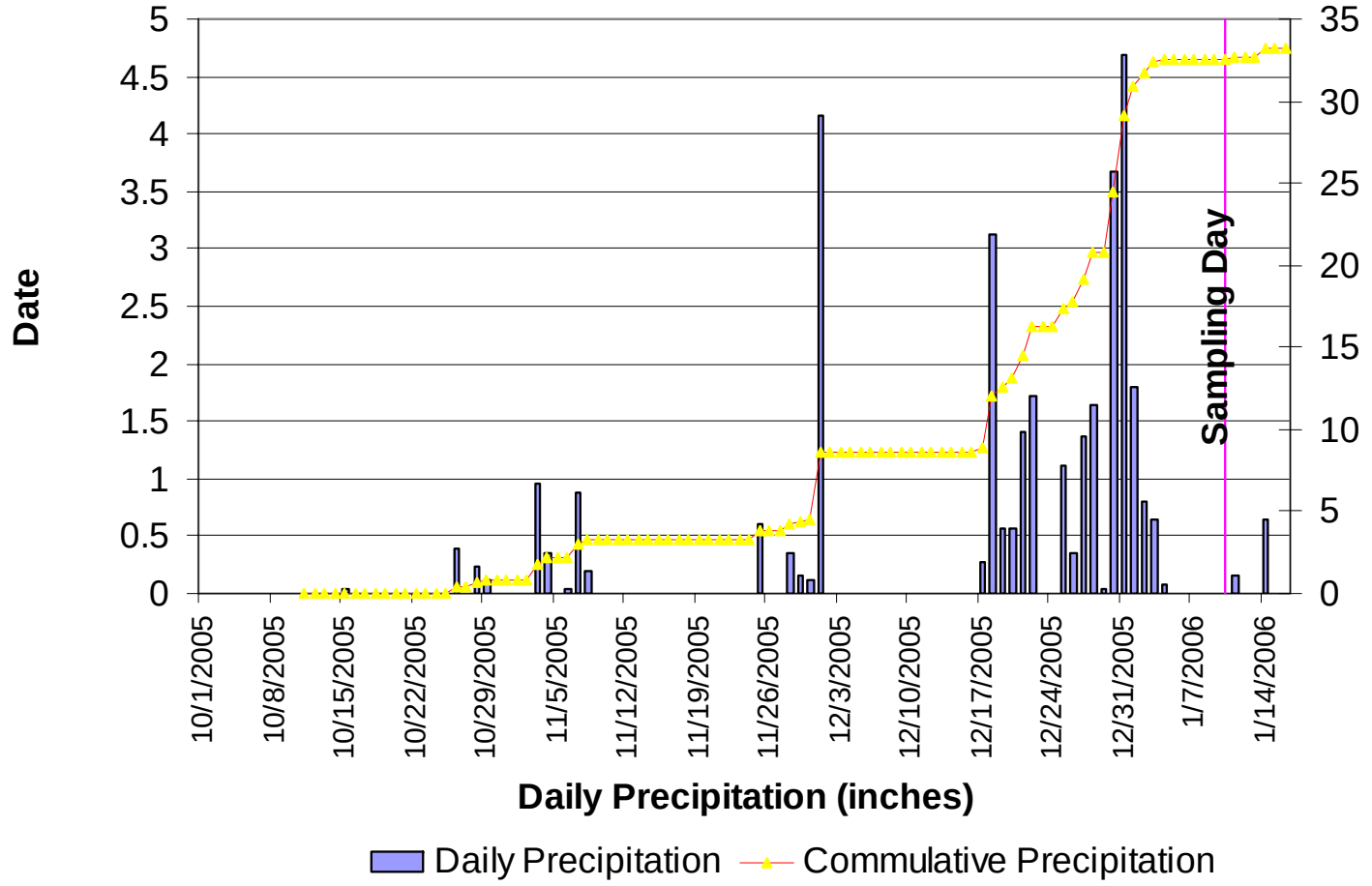

Table 8

Input Data Used in the Salinity Diffusion Analysis

Parameter	Units	Value	Other unit values	Notes
Mixing Input Data				
Length of mixing layer above soil surface	feet	0.1		Assumed
Concentration of Salt in Groundwater	g/L	57		Average of measured soil data from Ponds 9 and 10 composites (Wallace Laboratories) – see Appendix A
Diffusion coefficient from soil to surface water	m^2/s	1.50E-09	1.21E-09 ft^2/s	Molecular diffusion coefficient. Value in ft2/s was reduced from literature value by factor of 0.08 for calibration
Average wind speed	m/s	1.80E+00	5.90E+00 ft/s or 4 MPH	CIMIS Station #123 Suisun Valley, 90 percentile daily average wind speed
Physical Properties				
Tidal period	hours	12.5		
Surface Area of wetland	acres	79		Pond 9
Elevation of wetland bottom	feet	2.39		
MHW	feet	5.62		
Average width of Pond	feet	600		
Depth of water column	ft	2		
Density of water	kg/m^3	1010		
density of air	kg/m^3	1.4		
Calculated Values				
Average Depth	ft/s	3.23		
Average flow rate	cfs	494.0		
Average velocity	ft/s	0.000152944		
Vertical dispersion coefficient from tidal flows	ft^2/s	5.52E-03	3.08E-07 m^2/s	
Wind mixing	ft^2/s	1.72E-03		

Figure 50 Predicted Salinity in Ponds 9 and 10 Compared to Measured Values for Existing Conditions

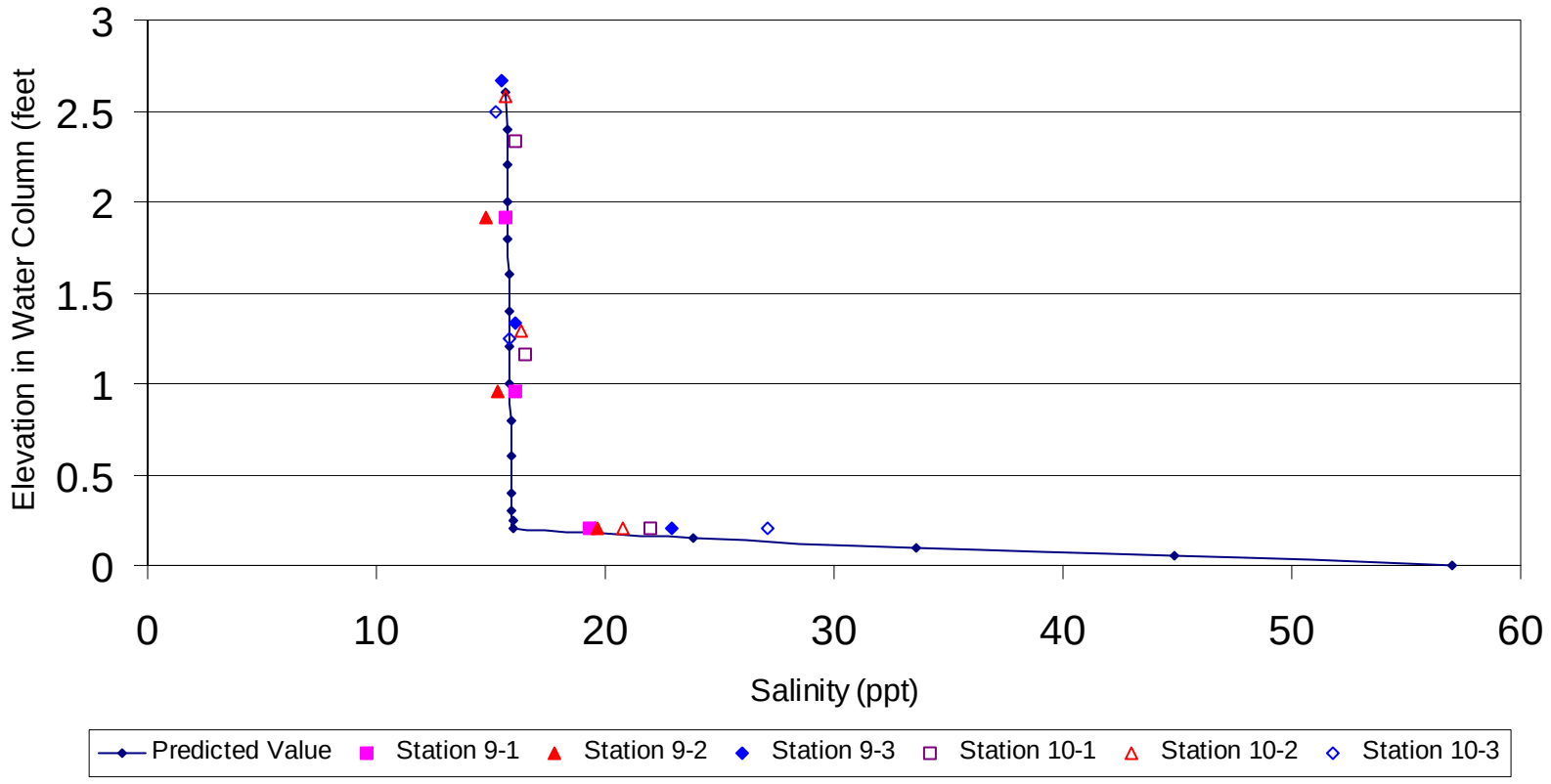

13.4.2 Sediment Salinity Characterization

13.4.2.1 Purpose

To determine salinity diffusion rates from the top 4 inches (10 cm) of pond sediment into overlying water. Diffusion coefficients will be applied across the ponds during various tidal events to determine the salinity of the outgoing tidal waters into Napa River.

13.4.2.2 Field sampling

Sediment cores were collected from Ponds 9 and 10 on January 10, 2005. Samples were collected near the margins of the salt ponds because the water depth prohibited access to the center of the ponds. To properly characterize the pond sediments and avoid an "edge effect", samples were collected from approximately 20 to 40 feet from the edge at a point where the pond bottom was relatively flat and no distinct changes in sediment characteristics were detectable (determined by the texture of the pond bottom). Three sampling stations were established in each pond. Locations of the sampling stations were recorded using a Trimble GeoExplorer 3 GPS receiver, and are shown on Figure 51.

Ambient water chemistry conditions were recorded at each sampling station prior to collecting sediment samples. Water temperature, salinity and conductivity were measured with a YSI 30 meter at three depths: pond bottom, near the middle of the water column and near the surface. Depth of the water column was measured and distance from the pond edge was estimated. These data are provided in Table 9.

Sediment cores were collected in 2-inch diameter by 30-inch length acrylic tubing. Three sediment samples were collected at each station. The sampling tubes were manually pushed into the pond bottom to a depth of approximately 5 inches. At stations 9-1 and 10-3, a fourth sediment sample was collected by pushing the acrylic tube far as possible into the pond bottom to retrieve a deeper sediment core. To draw an intact sediment core from the pond bottom it was necessary to maintain pressure in the sampling tube. Pressure was maintained in the tube by cupping the top of the tube with the palm of the sampler's hand. When the samples were retrieved both ends of the tube were sealed with plastic end caps. Pond water that entered the tube during sampling was retained in the tube. Samples were transported to the URS Oakland office for water chemistry characterization. A grab sample of Napa River water (to be used in laboratory analysis) was also collected at approximately 17:00, just downstream of the Brazos Drawbridge.

13.4.2.3 Laboratory Analysis

13.4.2.3.1 Water Chemistry

Water chemistry analysis was conducted 18 to 21 hours after field collection. Temperature, conductivity, and salinity measurements were taken from the top and bottom of the water column in the sediment core tubes. The average pond water salinities in the bottom of the sediment cores increased over that of the field salinity measurements by 2.9 ppt for site 10-1 to 9.0 ppt for site 9-2. Site 10-3 was the only location where the

bottom water salinities decreases an average of 4.1 ppt over the salinity measurement recorded in the field. Site 10-3 was located next to a thick salt crust, which may have contributed to the high bottom field salinity. The data in Tables 9 and 10 indicate a salinity diffusion gradient consistent with that measured in the field from the top to the bottom of the water column. The water salinity diffusion gradient was much higher at the bottom of the water column compared to the top as indicated in the field sampling data (Table 9). The lab data shows a similar trend with an average salinity difference from the top to the bottom of the cores of 4.7 ppt and gradient of 0.26 ppt/in (Table 10). Mixing of the water column effectively lowers the salinity of the water at the soil interaction zone allowing further salt diffusion from the soil to the water to occur.

In order to simulate the salt diffusion from soil to water column following the breaching of the levees in the summer months, water of equivalent summer time salinity was added to the sediment cores. The salinity of the water that would enter Napa Plant Site during the summer months was estimated to be 15 ppt, the lowest summer time salinity recorded for the top of the water column at the USGS station on Mare Island in 1997 (CSCC et al. 2003). The lowest salinity recorded during the summer months was chosen because lower salinity water would result in the highest possible salt diffusion. The 15 ppt water was mixed by gradually adding table salt to five gallons of tap water. An equivalent amount of salt "summer" water was added atop the first ("A") sediment core sampled at each site and the replicate ("R") samples taken from each pond. The third sediment samples ("C") taken from each site in each pond was mixed together thoroughly making a composite for each pond. Four inches of the mixed sediment was filled back into an acrylic core and 15 ppt water was added. To simulate winter salt diffusion 0.3 ppt fresh water collected from Napa River during the field sampling was added to the second or "B" samples taken from each sample site. To mimic a tidal cycle the water was allowed to sit atop the sediment cores for a period of approximately six hours.

Following the 6-hour lapse time temperature, conductivity, and salinity were measured at the top and bottom of the water column as shown in Table 11. The results of the summer tidal water simulation indicate that there was an increase (above 15 ppt) in the bottom water column salinities ranging from a 0.5 ppt increase at site 9-1 to a 6.8 ppt increase at site 9-2. The winter tidal water simulation using Napa River water at 0.3 ppt indicates bottom salinity increases ranging 0.5 ppt at sites 10-2 and 10-3 to 2.4 ppt at site 9-2. Consistently site 9-2 diffused the highest amount of salt into the bottom of the water column (Figure 52). Overall, pond 10 (Figure 53) appears to diffuse slightly less salt and have slightly lower salinity difference or gradient from the top to the bottom of the water column than pond 9 (Figure 52). A comparison summary table of the average salinities measured for each sample site is provided in Table 12 for the field, lab pond water, and summer and winter simulations. Other than site 9-2 the composite samples for both ponds 9 and 10 showed the greatest salinity difference in summer water salinity (Table 12). It seems the mixing of the pond sediments allowed for a higher diffusion rate. This condition is more indicative of the conditions, which may occur once the ponds are ripped or plowed. Table 12 also indicates that there was not much of a salinity gradient from the bottom to the top of the water column for both the summer and winter water simulations.

13.4.2.3.2 Sediment Analysis

Sediment samples from ponds 9 and 10 were sent to Wallace Laboratories in El Segundo, CA for electrical conductivity analysis. A conversion factor was given to convert the conductivity measurements (millimho/cm) to salinity (ppt). Samples analyzed included a composite of the three sampling locations for both ponds 9 and 10, and a sample of the top and bottom half of the cores sampled at locations 9-1 and 10-3.

The data from the pond sediment analysis is depicted in Figure 54. The soil salinities ranged from 51.6 ppt for the composite of the sediments from pond 10 to 85.1 ppt for the top sediments at site 9-1. The salinities of these sediments indicate a capacity to diffuse additional salt into the water column. This may particularly be the case when the sediments are mixed rather than stratified allowing more surface area water interaction with sediment colloids. This was observed in the composite analysis as mentioned above. Using the salinity diffusion data collected from the laboratory analysis, a model can be created that simulates the salinity diffusion for the entire Napa Plant Site following the restoration.

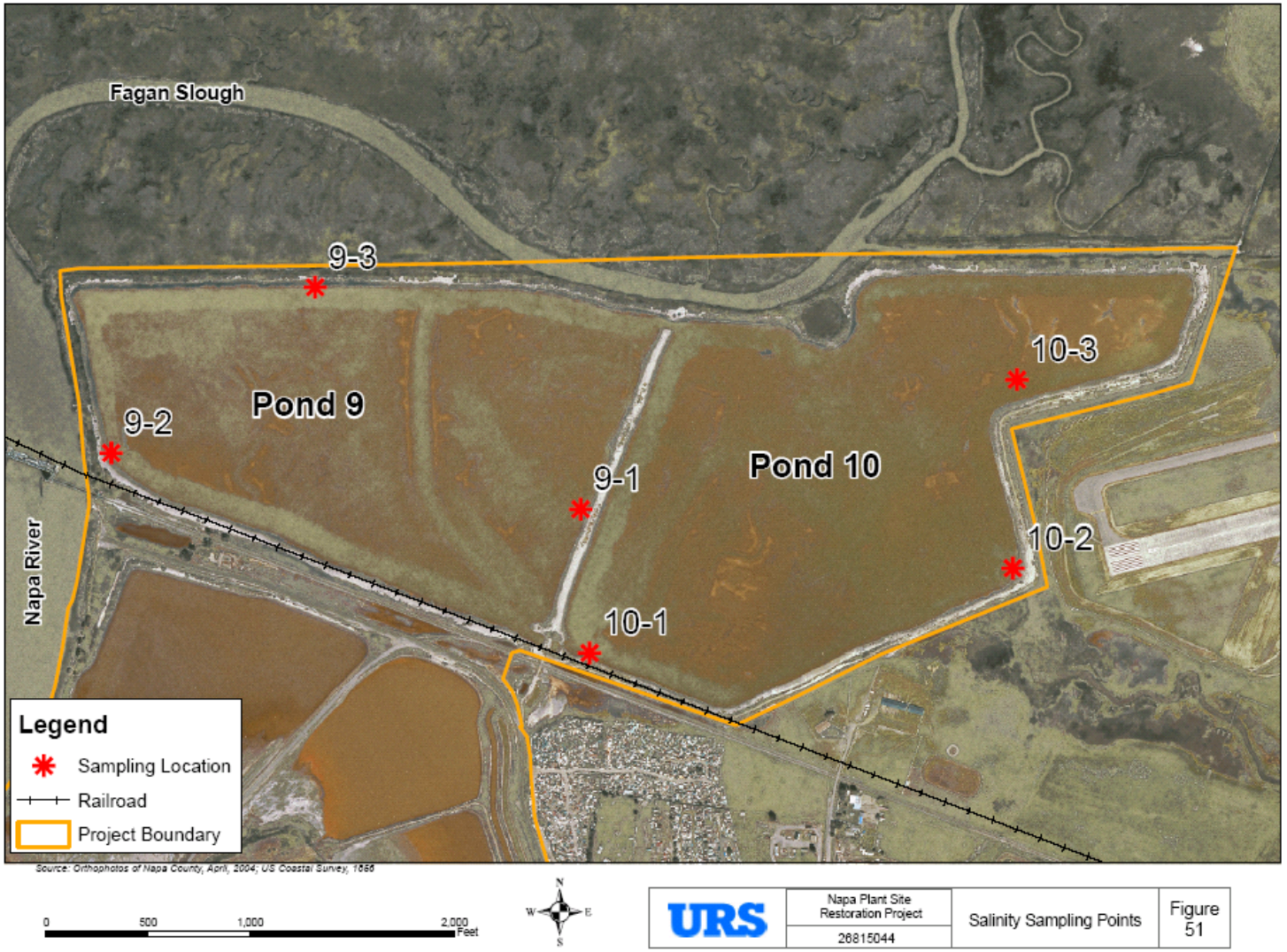
Fagan Slough
9-3
Pond 9
9-2
9-1
Pond 10
10-3
10-2
10-1
Napa River
Legend
Sampling Location
Railroad
Project Boundary
Source: Orthophotos of Napa County, April, 2004; US Coastal Survey, 1856
0
500
1,000
2,000
Feet
N
W
E
S
URS
Napa Plant Site Restoration Project
26815044
Salinity Sampling Points
Figure 51

Table 9. Ambient water chemistry conditions recorded at each sampling station prior to collecting sediment samples.

Site	Time	Approx. Distance from Waters Edge (ft)	Water Depth (in)	Temp (C)	Specific Conductivity[1] (µS)	Conductivity (µS)	Salinity (ppt)	Salinity Gradient (ppt/in)[2]	
9-1 top	16:40	25	23	11.7	25.40	18.90	15.6	0.04	0.16
9-1 middle				11.8	26.10	19.40	16.1		
9-1 bottom				13.0	31.20	24.30	19.3	0.28	
9-2 top	17:08	25	23	11.0	24.30	17.70	14.8	0.04	0.21
9-2 middle				11.2	24.80	18.10	15.3		
9-2 bottom				13.8	31.40	24.90	19.7	0.38	
9-3 top	17:40	20	32	11.8	25.30	18.80	15.5	0.04	0.23
9-3 middle				11.6	26.20	19.20	16.1		
9-3 bottom				14.8	36.70	29.90	22.9	0.43	
10-1 top	14:37	20	28	11.2	26.40	19.40	16.1	0.03	0.21
10-1 middle				11.0	27.20	19.70	16.5		
10-1 bottom				13.0	33.20	26.00	22.0	0.39	
10-2 top	15:06	30	31	11.2	25.30	18.60	15.6	0.05	0.17
10-2 middle				11.3	26.00	19.10	16.3		
10-2 bottom				14.1	33.30	26.60	20.8	0.29	

Site	Time	Approx. Distance from Waters Edge (ft)	Water Depth (in)	Temp (C)	Specific Conductivity[1] (µS)	Conductivity (µS)	Salinity (ppt)	Salinity Gradient (ppt/in)[2]	
10-3 top	15:32	60	30	11.6	24.90	18.50	15.2	0.04	0.40
10-3 middle				11.6	25.80	19.00	15.8		
10-3 bottom				14.3	42.40	34.00	27.1	0.75	

[1]Specific Conductivity is corrected for temperature at 25ºC, whereas conductivity is temperature dependent

[2]Salinity gradient calculated based on the upper half, lower half, and entire water column depth

Table 10. Water chemistry measurements recorded for each sample and sampling station 18-21 hours following field collection

Site[1]	Time	Water Depth	Temp (°C)	Specific Conductivity[2] (mS)	Conductivity (mS)	Salinity (ppt)	Salinity Difference Top to Bottom (ppt)	Salinity Gradient (ppt/in)
9-1-A top	11:03	15.8	22.8	37.19	35.59	24.5	3.7	0.23
9-1-A bottom	11:06		21.9	43.61	40.63	28.2		
9-1-B top	11:17	17.0	23.0	36.39	35.02	23.1	0.0	0.00
9-1-B bottom	11:24		21.0	36.48	33.69	23.1		
9-1-C top	11:23	17.4	23.3	35.13	34.02	22.1	3.3	0.19
9-1-C bottom	11:25		21.0	39.7	36.68	25.4		
9-1-R top	11:49	17.4	23.1	34.56	33.29	21.7	2.6	0.15
9-1-R bottom	11:51		21.2	38.15	35.42	24.3		
9-2-A top	11:59	16.1	23.1	34.28	33.05	21.6	7.2	0.45
9-2-A bottom	12:02		22.6	44.58	42.58	28.8		
9-2-B top	12:06	18.8	23.3	35.54	34.38	22.4	7.4	0.39
9-2-B bottom	12:09		22.4	45.69	43.49	29.8		
9-2-C top	12:15	20.0	23.3	33.7	32.56	21.1	6.4	0.32
9-2-C bottom	12:17		22.1	42.66	40.34	27.5		
9-3-A top	12:28	18.8	23.2	33.42	32.24	21.0	7.1	0.38
9-3-A bottom	12:31		22.8	43.57	41.71	28.1		
9-3-B top	12:34	14.8	23.0	33.11	31.83	20.8	6.8	0.46

Site[1]	Time	Water Depth	Temp (°C)	Specific Conductivity[2] (mS)	Conductivity (mS)	Salinity (ppt)	Salinity Difference Top to Bottom (ppt)	Salinity Gradient (ppt/in)
9-3-B bottom	12:36		22.6	42.91	41.05	27.6		
9-3-C top	12:39	17.4	23.1	33.23	32	20.9	3.4	0.20
9-3-C bottom	12:44		22.7	38.17	36.46	24.3		
10-1-A top	12:46	18.1	23.1	32.4	31.18	20.3	7.0	0.39
10-1-A bottom	12:50		21.3	42.43	39.46	27.3		
10-1-B top	12:53	18.7	23.1	32.4	31.23	20.3	5.7	0.30
10-1-B bottom	12:55		20.9	40.55	37.43	26.0		
10-1-C top	12:58	18.6	23.0	34.35	33.04	21.6	5.3	0.28
10-1-C bottom	13:00		21.0	41.83	38.61	26.9		
10-2-A top	13:02	18.5	23.2	33.33	32.19	20.9	4.1	0.22
10-2-A bottom	13:05		21.5	39.13	36.52	25.0		
10-2-B top	13:09	19.0	23.3	31.78	30.71	19.8	5.9	0.31
10-2-B bottom	13:12		21.5	40.15	37.46	25.7		
10-2-C top	13:15	18.8	23.1	32.25	31.06	20.2	3.7	0.20
10-2-C bottom	13:17		21.1	37.58	34.8	23.9		
10-3-A top	13:20	16.1	23.1	31.56	30.39	19.7	3.7	0.23
10-3-A bottom	13:23		21.3	36.89	34.31	23.4		
10-3-B top	13:26	17.4	23.1	31.5	30.34	19.6	3.5	0.20

Site[1]	Time	Water Depth	Temp (°C)	Specific Conductivity[2] (mS)	Conductivity (mS)	Salinity (ppt)	Salinity Difference Top to Bottom (ppt)	Salinity Gradient (ppt/in)
10-3-B bottom	13:29		21.8	36.42	34.15	23.1		
10-3-C top	13:32	17.0	23.1	31.39	30.19	19.6	3.5	0.21
10-3-C bottom	13:35		21.2	36.49	33.82	23.1		
10-3-R top	13:39	18.0	23.1	31.3	30.18	19.5	3.1	0.17
10-3-R bottom	13:42		21.7	35.7	33.49	22.6		
						Average Top to Bottom:	4.7	0.26

[1]A, B, C refers to the three sample cores taken at each sampling site. R refers to the replicate sample core taken at sites 9-1 and 10-3

[2]Specific Conductivity is corrected for temperature at 25ºC, whereas conductivity is temperature dependent

Table 11. Water chemistry measurements made following the 6-hour summer and winter tidal simulations.

Site	Start Time	Sampling Time	Water Depth (in)	Water Volume (ml)	Temp (°C)	Specific Conductivity[1] (mS)	Conductivity (mS)	Salinity (ppt)	Salinity Difference Top to Bottom (ppt)	Salinity Gradient (ppt/in)
9-1-A top	13:34	20:07	15.8	635	16.1	24.76	20.61	15.1	0.4	0.03
9-1-A bottom		20:11			17.1	25.33	21.53	15.5		
9-1-B top	12:40	20:30	17.0	675	17.0	1.524	1.294	0.8	0.4	0.02
9-1-B bottom		20:33			17.8	2.247	1.942	1.2		
9-1-R top	13:40	20:14	17.4	740	16.3	25.23	21.05	15.4	0.4	0.02
9-1-R bottom		20:16			16.9	25.84	21.83	15.8		
9-2-A top	13:53	20:45	16.1	675	16.8	25.09	21.21	15.3	6.5	0.40
9-2-A bottom		20:47			18.0	34.58	29.98	21.8		
9-2-B top	12:44	20:25	18.8	740	16.0	1.690	1.402	0.9	1.8	0.10
9-2-B bottom		20:40			18.1	4.960	4.319	2.7		
9-3-A top	13:55	20:51	18.8	745	17.9	25.41	21.96	15.5	0.5	0.03
9-3-A bottom		20:53			17.8	26.09	22.51	16.0		
9-3-B top	12:48	20:54	14.8	585	17.6	1.726	1.484	0.9	0.4	0.03
9-3-B bottom		20:56			17.4	2.462	2.109	1.3		
9-Comp top	13:45	20:21	17.4	690	16.0	29.60	24.53	18.4	2.9	0.17
9-Comp bottom		20:24			18.0	33.95	29.45	21.3		

Site	Start Time	Sampling Time	Water Depth (in)	Water Volume (ml)	Temp (°C)	Specific Conductivity[1] (mS)	Conductivity (mS)	Salinity (ppt)	Salinity Difference Top to Bottom (ppt)	Salinity Gradient (ppt/in)
10-1-A top	14:00	20:58	18.1	720	16.9	25.57	21.62	15.6	0.4	0.02
10-1-A bottom		20:59			15.7	22.07	21.44	16.0		
10-1-B top	12:55	21:02	18.7	740	17.2	1.416	1.207	0.7	0.2	0.01
10-1-B bottom		21:04			15.9	1.792	1.482	0.9		
10-2-A top	14:05	21:05	18.5	730	17.3	25.23	21.54	15.4	1.1	0.06
10-2-A bottom		21:07			17.2	26.87	22.88	16.5		
10-2-B top	12:51	21:09	19.0	755	17.6	1.243	1.086	0.6	0.2	0.01
10-2-B bottom		21:12			16.8	1.665	1.406	0.8		
10-3-A top	14:13	21:13	16.1	645	17.0	25.10	21.28	15.3	1.3	0.08
10-3-A bottom		21:15			16.3	26.97	22.50	16.6		
10-3-B top	13:01	21:22	17.4	690	17.7	1.268	1.092	0.6	0.2	0.01
10-3-B bottom		21:23			16.1	1.662	1.381	0.8		
10-3-R top	14:15	21:16	18.0	715	17.5	25.67	22.00	15.7	0.4	0.02
10-3-R bottom		21:17			15.7	26.18	21.56	16.1		
10-Comp top	14:05	21:20	17.0	635	17.1	26.69	22.68	16.4	1.6	0.09
10-Comp bottom		21:21			17.4	29.02	24.80	18.0		
								Average Salinity Difference Top to Bottom:	1.2	0.07

Site	Start Time	Sampling Time	Water Depth (in)	Water Volume (ml)	Temp (°C)	Specific Conductivity[1] (mS)	Conductivity (mS)	Salinity (ppt)	Salinity Difference Top to Bottom (ppt)	Salinity Gradient (ppt/in)

[1]Specific Conductivity is corrected for temperature at 25ºC, whereas conductivity is temperature dependent

Table 12. Summary table of the salinity diffusion differences for each method

Site	Field Pond Water		Lab Pond Water		Summer Water (15 ppt)		Winter Water (0.3 ppt)	
	Field Pond Salinity (ppt)	Salinity Difference Middle to Bottom (ppt)	Average Lab Pond Water (for each site) (ppt)	Average Salinity Difference Top to Bottom (for each site) (ppt)	Summer Salinity Simulation	Summer Salinity Difference Top to Bottom (ppt)	Winter Salinity Simulation	Winter Salinity Difference Top to Bottom (ppt)
9-1 top	16.1	3.2	22.9	2.4	15.1	0.4	0.8	0.4
9-1 bottom	19.3		25.3		15.5		1.2	
9-2 top	15.3	4.4	21.7	7.0	15.3	6.5	0.9	1.8
9-2 bottom	19.7		28.7		21.8		2.7	
9-3 top	16.1	6.8	20.9	5.8	15.5	0.5	0.9	0.4
9-3 bottom	22.9		26.7		16.0		1.3	
10-1 top	16.5	5.5	20.3	4.6	15.6	0.4	0.7	0.2
10-1 bottom	22.0		24.9		16.0		0.9	
10-2 top	16.3	4.5	20.3	4.6	15.4	1.1	0.6	0.2
10-2 bottom	20.8		24.9		16.5		0.8	
10-3 top	15.8	11.3	19.6	3.5	15.3	1.3	0.6	0.2
10-3 bottom	27.1		23.1		16.6		0.8	
9-Composite top					18.4	2.9		
9-Composite bottom					21.3			

10-Composite top			16.4	1.6	
10-Composite bottom			18.0		

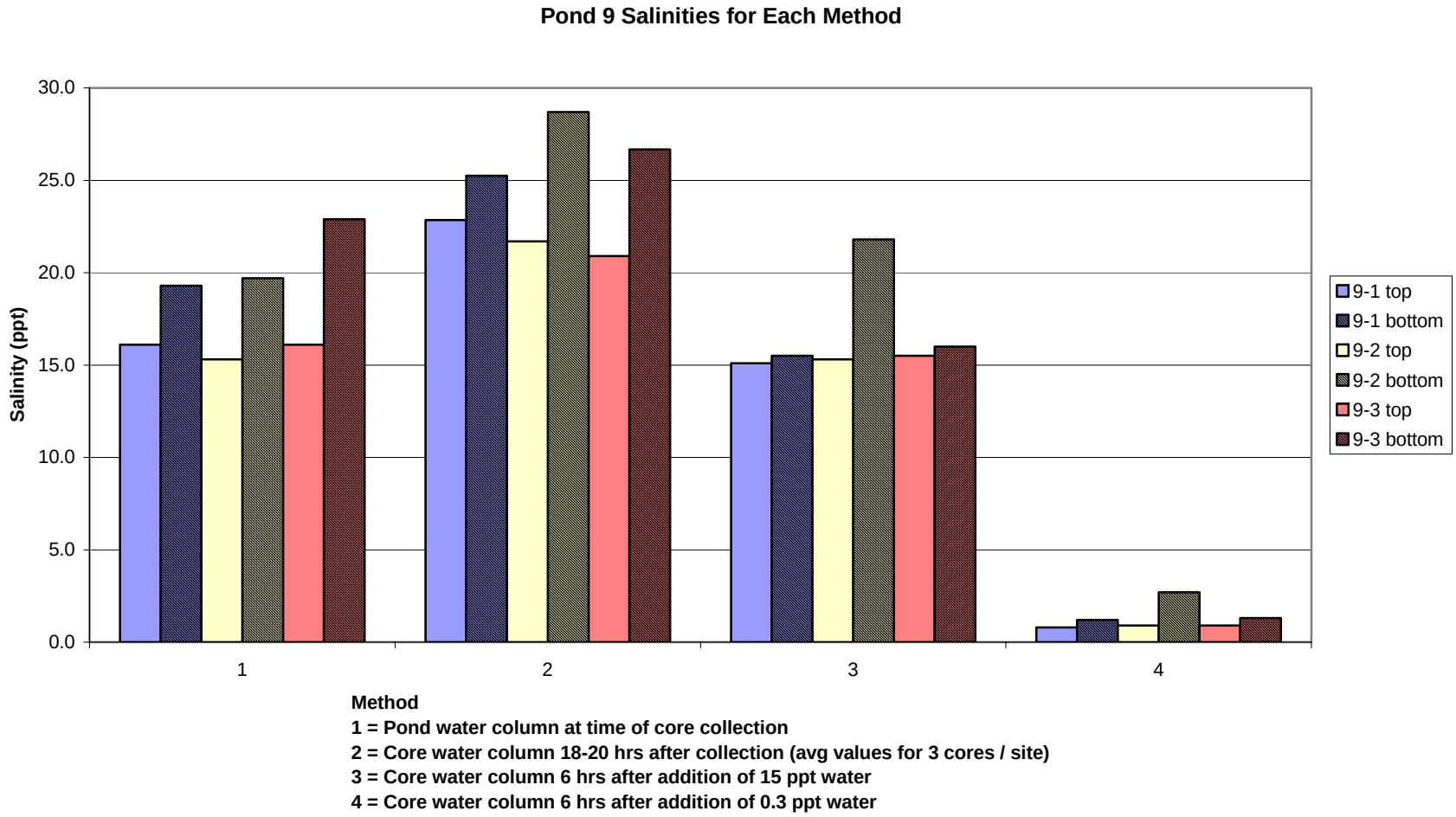

Figure 52. Pond 9 salinities at the time of field collection and for each analysis method

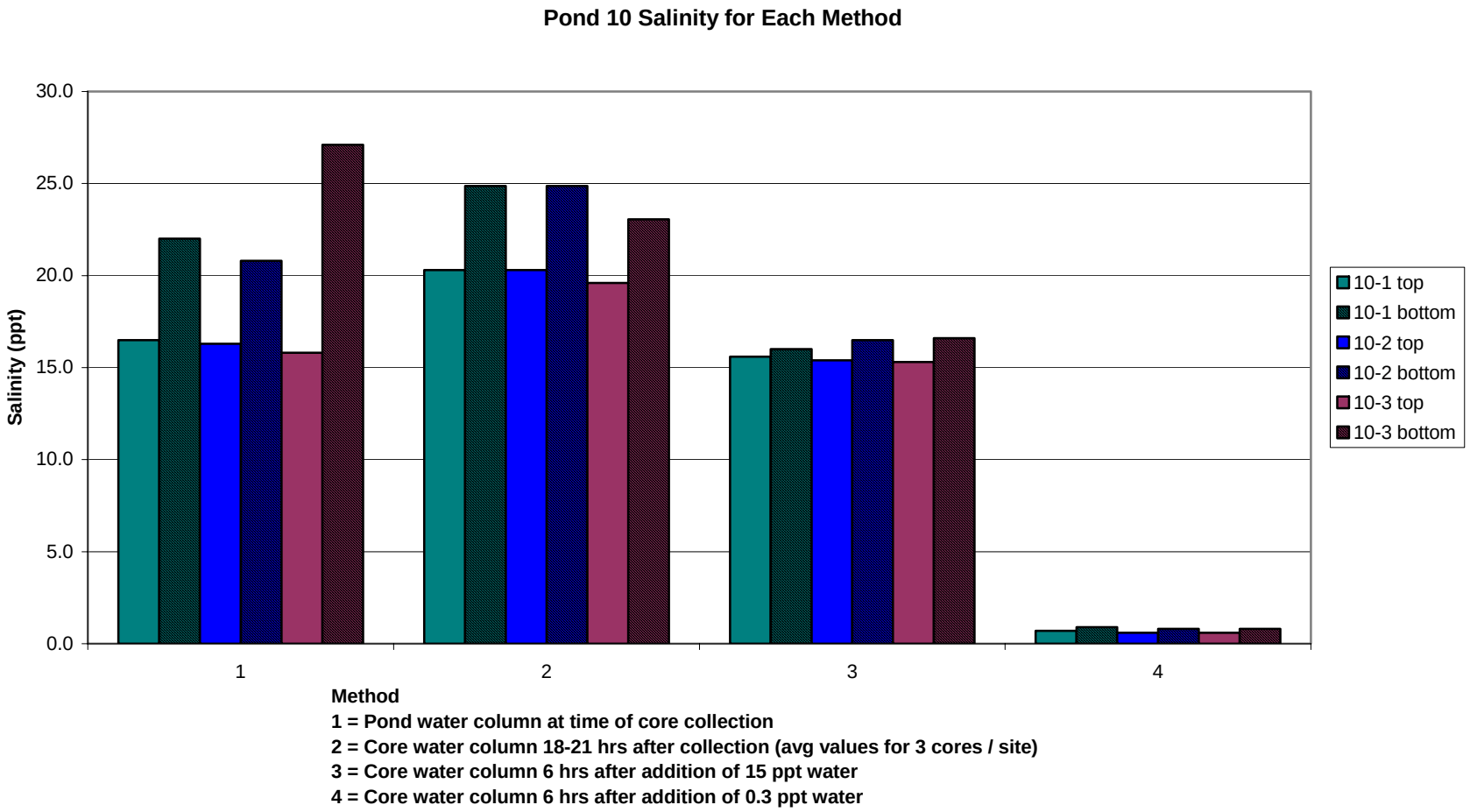

Figure 53. Pond 10 salinities at the time of field collection and for each analysis method

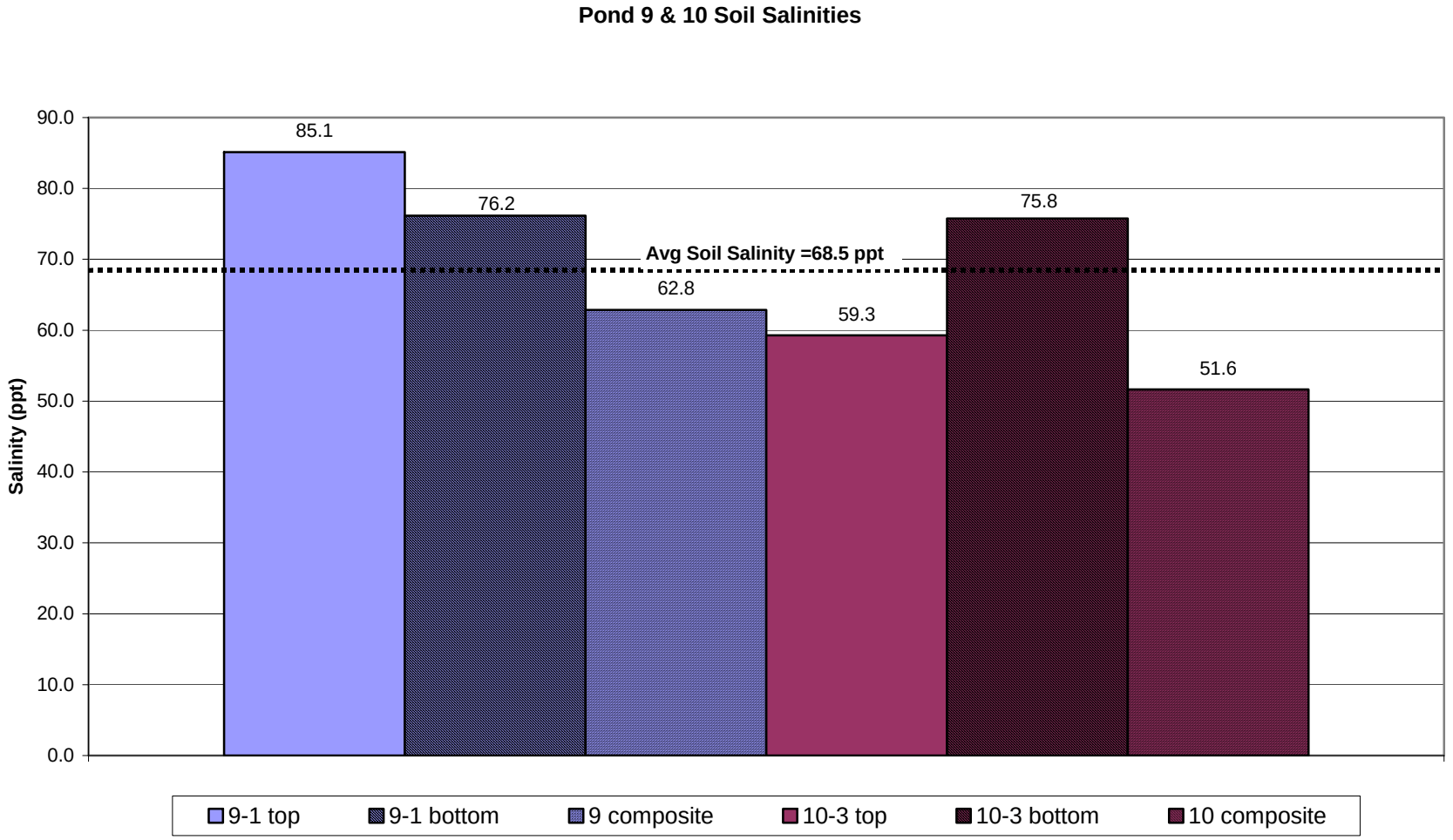

Figure 54. Pond 9 and 10 soil salinity analysis

The following is a summary of modeling results and suggestions for additional analysis that can be performed during final design:

- Preliminary design of breach size, and channel geometry/location has been determined for the various alternatives to meet project goals;
- Tidal channels will need to be included in the design, particularly in sub-area 3, if complete drainage of the wetland is desired soon after construction. Without construction of internal channels, full drainage may not occur until internal channels are formed naturally. Drainage improves with the length and extensiveness of tidal channel. Additional sensitivity analyses as to the extent and size of channels required to achieve desired flooding and draining characteristics can be performed at the final design stage for the preferred alternative. This sensitivity analysis will allow an evaluation of the effect "puddles" can have on the size of channels. We propose to perform simulations using a constant marsh surface by computing the average elevations in each respective area and thus determining if this results in different channel sizes;
- Results indicate that the restoration of the Site under all Alternatives has no bearing on the water level at the Napa River;
- Velocities in Fagan Slough and Napa River increase as a result of the proposed restoration alternatives. The increase in the Napa River is minor. The increase in Fagan Slough is significant and may result in an enlargement of Fagan Slough's cross-section.
- Extreme flood elevations have preliminarily been determined in the ponds to plan for flood control.
- Geomorphic analysis indicates that the ponds should start to vegetate within 3 to 5 years. Development of mature marshes may take 50 years or more.

California State Coastal Conservancy (CSCC), U.S. Army Corps of Engineers (USACE), California Depatment of Fish and Game (CDFG). 2003. Napa River Salt Marsh Restoration Project; Feasibility Report and Technical Appendices, Figures 4-21 to 4-30. Available online at: http://www.napa-sonoma-marsh.org/documents/Feasibility/appendices/AppD/phase2.html

Chow, V.T. 1959. Open Channel Hydraulics, McGraw Hill.

Federal Emergency Management Agency. 1990. Flood Insurance Study: Napa County, Unincorporated Areas, Community Number 060205. http://store.msc.fema.gov/

Hines, Anthony L. and Robert N. Maddox. 1985. Mass Transfer. Fundamentals and Applications. PTR Prentice Hall, Englewood Cliffs, N.J.

PWA, 1995. Design Guidelines for Tidal Channels in Coastal Wetlands, PWA Ref. # 934. Prepared for U.S. Army Corps of Engineers Waterways Experiment Station.

PWA. 2002a. Napa-Sonoma Marsh Restoration Feasibility Study – Hydrodynamic Modeling Analyses of Existing Conditions – Phase 1, PWA Ref. # 1174. Prepared for U.S. Army Corps of Engineers, San Francisco Office.

PWA. 2002b. Napa Sonoma Marsh Restoration Feasibility Study, Phase 2 Stage 1, PWA Ref. # 1545/46. Prepared for the California State Coastal Conservancy.

PWA. 2002c. Napa River Salt Marsh Restoration – Habitat Restoration Preliminary Design, Phase 2 Stage 2 of the Hydrology and Geomorphology Assessment in Support of the Feasibility Study, Final Report, PWA Ref. # 1591. Prepared for the California State Coastal Conservancy.

PWA. 2004. CD of MIKEFLOOD input files for Napa Salt Ponds. Files from PWA projects 1545 (PWA 2002b) and 1591 (PWA 2002c). Transmitted to URS from PWA.

Towill, Inc. 2001. Napa Salt Marsh Restoration Project, Topographic and Hydrographic Surveys; Ground Control and Hydrographic Survey Report. Prepared for the U.S. Army Corps of Engineers, San Francisco District, California.

USACE. 1998. Napa River Flood Protection Project. U.S. Army Corps of Engineers, Sacramento District, California.

Warner, J.C., S.G. Schladow, and D.H. Schoellhamer. 1999. Summary and Analysis Hydrodynamics and Water-Quality Data for the Napa/Sonoma Marsh Complex, Final Report, Equipment Deployment from September 1997 to March 1998, University of California, Davis, Environmental Dynamics Laboratory Report No. 98-07.

Warner, J.C. 2000. Barotropic and Baroclinic Convergence Zones in Tidal Channels, Ph.D. Dissertation, University of California, Davis.

Weast, Robert, Ph.D., Editor. 1980. CRC. 60th Edition. CRC Press, Inc. Boca Raton, FL.

Zlomke, B. 1996. Napa County Resource Conservation District (NRCD), Inter-office memo with PWA on Napa River Flood Protection Project Phase 1 Model Report.